SULFENYLATION OF CYTOCHROMES P450 IN RESPONSE TO REDOX ALTERATION

by

Matthew E. Albertolle

Dissertation

Submitted to the Faculty of the

Graduate School of Vanderbilt University

in partial fulfillment of the requirements

for the degree of

DOCTOR OF PHILOSOPHY

in

Biochemistry

January 31, 2019

Nashville, Tennessee

F. Peter Guengerich, PhD

Kevin L. Schey, PhD

Manuel Ascano, PhD

Richard M. Breyer, PhD

Ambra A. Pozzi, PhD

To my beloved wife, Elizabeth, who always encouraged me to pursue my dreams and healthy habits.

And

To my parents, who let me play in the dirt and fostered my relationship with and appreciation of Nature.

ACKNOWLEDGEMENTS

I have been very fortunate to have many mentors through my journey into a scientific career. First, I would like the thank the San Mateo Community College District for providing high quality training in the sciences and for allowing me to decide a career path in an affordable fashion.

I had many amazing mentors and coaches at the University of San Francisco during my undergraduate tenure. I would like to thank Dr. Juliet V. Spencer for allowing me to intern in her lab and learn the basics of molecular biology. Also Drs. William Melaugh and John G. Cobley for fostering my interests, helping me find a position as a technician at UCSF, and talking science over a few beers.

Working as a technician in the Sandler-Moore Mass Spectrometry Core Facility at UCSF provided me with excellent training in preparation for my PhD training. Dr. Susan J. Fisher was instrumental in her trust of my work and her help getting admitted to Vanderbilt University. My three bosses Drs. Steven C. Hall, Katherine E. Williams, and H. Ewa Witkowska gave me projects that were challenging and allowed me to discover on my own. They fostered my creativity and independence. This vein of thinking has continued to evolve throughout my thesis.

I have much gratitude to the Vanderbilt IGP Graduate Program and rotation mentors Drs. Eric Skaar, Adam Seegmiller, and Daniel Liebler. I learned a lot about various techniques that I carried over to my thesis work in the Guengerich laboratory. In particular, Dr. Dan Liebler has helped me immensely in terms of designing and implementing chemoproteomic experiments and as a general science life coach.

Dr. Guengerich has been an amazing mentor. I couldn't have asked for a better scientist to aspire to. His work ethic and efficiency are unparalleled, which made my writing and experiments proceed quickly. His style of mentoring evolved as I progressed into a senior graduate, to still provide me with advice and act as a sounding board for new scientific ideas and questions. I continue to learn from him and believe I still in the following years as I progress in my career. I understand the strength of the fraternity of "ex-dogs" and am happy I am to be a member of this group.

I would also like to thank my committee for mentoring me through my PhD. I had different, but equally beneficial relationships with Drs. Ascano, Breyer, Pozzi, and Schey. They encouraged me to think critically and helped to improve my presentation skills.

During my tenure in the Guengerich laboratory, I have had interactions with great scientists including Eric Gonzalez, Valerie Kramlinger, Kevin Johnson, Carl Sedgeman, Francis Yoshimoto, Michael Reddish, Pratibha Ghodke, and Kathy Trisler. I'm thankful for all of the friendships I have developed in the lab and have learned a lot from each of these researchers.

I am particularly grateful for the mass spectrometry core facility at Vanderbilt. The staff both on the proteomics and small molecule sides were always helpful and willing to talk if I had specific questions. Hayes McDonald, Kristie Rose, and Salisha Hill were all so helpful when I was initially getting my footing running instruments by myself in the core. Thanks in particular goes to Hayes for the time I spent in his office seeking advice for dealing with difficult problems and pushing instrument limitations. Wade Calcutt, Emilio Rivera, and Julie Coleman were excellent at keeping the instruments I used maintained

and functional. Wade always has time to help with troubleshooting instrument errors or with advice on analytical chemistry issues.

I would also like to thank Dr. Guengerich's and my funding sources including the National Institute of Health (R01 GM118122, T32 ES007028, F31 HL136133) and the American Heart Association (PRE33410007).

Despite moving away from my hometown, my family has always been supportive of my decisions. My parents are the second people (behind my wife) I call if I have anything to talk about, good or bad. They are both great listeners and were there for every step of my life.

Lastly, Elizabeth has been the most important person in my life for nine years. Thanks for keeping me in check and providing a sometimes much needed voice of reason. Thanks for all the sweet treats and understanding when I went into the lab "for just twenty minutes" on a Sunday.

TABLE OF CONTENTS PAGE

LIST OF TABLES PAGE

LIST OF FIGURES PAGE

20-HETE	20-Hydroxyeicosatetraenoic Acid
AAALAC	Association for the Assessment and Accreditation of Laboratory Animal Care
AGC	Automatic Gain Control
AUC	Area Under the Curve
BCA	Bicinchoninic Acid
CHTN	Cooperative Human Tissue Network
CID	Collision-Induced Dissociation
CPR	NADPH-P450 Reductase
DDA	Data-Dependent Analysis
DIA	Data-Independent Analysis
DLPC	L-*α*-dilauroyl-*sn*-glycero-3-phosphocholine
DTT	Dithiothreitol
EET	Epoxyeicosatrienoic Acid
EGFR	Epidermal Growth Factor Receptor
ER	Endoplasmic Reticulum
FAD	Flavin Adenine Dinucleotide
FDR	False Discovery Rate
FMN	Flavin Mononucleotide
FMO	Flavin-containing Monooxygenase
GAPDH	Glyceraldehyde-Phosphate Dehydrogenase
GSH	Glutathione
HCD	Higher Energy Collisional Dissociation
HEPPS	3-[4-(2-hydroxyethyl)-1-piperazinyl]propanesulfonate
HRMS	High Resolution Mass Spectrometry
ICAT	Isotope-Coded Affinity Tag
ICDID	Isotope-Coded Dimedone/Iododimedone
Keap1	Kelch-like ECH-associated Protein-1
MAO	Monoamine Oxygenase
MD	Molecular Dynamics
MRM	Multiple Reaction Monitoring
NCE	Normalized Collison Energy
NTA-Ni^{2+}	His_6-nitrilotriacetic acid/nickel
OH	Hydroxylation
P450, CYP	Cytochrome P450
PK	Pharmacokinetics
POR	Cytochrome P450 Oxidoreductase, Also CPR
PRM	Precursor Reaction Monitoring

PTP1B	Tyrosine Phosphoprotein Phosphatase 1B
ROS	Reactive Oxygen Species
SILAC	Stable Isotope Labeling of Amino Acids in Cell Culture
TCA	Trichloroacetic Acid
TCEP	*tris*-(Carboxyethyl)phosphine
UGT	UDP-Glucuronyltransferase

CHAPTER 1

1. Introduction

1.1. Cytochrome P450 Enzymes

Cytochrome P450 (CYP, P450) enzymes were initially named for the change in absorbance found from the reduced form of the enzyme in the presence of CO which provided an absorbance maxima of 450 nm (1). Initially, P450 enzymes were investigated and purified for roles played in drug metabolism, especially in the liver (2-4). More recently with the rapid expansion of genomic data, there has been an initiative to follow a naming convention. The nomenclature guidelines for P450 families share at least 40% amino acid identity, while members of subfamilies must share at least 55% amino acid identity (i.e., P450 3A4: 3 (family) A (subfamily) 4 (enzyme) (5). Additionally, when referring to the P450 gene, the name would be italicized (i.e., *CYP3A4*) and the protein name is not (i.e., P450 3A4). Capitalization also may denote species-specific P450 enzymes (i.e., human P450 4A11, mouse P450 4a12, rat P450 4A12).

P450 enzymes are localized to either the endoplasmic reticulum (ER) or the mitochondria. The endoplasmic reticulum is a site of protein translation, posttranslational processing, and small molecule metabolism (6). Posttranslational processing includes glycosylation of proteins for sorting, disulfide bond formation, and specific proteolytic cleavages. The ER lumen is an oxidizing environment that aids in the production of disulfide bonds, which is maintained at a homeostatic level by both small molecules (ascorbate and glutathione (GSH)) and proteins (protein disulfide isomerases) (7,8). The cytosolic side of the ER remains a reducing environment to preserve the normal function of integral ER proteins (Figure 1).

P450 enzymes are found in the cytoplasmic side of the ER and are most well-known for the ability to metabolize xenobiotics and important endogenous substrates (e.g., steroids and vitamins) (9). These proteins have been of interest in the pharmaceutical industry since their initial discovery, and enzymes mainly in P450 Subfamilies 1A, 2C, 2D, and 3A are involved in the metabolism and clearance of a large majority of small molecule drugs currently approved for clinical use in humans (9). P450 regulation involves genetic and epigenetic aspects, as well as transcriptional regulation by both endogenous and exogenous factors (10). Post-transcriptional mRNA processing is also known and has also been found to be highly controlled (10).

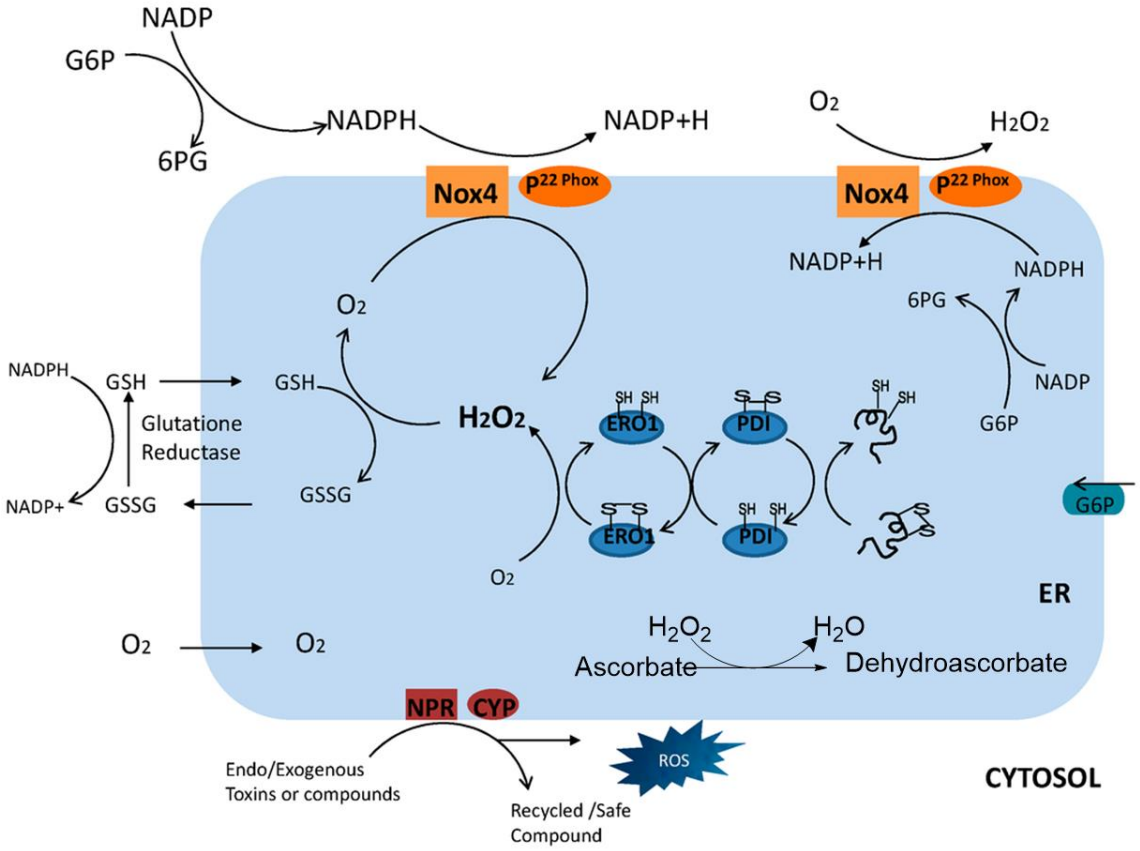

Figure 1. **The Lumen of the Endoplasmic Reticulum.** Oxidizing environment inside the lumen of the endoplasmic reticulum maintained at homeostasis by various small molecules and proteins. During the protein folding process, production of reactive oxygen species (ROS) by possible surrounding sources, such as NADPH oxidase 4 (Nox4), NADPH-P450 reductase (NPR), and GSH topologies, along with their functions in the outer ER environment. NADPH, Nicotinamide adenine dinucleotide phosphate; G6P, glucose-6-phosphate; 6PG, 6-phospho gluconate; Nox4, NADPH oxidase 4; GSH, glutathione; GSSG, glutathione disulfide; ERO1, ER oxidoreductin 1; PDI, protein disulfide isomerase. CYP; Cytochrome p450. Adapted from (11)

P450s play two major biological roles: (1) xenobiotic metabolism, with the goal being a decrease in the hydrophobicity of compound for ease of excretion and for further metabolism by enzymes such as sulfotransferases and UDP-glucuronyltransferases (UGT), and (2) biosynthesis of bioactive molecules including steroids, vitamins, and oxidized fatty acids (Table 1) (9). A subset of the latter role is the activation, deactivation, and turnover of bioactive molecules, e.g. vitamins A and D (12,13). Also, a small subset of P450s are still considered “orphan” enzymes which have unknown function or substrates. Many diseases are associated with specific P450 variants, and other diseases result from a lack of genes or the substitution of functionally inactive mutants (14-16).

The various P450s are diverse despite sharing common structural features. P450s are also some of the most promiscuous enzymes, with human P450 3A4 having thousands of reported substrates (17,18). Plants have greater numbers of P450-encoded genes than any other kingdom of organisms (e.g., wheat has 1476). These are extensively involved in the synthesis of secondary metabolites and defense molecules (19). Prokaryotic P450s synthesize important secondary metabolites such as antibiotics and have also been used as model enzymes for the study of all aspects of the general P450 catalytic cycle (20). The use of prokaryotic P450s to catalyze diverse chemical reactions that are difficult to perform synthetically has proved to be promising as well (21). This includes the use of H_2O_2 and oxygen compounds as oxygen surrogates (e.g., peracids, hydroperoxides, iodosylbenzene) for chemical reactions (22). This oxidative chemistry has implications important to the understanding of P450s in a biological context.

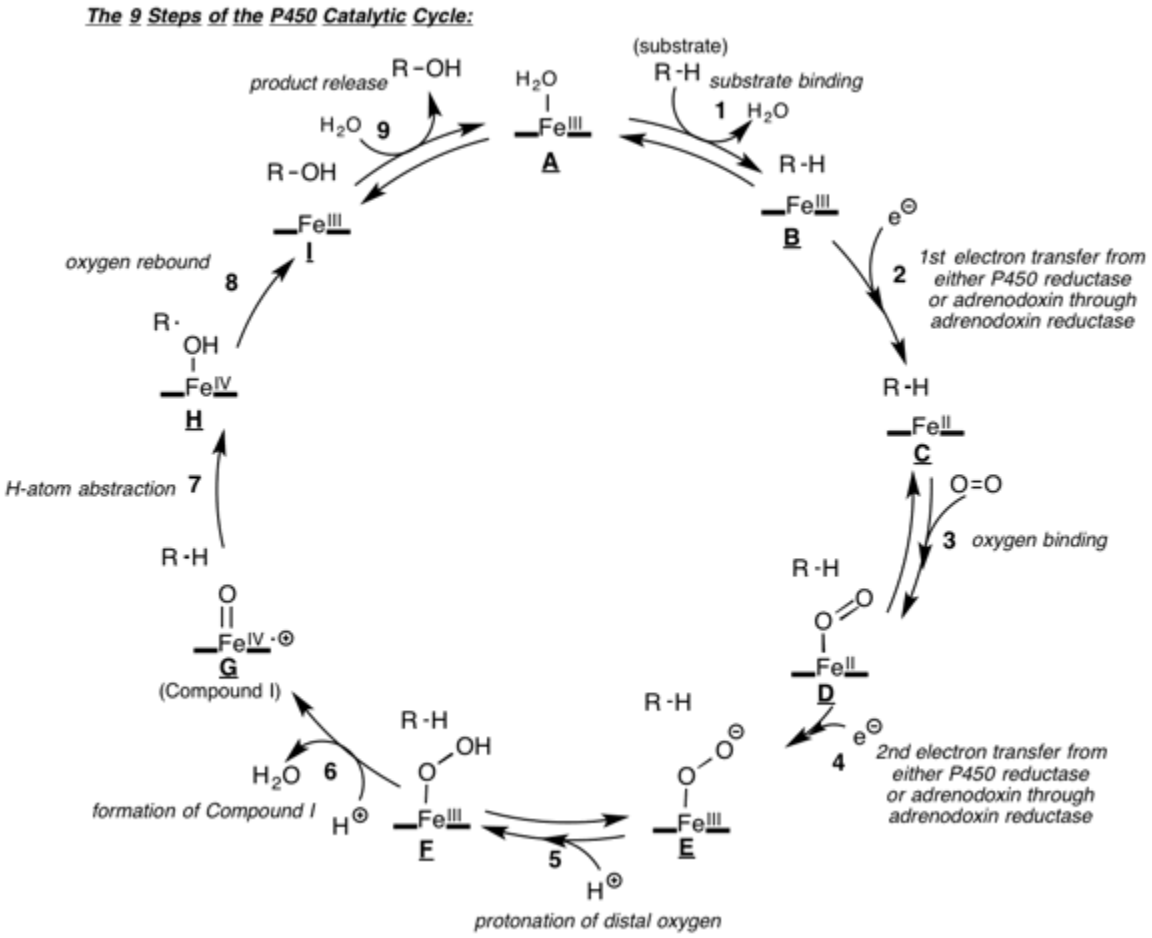

Figure 2. **The General P450 Catalytic Cycle** (from (23)

Steroids	Xenobiotics	Fatty Acids	Eicosanoids	Vitamins	Unknown (Orphan)
1B1	1A1	2J2	4F2	2R1	2A7
7A1	1A2	2U1	4F3	24A1	2S1
7B1	2A6	4A11	4F8	26A1	2W1
8B1	2A13	4B11	5A1	26B1	4A22
11A1	2B6	4F11	8A1	26C1	4X1
11B1	2C8	4F12		27B1	4Z1
11B2	2C9	4F22		27C1	20A1
17A1	2C18	4V2			
19A1	2C19				
21A2	2D6				
27A1	2E1				
39A1	2F1				
46A1	3A4				
51A1	3A5				
	3A7				
	3A43				

Table 1. **Cytochrome P450s with Specific Substrate Classes Highlighted.**

The general reaction scheme for P450-catalyzed reaction are as follows with RH as substrate

$$RH + NADPH + O_2 + H^+ \rightarrow ROH + NADP^+ + H_2O$$

This hydroxylation reaction involves a complex cycle which can be visualized in Figure 2. In the resting state, P450s are generally thought to have a water molecule as the sixth ligand coordinated to the ferric iron of the heme prosthetic group (Fig. 2, **A**). Upon substrate binding, the water ligand is often displaced, and an electron is donated from a redox partner, either cytochrome NADPH-P450 reductase (endoplasmic reticulum) or adrenodoxin (mitochondria), oxidizing NAD(P)H and reducing the iron to its ferrous form. Ferrous heme can then bind oxygen forming the formal ferric superoxide complex (Fig. 2, **D**). Another electron is supplied from a redox partner producing the P450-peroxo complex (Fig. 2, **E**). This is quickly protonated to form the P450-hydroperoxo complex (Fig. 2, **F**). This complex is protonated which destabilizes the oxygen-oxygen bond, forming Compound I ((Fig. 2, **G**) and water. This highly electrophilic species readily abstracts a proton from the substrate leaving a free radical substrate species that facilitates a homolytic cleavage reaction with the Fe^{IV}- oxygen bond-forming a hydroxylated product and ferric heme iron. Water then displaces the product returning the P450 to its resting state.

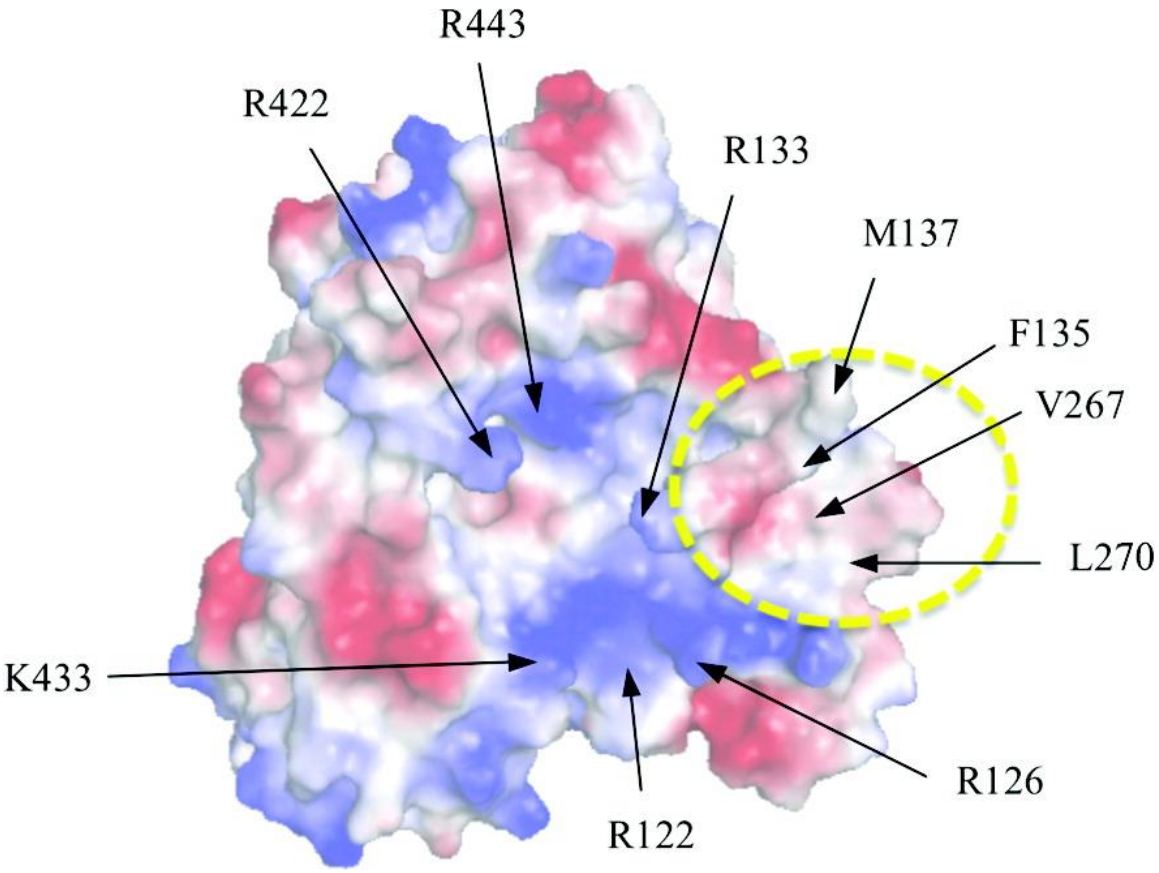

Figure 3. **Surface Electrostatic Plot of Human P450 2B4**. Electrostatic surface of P450 2B4 shows the central basic residues proposed to be involved in P450-reductase binding and a hydrophobic patch that includes V267 and L270 indicated by the dashed yellow circle. Red represents acidic residues while blue represents basic residues on the surface of P450 2B4.From (24)

The interaction of P450 and its redox partners is still not completely understood. From a crystal structure of rat NADPH-P450 reductase, it was apparent that there are three domains of the protein: the NADPH/flavin-adenine dinucleotide (FAD) binding domain in which the FAD moiety accepts electrons from NADPH, a linker domain, and a flavin mononucleotide (FMN) domain which interacts with P450s and is involved in electron transfer to the heme (25). The reductase is thought to interact with P450s through both electrostatic and van der Waals interactions as well as membrane anchoring topologies (Fig. 3) (24). Considering that this reductase has to provide electrons to all P450s located in the ER and there is not a conserved CPR binding region among P450s, the mechanism of interaction and electron transfer is of great interest.

1.2. P450 Interactions with Hydrogen Peroxide

1.2.1. Reactions with Iron and H_2O_2

Iron reacts readily with molecular oxygen and H_2O_2 to produce species capable of performing a diverse array of oxidation reactions. Known broadly as Fenton reactions (26), when this chemistry is uncontrolled it can generate a mixture of nonspecific products with organic reactants and is generally undesired in most biochemical systems (27). These are generally controlled *in vitro* by the addition of iron chelating reagents such as EDTA. P450s, as well as some other iron-centered enzymes (28), control the reaction of oxygen with iron in a stereospecific and regiospecific manner. These enzymes have varying efficiencies and are dependent on numerous factors. The iron-oxo reaction also allows for action on a varied number of substrates, because a general role in much of xenobiotic metabolism is to produce more hydrophilic compounds for facile excretion and also allows for so-called “secondary” metabolism of xenobiotics (e.g., sulfation and glucuronidation).

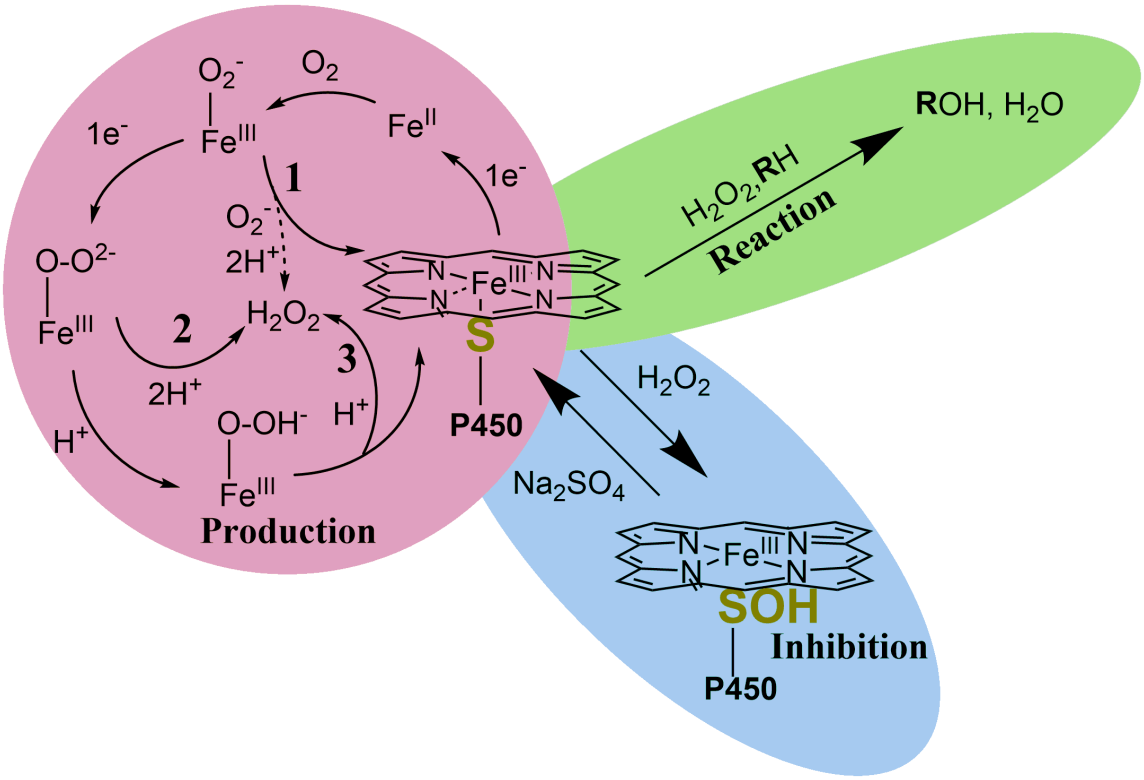

Figure 4. **P450 Production, Reaction, and Inhibition with H_2O_2.** P450s can produce H_2O_2 in three separate reactions after molecular oxygen binds to the ferrous heme (red circle, numbered reactions). H_2O_2 can also be used as a co-substrate and oxygen donor in peroxygenase and peroxidase reactions (green oval). Additionally, H_2O_2 can inhibit catalysis through sulfenylation of the heme-thiolate ligand (blue oval). From (29)

1.2.2. H_2O_2 Production Through Pathway Uncoupling

Since the report of Gillette *et al.* (30) on the NADPH-dependent production of H_2O_2 in liver microsomes, there has been interest in this area of study. Several years later, a stoichiometric anomaly observed between NADPH, oxygen consumption, and product formation in liver microsomes (31) was accounted for when H_2O_2 and H_2O production were measured as side products in P450 reactions (32,33). H_2O_2 production, plus the generation of superoxide anion by NADPH-P450 reductase (34) and P450 (35), led to the hypothesis that P450 induction may be related to hepatic disfunctions such as ethanol-induced liver damage (36-38). Uncoupling has been proposed to have potentially damaging circumstances by contributing to reactive oxygen species (ROS) production and to accelerating the aging process (39).

ROS production can, at least in principle, occur at three intermediate stages during the normal P450 catalytic cycle (Fig. 4). The first is directly after molecular oxygen binding to the ferrous heme (Fig. 4, Reaction **1**, dashed line). This has been described as the ferric superoxide complex, Fe^{III}-O_2^- (40). This state is only 1 kcal mol^{-1} above the heme resting state (Fe^{III}), and the oxygen-iron bond can easily be broken to form superoxide anion ($O_2^{\bullet-}$) and iron (III) heme (41). The rate of this process (Fe^{II} —> Fe^{III} + $O_2^{\bullet-}$), termed autoxidation, is related to the stability of the Fe^{II}-O_2 complex and varies among P450s (42), and the rate of autooxidation is dependent on temperature (43,44). Superoxide is quickly dismutated (non-enzymatically) to H_2O_2. Structural studies with $P450_{cam}$ have elucidated a coordination sphere surrounding the heme-thiolate ligand, which reduces the sulfur charge and allows for reduction to ferrous heme (45). This hydrogen bonding

network appears to fine-tune the positioning and electron donating ability of cysteine sulfur (46).

The second and third stages at which ROS can be produced, following the second reduction step, are from the P450 peroxo (Fe^{III}-O-O^{2-}) and hydroperoxo (Fe^{III}-O-OH^{-}) complexes ("Compound 0"). The Fe-O bond of the peroxo complex can be broken, and the oxygen species can be doubly protonated to form H_2O_2 (Fig. 4, Reaction **2**). In a similar fashion, after protonation the hydroperoxo complex can either be further protonated, forming Compound I (Fe^{IV}=O^{3+}) and H_2O, or the Fe-O bond can break, once again forming H_2O_2 (Fig. 4, Reaction **3).**

This uncoupling appears to be dependent on several factors, including pH, substrate positioning in the active site, and a disturbed substrate binding pocket. The heme thiolate allows for the correct amount of "push" and "pull" of electrons for the successful completion of the P450 catalytic cycle (47). Bacterial enzymes generally have very high coupling efficiencies for native substrates compared to mammalian P450s (Table 2). This difference in coupling efficiency may be due to the number of substrates mammalian P450s can accommodate compared to bacterial enzymes.

ROS generated by P450 from inefficient reaction cycles can, in principle, oxidize cellular proteins, lipids, and DNA. This alteration in cellular redox balance can lead to signaling involved in antioxidant responses, create an oxidatively stressed environment, and potentially lead to disease (48). Evidence has amassed for potential ROS-dependent toxicity involving P450s in the *CYP* Subfamilies 1, 2, 3, and 4 (39,49).

P450	Substrate	% coupling efficiency	Reference
1A1	Phenacetin	2.5	(50)
1A2	Methanol 7-Ethoxycoumarin Phenacetin	7.5 1.2 5.1	(50,51)
2A6	Coumarin	25	(52)
2B6	17-α-ethynylestradiol Efavirenz	48 42	(53)
2C9	*(S)*-flurbiprofen *(S)*-Warfarin	21 4	(54)
2D6	Bufuralol 3-Methoxyphenylethylamine 4-Methoxyphenylethylamine	39 43 42	(55,56)
2E1	*N*-Nitrosodimethylamine	5.6 and 59 (±*b5*)	(57)
2J2	Ebastine	2-17	(58)
3A4	Testosterone	10-16	(59)
4A11	Lauric acid	31	(60)
17A1	Progesterone 17*α*-Hydroxyprogesterone Pregnenolone 17*α*-Hydroxypregnenolone	22, 41 1.3, 10 97, 61 4,44	(61,62)
19A1	Androstenedione 19-Hydroxy androstenedione 19-Aldehyde androstenedione	5 34 33	(63)

Table 2. **Human P450: Coupling Efficiency (Product/NADPH Ratio)**

ROS-dependent toxicity originating from P450-mediated uncoupling has been difficult to establish *in vivo*. Many *in vitro* reconstituted, microsomal, mitochondrial, and cellular studies have provided evidence that induction of P450s can cause elevated ROS production (59,64-70). However, *in vivo* studies in rodents indicate that toxicity may stem from depletion of reducing pools found in cells, such as GSH and reduced pyridine nucleotides (NADPH and NADH) (71,72). Conversely, other studies indicate that P450s may have protective effects in the case of the P450 1A subfamily (73,74). A major unanswered question in this field is how much do P450s contribute to ROS production? Although much has been written about both topics, there are major issues. One is that much of the experimental work has been done in cell culture, often with the use of inappropriate cellular models (e.g., that do not normally express P450s), or ROS has been measured using inadequate methods (e.g., several fluorescent dyes (75-77).) A number of papers have touted P450s as a major source of ROS (78-80) although others do not consider this to be as important as mitochondrial leakage, NADPH oxidase, and other sources (81). *In vivo* work with both rats and mice, using F_2-isoprostane formation (82) (still accepted as the "gold standard" for measurement of oxidative stress (77)) showed that P450 induction elevated total tissue or urinary ROS only in the case of barbiturate induction, and that was at least in part due to an alteration in levels of pyridine nucleotides resulting from altered methyl transferase activity (71,72). However, other work done has shown that some localized changes (e.g., translocation of P450 2E1 to mitochondria and uncoupling there) may occur and be detrimental (64) (and these ROS changes were confirmed with isoprostane analysis). More *in vivo* studies will be needed to determine the contribution of P450s to proposed ROS-related toxicities (48).

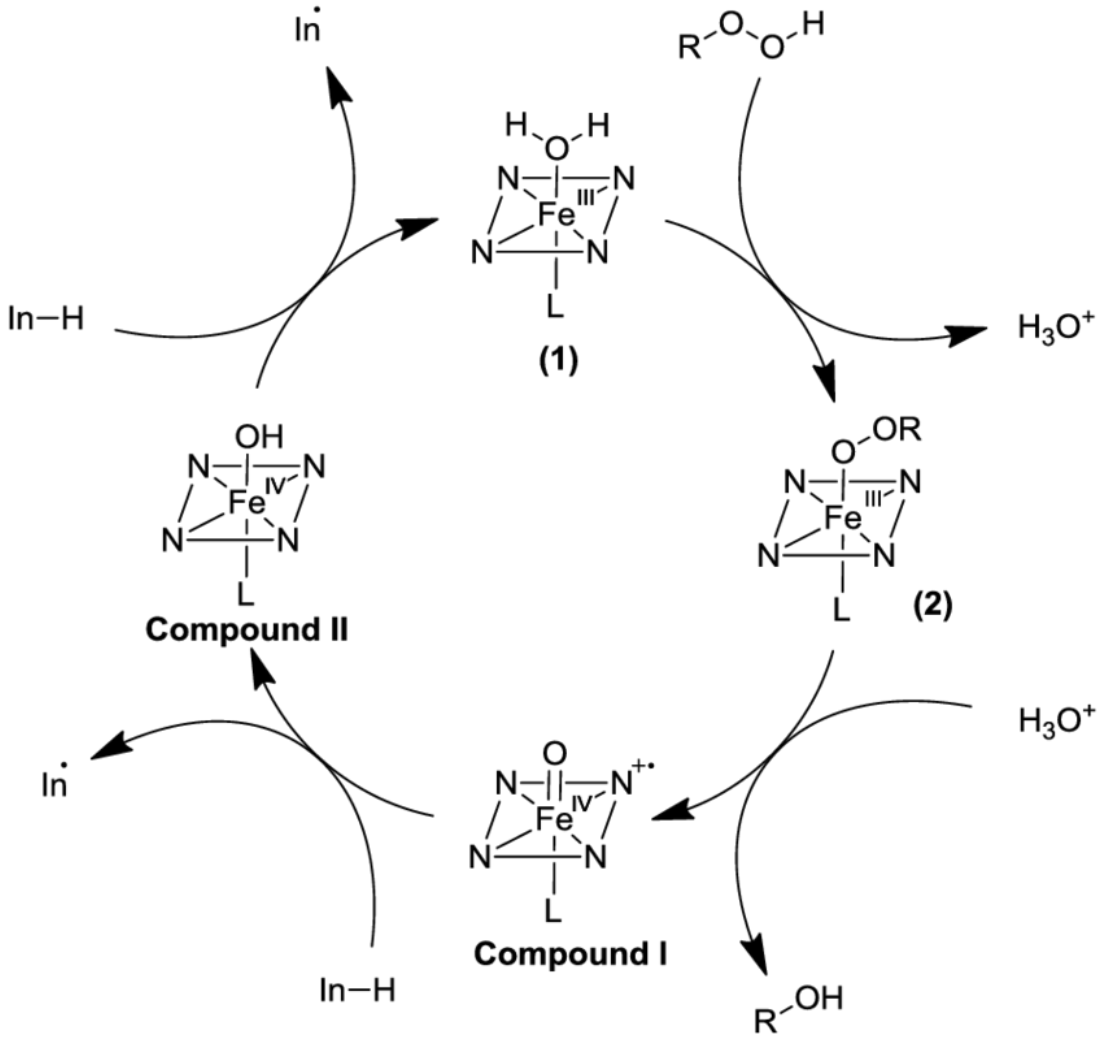

Figure 5. **Generalized Peroxidase Mechanism.** L is either a histidine ligand or cysteine. From (83).

1.2.3. H_2O_2 as a P450 Co-substrate

Reactions with H_2O_2 as the oxygen donor for P450 peroxygenase and peroxidase reactions are known (84,85). In these reactions, the ferric heme reacts directly with an oxygen of H_2O_2 or other hydroperoxide species and proceeds with heterolytic cleavage of the oxygen-oxygen bond to form Compound I (86). Other oxygen donating molecules ("oxygen surrogates") have been noted to have oxidation activity including iodosylbenzene (87) and sodium chlorite (88). Additionally, Rittle and Green used *m*-chloroperbenzoic acid as an oxygen surrogate for CYP119 to successfully isolate Compound I (89).

In the case of the peroxidase function of P450s, once Compound I is formed by either H_2O_2 or an organic hydroperoxide, a one-electron oxidation is performed on a substrate, resolving the porphyrin radical of Compound I to form Compound II (Fe^{IV}-OH) and a radical product. Compound II performs a subsequent one-electron reduction on another substrate generating ferric heme, water, and a second radical product (Fig. 5) (22). Mammalian P450s are known to act on endogenous hydroperoxide species, reducing them to their corresponding alcohols (90,91). This may be one of the metabolic mechanisms to reduce the levels of reactive hydroperoxides in cells.

P450s can also perform peroxygenase reactions in which the enzyme can catalyze monooxygenase reactions without the requirement for ferric iron reduction or redox partner proteins. Peroxygenase reactions are thought to react in a chemically similar way to the monooxygenase activity. Various hydroperoxide substrates have been explored in the oxidation of P450 substrates (92-95). This reactivity provides further evidence that P450s may utilize endogenous hydroperoxides as co-substrates *in vivo.* However, there

are many technological challenges to study this hypothesis including the need for highly sensitive detection methods and the inherent instability of hydroperoxides (96).

In mammalian P450s the reaction with H_2O_2 is generally very inefficient and is dependent on high concentrations of H_2O_2 that are well above estimated physiological concentrations, suggesting that this reaction does not occur *in vivo* (97). However, some bacterial enzymes are known to have fast catalytic rates and highly specific decarboxylation products of saturated fatty acids, e.g. $P450_{SP\alpha}$, $P450_{BS\beta}$ (98), and OleT (99-101). These enzymes and other bacterial P450s are highly stable in the presence of H_2O_2. P450 BM3 (102A1) has been an important enzyme in the study of peroxygenases, especially after engineering an increase in stability (102-104). Other bacterial enzymes have also shown high stability in the presence of H_2O_2 (105,106).

More recently, scientists have recognized the utility of peroxygenase reactions in the development of P450s as industrial biocatalysts (107,108). This industrial role has potential, and ongoing discovery and characterization of novel peroxygenase- and peroxidase-catalyzing P450s may lead to biocatalysts that produce useful products, e.g., biofuels and molecules that are difficult or expensive to synthesize.

1.2.4. H_2O_2 as a P450 Inhibitor

It has been known that H_2O_2 and other peroxides can inhibit P450 activity through heme degradation (109,110). Furthermore, this thesis focuses on the observation that incubation with H_2O_2 can also inhibit P450 by oxidizing the heme thiolate ligand to a sulfenic acid, thus inhibiting P450 catalysis (111,112). This phenomenon, first identified in human recombinant P450 4A11 (112), can affect other human P450 enzymes, as well as

other drug metabolizing enzymes. Spectral studies indicated that loss of the proximal heme ligand inhibited carbon monoxide binding and/or ferric heme iron reduction by NADPH-P450 reductase but can be reversed using a reducing agent, e.g., dithiothreitol (DTT), *tris*-(carboxyethyl)phosphine (TCEP), or sodium dithionite ($Na_2S_2O_4$). In these studies, human P450s 2D6, 2C8, 3A4, and 4A11 exhibited redox sensitivity and P450 1A2 was redox insensitive, suggesting that there is differential redox regulation among P450s (111). P450 1A2 was found to undergo extensive oxidation of one ancillary cysteine (Cys-159) that had no effect on catalysis. This was contrary to the case of P450 3A4, which showed an irreversible inhibition related to hyperoxidation of ancillary Cys-468. This may be reasonable, as Sevrioukova has recently reported a cysteine-depleted P450 3A4 enzyme with higher catalytic activity (113).

P450s 2D6, 2C8, and 4A11 behaved similarly both in inhibitory and spectral aspects (112). In anaerobic spectral studies, P450s in the presence of CO, NADPH-P450 reductase, and NADPH exhibited a maximal absorbance of 420 nm, indicating a 5-coordinate heme center. After the addition of dithionite, the typical 450 nm absorbance was observed. This change was interpreted as H_2O_2-dependent oxidation of the heme-thiolate ligand to a sulfenic acid which lost iron coordination. Dithionite was then able to reduce the sulfenic acid, allowing for re-liganding of the thiolate to the iron (Figure 6).

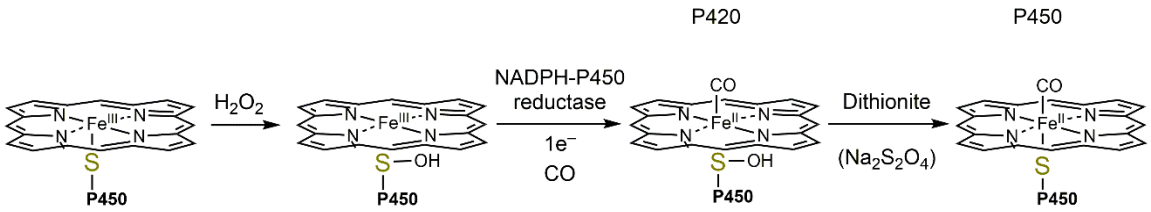

Figure 6. **Sulfenylation of the Heme-Thiolate Ligand.** The heme-thiolate cysteine is oxidized to a sulfenic acid. NADPH-P450 reductase cannot reduce the sulfenic acid, but can reduce the heme iron, allowing iron to bind CO and produce a 420 nm absorbance band. Adding dithionite reduces the sulfenic acid, allowing the thiolate to religand red shifting the absorbance band to 450 nm.

There have been multiple reports of variation in pharmacokinetics (PK) of drugs due to disease and/or inflammation (114). PK differences have been observed in celiac patients (which were reversed with treatment (115)) in which ROS levels are elevated, in untreated rheumatoid arthritis patients with extended verapamil half-lives compared to treated patients (116), and in P450 1A2 activity in patients with heart failure (117). Other reports highlighting a two- to five-fold change increase in the area under the curve (AUC) in P450 substrates has been reviewed in detail recently by Coutant and Hall (118,119). There is a strong link between autoimmune and inflammatory diseases to increased ROS production and also transcriptional downregulation of P450s (118-120). The redox sensitivity observed with some P450s may explain this variability, or at least contribute to it. Further testing in cellular and animal models is needed to confirm this, in that an alternate explanation is that the inflammation lowers overall levels of P450s at a pre-translational level or through other phenomena (121,122).

This inhibition may function as a sensor where P450s are switched off when there is a high oxidizing environment and a low amount of NADPH may be present. The reducing equivalents of NADPH and/or NADH may be required to perform functions critical for life such as reversing glutathionylated glyceraldehyde-phosphate dehydrogenase (GAPDH) (123) or maintaining general redox homeostasis (124-126). This may also be a negative feedback loop in place to limit uncoupling and further H_2O_2 production. Interestingly, in 1971 Hrycay and O'Brien hypothesized that heme-thiolate sulfenylation could occur and that modified P450s would preferentially catalyze peroxidase reactions over monooxygenase reactions (110). This hypothesis requires further testing, however

switching the P450 oxygen donor to H_2O_2 and reducing the need for electrons from a redox partner could be beneficial in times of ROS stress.

1.3. H_2O_2 in Signaling

In recent years H_2O_2 has been recognized as an important secondary signaling molecule, and several laboratories have characterized redox sensitive enzymes (127,128). ROS have been shown to react specifically with several amino acids, but the sulfur-containing residues cysteine and methionine are the most susceptible to oxidation. The first step of cysteine oxidation by H_2O_2 is formation of a sulfenic acid (-SOH), initially characterized as an anthraquinone-sulfenic acid by Fries (129) and later by Bruice (130). This oxidation can occur at rates between 10^{-1} M^{-1} s^{-1} (GSH) and 10^{8} M^{-1} s^{-1} (peroxiredoxin) (128) (Fig. 7). This large variation in reactivity is due at least in part to the pK_a of the particular oxidized cysteine. Sulfenic acids are reactive species and readily react with free thiols to form disulfide bonds through a dehydration reaction or through a sulfenamide intermediate (131). This is thought to be the general mechanism of physiological disulfide bond formation (Fig. 7). The reaction can occur in an intra- or intermolecular fashion with free thiols (including GSH) and can be reversed by an NADPH-dependent reaction catalyzed by glutaredoxin (132). Sulfenic acids can be further oxidized to dioxidation (sulfinic acid, SO_2^-) and trioxidation products (sulfonic acid, SO_3^-), which are mostly irreversible and induce protein degradation and cellular stress responses (Fig. 1) (133).

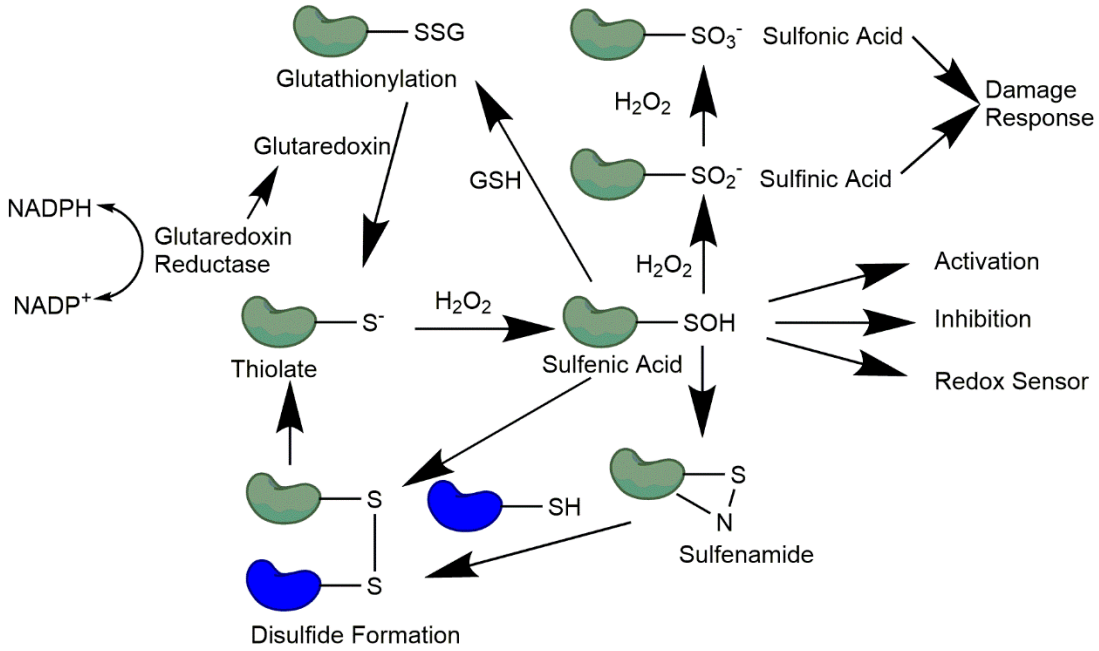

Figure 7. **General Redox Cycle of Protein Thiols.** In the presence of H_2O_2, thiols can be oxidized to sulfenic acids, which may elicit a physiological response. Sulfenic acids can then form disulfide bonds, which can be reduced to free thiols. Sulfenic acids can also be further oxidized to sulfinic or sulfonic acids, which can trigger cellular damage responses. From (29)

Oxidative regulation of cysteines in proteins have been known for quite some time. Evidence of oxidative inhibition of GAPDH (134) and papain (135) led to an interest in the field (136). After researchers determined conditions to promote the stability of sulfenic acids, they could be studied in a more systematic fashion (137-139). Recently, mechanisms of stability and function have been elucidated. In the case of epidermal growth factor receptor (EGFR), a sulfenic acid is formed in the kinase domain of the protein (Cys-797) in an H_2O_2-dependent fashion, causing autophosphorylation and activating the EGFR signaling cascade in an EGF-independent manner. This sulfenic acid is stabilized by a hydrogen bond with Arg-841, which, when mutated confers resistance to oxidative activation (140). Additionally, tyrosine phosphoprotein phosphatase 1B (PTP1B) (141), GAPDH (123), Kelch-like ECH-associated protein-1 (Keap1) (142,143), P450s (111,112), and many others (144) have been found to be regulated by sulfenic acid formation. Methods for detecting and analyzing cysteine oxidation have remained challenging, but recent advances in chemical trapping methods and in our understanding of redox biology provide promising new ways to elucidate redox functions of cysteines (145,146).

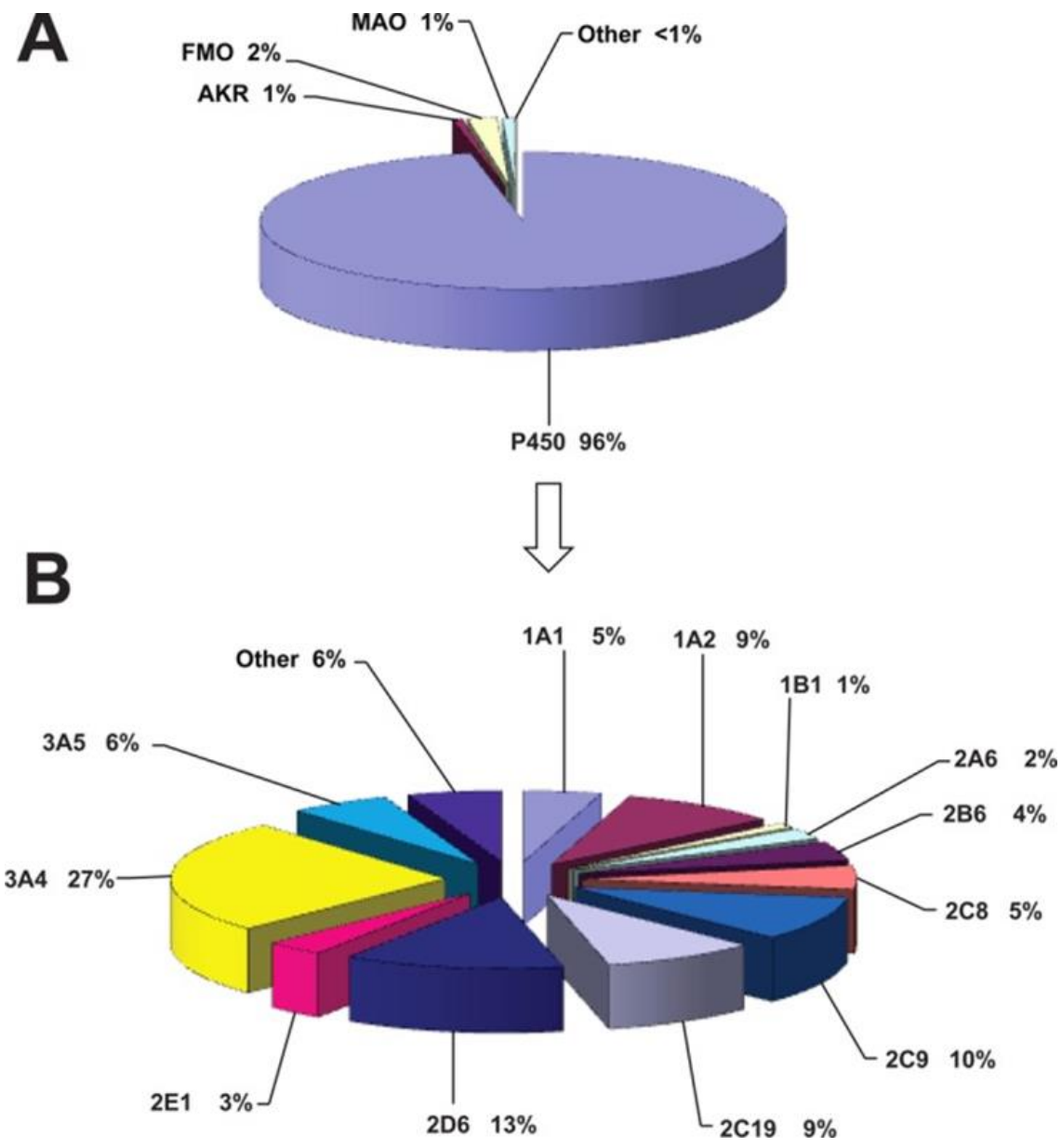

Figure 8. **Drug Metabolism Enzyme Contribution.** (A) Human oxidoreductases participating in the metabolism of drugs. (B) Human P450 enzymes in the metabolism of drugs. From (17)

1.4. P450 Posttranslational Regulation

There is extensive knowledge on the transcriptional regulation of P450s, but knowledge of the posttranslational regulation of P450 enzymes is limited (147). P450 transcriptional induction by xenobiotics such as barbiturates and polyaromatic hydrocarbons has been studied extensively because this upregulation potentially effects drug-drug interactions and pharmacokinetic profiles of administered drugs (148).

The study of posttranslational regulation of P450 enzymes has not been fully evaluated. Several studies have assessed P450 phosphorylation but is not a field that has garnered much attention. Of the phosphorylation sites identified, they have been characterized as inhibitory either directly or as phosphodegrons involved in the ER-associated degradation (ERAD) pathway (149-151).

1.5. Specific P450 Enzymes Studied in this Thesis

1.5.1. Rationale

The redox sensitivity of P450 enzymes was first observed by the laboratory of Jorge Capdevila and Donghak Kim performed initial investigations in the redox sensitivity of P450 4A11. P450 4A11 was chosen because this was the first enzyme where the response was seen. P450s 1A2, 2C8, 2D6, and 3A4 were selected for three reasons: (1) these enzymes have been expressed and purified in this laboratory with established protocols to monitor and assess modulations in enzymatic catalysis, (2) these four subfamilies of P450 are diverse in substrate recognition and major contributors to drug metabolism (Fig. 8), and (3) the data indicate that these enzymes have different responses to oxidation which is notable for discerning the mechanism of action.

1.5.2. P450 1A2

P450 1A2 makes up a considerable amount of the total P450 in microsomes with approximately 10% of total P450 content (152). Known inducers include polyaromatic hydrocarbons (which are also substrates that can be bioactivated to carcinogens) and cruciferous vegetables. Some xenobiotic substrates for P450 1A2 are acetaminophen, phenacetin, caffeine, and theophylline among many others (153).

1.5.3. P450 2C8

This enzyme is not as well-known as a drug metabolizing enzyme but is closely related to 2C9 and 2C19 which are both major metabolizers of xenobiotics. P450 2C8 is involved in the metabolism of taxol and the production of epoxyeicosatrienoic acids (EETs) from arachidonic acid. P450 2C8 is mostly expressed in the liver and kidney but is also found in many other tissues. P450 2C8 was found to be a cause of the withdrawal of the HMG-CoA inhibitor cerivastatin due to a drug-drug interaction with gemfibrozil which caused rhabdomyolysis (154).

1.5.4. P450 2D6

P450 2D6 is a very important enzyme for drug metabolism. To date there are over 160 variants (www.pharmvar.org) with varying abilities to catalyze metabolism of drugs. P450 2D6 is known to metabolize opioids, debrisoquine, and many others. During drug development, scientists try to design therapeutics that are not metabolized by P450 2D6 due to this high variability.

1.5.5. P450 3A4

P450 3A4 is the most abundant human P450 in the liver and is the major metabolizer of xenobiotics. P450 3A4 is involved in the metabolism of more than 50% of

all small molecule drugs developed in the last ten years (18). This enzyme has a very large substrate binding pocket (>1300 $Å^3$) that can facilitate many substrates (155). Because of this substrate promiscuity, there is large concern for possible drug-drug interactions that may cause toxicity. P450 3A4 is the main target of inhibition by molecular components in grapefruit juice, which leads to the recommendation for avoidance of the fruit when taking certain medications (156).

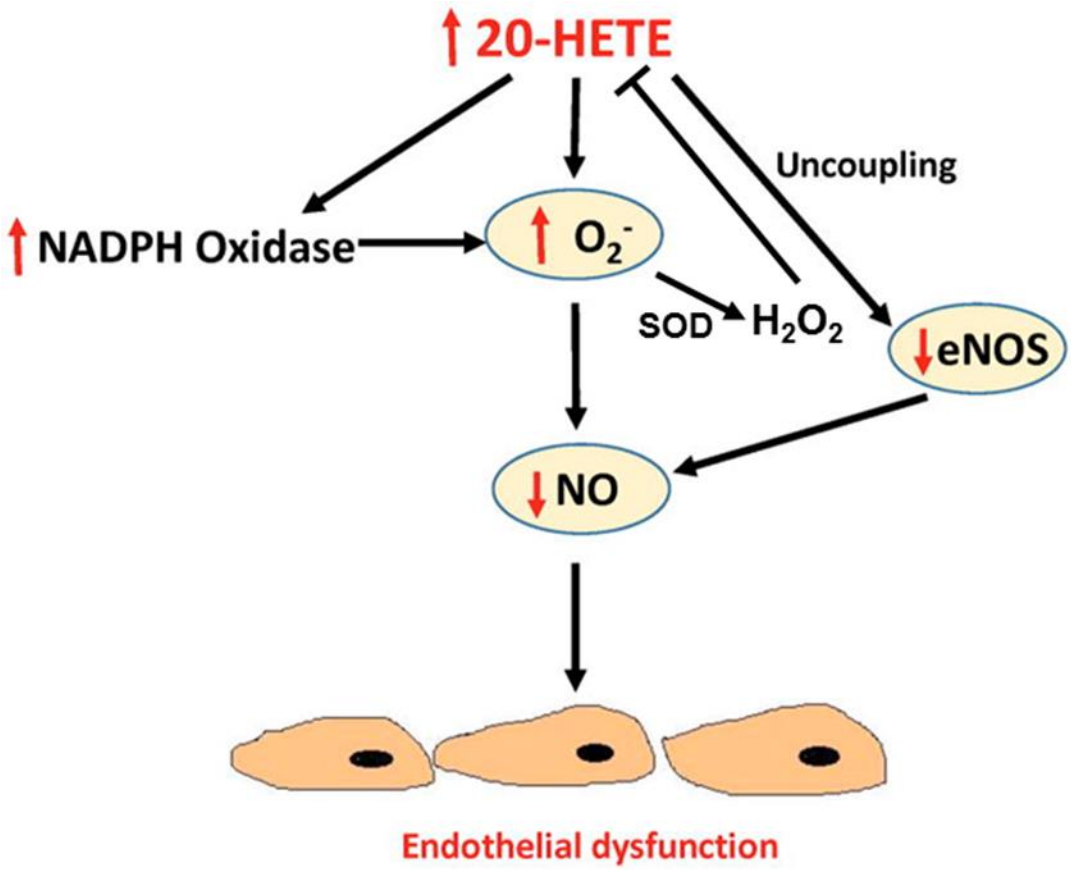

Figure 9. **20-HETE Contributes to Endothelial Dysfunction.** 20-HETE increases NADPH-oxidase function and uncouples nitric oxide synthase contributing to endothelial dysfunction. Superoxide produced dismutates to H_2O_2 which inhibits P450 4A11, reducing 20-HETE production in a putative negative feedback fashion. Adapted From (157)

1.5.6. P450 4A11

At least 13 human P450 enzymes (2C8, 2C9, 2J2, 2U1, 4A11, 4F22, 4F12, 4V2, 4F2, 4F3, 4F8, 5A1, and 8A1) utilize fatty acids and/or eicosanoids as substrates (9). P450 4A11 is primarily an *ω*-hydroxylase, with its main endogenous role apparently being the conversion of arachidonic acid to 20-hydroxyeicosatetraenoic acid (20-HETE) (158). P450 4A11 can also catalyze oxidations of other fatty acid substrates, including lauric acid (60):

$$CH_3(CH_2)_nCO_2H \text{ —> } HOCH_2(CH_2)_nCO_2H$$

P450 4A11 is expressed mainly in the liver, kidney, and vasculature (159,160), and Subfamily 4A P450 enzymes have been associated with vascular dysfunction and hypertension in rodent models and humans (161). The P450 4A11 F434S variant has been associated with increased blood pressure in several populations studied (162-167). 20-HETE plays opposing roles, having both pro- and anti-hypertensive actions by promoting vasoconstriction or natriuresis, respectively (168). 20-HETE has been reported to induce transcription of NADPH oxidase, activating this enzyme complex through protein kinase C (169-172), has been reported to increase mitochondrial reactive oxygen species (ROS) production (173), and is implicated in nitric oxide synthase uncoupling (157). It follows then, that the oxidative inhibition of P450 4A11 described in this thesis might act as a negative feedback loop to limit 20-HETE production (Fig. 9). Studies with P450 4A11 transgenic mice have identified P450 4A11 regulation via fasting and growth hormone (174) and that 20-HETE and P450 4A11 activity may uncouple the renal renin angiotensin system (175).

1.6. Research Aims

My dissertation research focuses on discerning the mechanism of redox dependent modulation of P450 activity. In this introduction I have tried to highlight the complex relationship between cytochrome P450 enzymes and H_2O_2. This redox relationship has been studied in some form or another for the last fifty years. Despite this effort, no one has reported the phenomenon of thiol redox-mediated activity modulation of P450s to my knowledge.

One of the more important questions is how would oxidation of some P450 enzymes confer a biological advantage through heme-thiolate sulfenylation? There are currently several hypotheses postulated:

(1) Limitation of futile cycling. Without substrate present P450 enzymes are still able to be reduced allowing the ferrous heme to bind oxygen. The activated oxygen will likely be released as superoxide if no substrate is present. The heme-thiolate ligand provides sufficient electronegativity to allow for this binding. It follows then, that the lack of this fifth ligand would prevent oxygen binding. This could be beneficial for the cell because it limits oxygen and NADPH consumption while reducing the amount of harmful ROS produced.

(2) Inactivation during an oxidative insult. In times of oxidative stress, cells require reducing equivalents in the forms of GSH and NAD(P)H to counteract and survive the stress. P450s that are mainly xenobiotic metabolizing enzymes (e.g. P450s 3A4 and 2D6) are not necessary for survival and can therefore be inactivated until the redox environment reaches homeostasis. This would allow NADPH to be diverted to enzymes devoted to combating oxidative stress, e.g. glutathione reductase and thioredoxin reductase.

(3) Oxidative modification as a degradation signal. Oxidation of cysteine thiols has been shown to signal proteins for degradation. This is likely a protective mechanism as oxidation can modify other amino acids, inactivating proteins. Since cysteines are the most easily oxidized amino acids in proteins, this process serves as a chemosensor for damage. Downregulation of P450s due as response to inflammation has been reported (118). Oxidation of thiols of P450s may be an acute response to inflammatory insults. With the goal of removing (in)active P450 enzyme before P450 genes are transcriptionally downregulated.

(4) Another reason for this modification would be the one originally proposed by Hrycay and O'Brien (110). They postulated that formation of a sulfenic acid on the heme-thiolate ligand would alter the spin state of the heme, allowing the enzyme to more easily catalyze peroxidatic reaction with H_2O_2 being a co-substrate, donating oxygen. This could be possible because P450 enzymes can utilize oxygen from peroxides and peracids as co-substrates. During oxidative stress events, highly reactive lipid peroxides and isoprostanes are produced. This P450 sulfenylation may allow for more facile metabolism of these damaging oxidative byproducts.

When I commenced work on this project, the original scope was centered around P450 4A11. This study involved specifically looking at redox sensitivity of the enzyme and then elucidating differences between single nucleotide variants of P450 4A11 with respect to blood pressure regulation. After the observation that other P450s are regulated in a similar fashion, the decision was made to pursue the mechanism behind this further.

My aims became centered around the hypothesis that P450 enzymes are (1) redox regulated and (2) this regulation is protective for the organism. To test the first part of this

hypothesis, I developed chemoproteomic and spectroscopic methods that were coupled with activity assays specific for each P450 tested. Selectively labeling sulfenic acids followed by LC-MS/MS quantitative analysis and verifying cysteine-heme ligandability spectroscopically proved to be a powerful technique that is outlined in Chapter II.

These techniques were first applied to P450 4A11. As this was the first enzyme discovered to have redox sensitivity, the resulting IC_{50} of ~140 μM for H_2O_2 preincubation was the lowest observed to date. This loss of activity correlated with heme-thiolate sulfenic acid formation in a H_2O_2 concentration-dependent manner. I was able to verify this correlation with spectroscopic techniques. Heme-thiolate sulfenylation of P450 4A11 was also observed in mouse liver and kidney microsomes via LC-MS/MS analysis. This work is further outlined in Chapter III.

The proteomic data obtained from the mouse liver and kidney microsomes mentioned above was acquired using a data-dependent analysis (DDA) “shotgun” approach and, interestingly, many other mouse P450s as well as other drug metabolizing enzymes showed evidence of heme-thiolate sulfenylation. Based on this data, I hypothesized that other human P450s are also redox sensitive. I repeated the microsome labeling experiment with human liver and kidney microsomes which showed evidence of sulfenylation of P450s and other enzymes. I tested other P450s for heme-thiolate sulfenylation as described previously and was able to classify P450s tested into three redox classes: (1) heme-thiolate sensitive (2) insensitive and (3) ancillary cysteine sensitive. This work is described in Chapter IV.

Chapter II

2. Techniques and Methods

2.1. Introduction

The analytical techniques developed during my thesis work allowed me to answer the questions posed and test proposed hypotheses efficiently. With that in mind, the optimized techniques utilized in Chapters III and IV are included here for reference. For methods that were challenging to develop and novel, a brief rationale is included to explain the reason

2.2. Chemical Synthesis

2.2.1. Rationale

Both the isotope-coded dimedone iododimedone labeling and iodoacetanilide alkylation methodologies and synthesis have previously been reported (176,177). Isotopically labeled iodoacetanilide was selected because of the ease of synthesis and the mass difference of 5 Da between the two molecules provided sufficient *m/z* separation between multiply charged peptide species (M + 2H, M + 3H, M+ 4H).

2.2.2. Iododimedone

Iododimedone was prepared from dimedone (4 mmol scale) by iodination with *N*-iodosuccinimide (178): Yield 48%, mp 145-146 °C; high resolution mass spectrometry (HRMS) for $C_8H_{12}O_2I$ *m/z* 266.9882 (MH^+), found 266.9881 (Δ 0.4 ppm); ^{1}H-NMR (400 MHz, $CDCl_3$) δ 1.04 (s, 6H, $(CH_3)_2$), 2.50 (d (splitting due to I), 4H, CH_2), 6.35 (s, 1H, CHI) (literature mp 155 °C (179)).

2.2.3. d_6-Dimedone

A modification of the basic procedure of Yeo and Carroll (177) was used. Diethyl malonate and mesityl-d_{10}-oxide were condensed in an ethanolic solution of $NaOC_2H_5$ under reflux, followed by decarboxylation with NaOH under reflux. After neutralization the filtrate was collected and extracted into ethyl acetate. The product was concentrated by partial removal of solvent *in vacuo* and trituration with hexanes to yield crystalline d_6-dimedone in 85% yield: mp 147-148 °C; HRMS for $C_8H_7D_6O_2$ *m/z* 147.1292 (MH^+), obs 147.1284 (Δ 5.4 ppm); ^{1}H-NMR (400 MHz, $CDCl_3$) δ 2.52 (s, 5H, -CH_2-), 3.33 (s, 2H, CO-CH_2-CO) (180) (lit mp 145-147 °C (180)).

2.2.4. d_0-Iodoacetanilide

Iodoacetanilide was prepared from iodoacetic acid (2.53 mmol, 470 mg) and aniline (2.53 mmol, 235 mg) by amide coupling with dicyclohexylcarbodiimide (2.53 mmol, 522 mg) (176): yield 70%, ^{1}H-NMR (600 MHz, acetone-d_6) δ 9.51 (bs, 1H, NH) 7.64 (d, 2H, *o*-Ar), 7.31 (t, 2H, *m*-Ar), 7.02 (t, 1H, *p*-Ar), 3.90 (s, 2H, CH_2I), ^{13}C-NMR (150 MHz, acetone-d_6) 167.0, 140.1, 129.7, 124.6, 120.0, 0.72.

2.2.5. d_5-Iodoacetanilide

d_5-Iodoacetanilide was prepared from iodoacetic acid (2.53 mmol, 470 mg) and d_5-aniline (2.53 mmol, 248 mg) by amide coupling with dicyclohexylcarbodiimide (2.53 mmol, 522 mg) (176): yield 89%, ^{1}H-NMR (600 MHz, acetone-d_6) δ 9.53 (bs, 1H, NH), 3.90 (s, 2H, CH_2I), ^{13}C-NMR (150 MHz, acetone-d_6) 167.0, 139.8, 129.1, 124.1, 119.6, 0.75.

2.3. Expression and Purification of Human Cytochrome P450 Enzymes

Human P450 4A11 (wild-type and F434S, C52S, C85S, C199S, C255S, and C512S mutants) was expressed and purified as described previously by Donghak Kim

(60,181). *Escherichia coli* recombinant rat NADPH-P450 reductase and human liver cytochrome b_5 (b_5) were prepared as described by Hanna et al. (182) and Guengerich (183), respectively.

Human P450s 1A2 (184), 2C8 (185), 2D6 (186), and 3A4 (187) (all with C-terminal $(His)_6$ tags) were expressed and purified. *E. coli* recombinant rat NADPH-P450 reductase and human liver b_5 were prepared as described by Hanna *et al*. (182) and Guengerich (183), respectively.

2.4. Cloning of P450 4A11

Site-Directed Mutagenesis—P450 4A11 was subcloned into a pBlueScript vector to preform site-directed mutagenesis. Residues from each site were converted to serine by using the QuikChange II Site-Directed Mutagenesis Kit (Agilent Technologies). The resulting plasmids were sequenced to confirm successful mutation and subcloned into a pCW expression vector.

2.5. Tissue Samples

2.5.1. Mouse Tissue

All experiments using mice were conducted with approved protocols by the Institutional Animal Care and Use Committee of Vanderbilt University and in accordance with the NIH Guide for the Care and Use of Laboratory animals. 129/Sv mice carrying one copy of the human P450 4A11 gene (*CYP4A11*) (under control of its native promoter were generated as previously described (175)) were provided normal chow diet (Purina Laboratory Rodent 5001; St. Louis, MO) with free access to water and were housed in an Association for the Assessment and Accreditation of Laboratory Animal Care (AAALAC)-accredited, temperature-controlled facility with a 12 h light–dark cycle. All

studies were conducted in mice aged 6-28 weeks of age. *CYP4A11* transgenic mice were crossed with pure Sv129 wild type mice and offspring were genotyped for the presence of a single copy of the human *CYP411* gene as previously described (175). Organs were collected from male transgenic mice immediately after sacrifice and used for microsomal preparations as described below.

2.5.2. Human Tissue

Tissues were collected and stored by the Vanderbilt University Medical Center Tissue Repository using Cooperative Human Tissue Network (CHTN) approved standard operating procedures, under a waiver of consent and anonymized. After collection, areas of necrosis or cauterized areas were removed and then sectioned into normal and tumor tissue. A representative section of each tissue type and/or disease type was fixed in formalin and processed, and a hematoxylin and eosin stained section was obtained and reviewed by a board-certified pathologist to ensure sample integrity and usefulness in research. Kidney and liver samples (five each, collected within one year of analysis, decoded) used for this study were snap-frozen in liquid nitrogen and stored at -80 °C.

2.6. Kinetic Assays

2.6.1. P450 4A11

Assays were done as described previously (60) with minor changes. Typical incubations included 0.2 *μ*M P450 4A11, 0.4 *μ*M NADPH-P450 reductase, 0.4 *μ*M b_5, 150 *μ*M L-*α*-dilauroyl-*sn*-glycero-3-phosphocholine (DLPC, Sigma Aldrich), 100 mM potassium phosphate buffer (pH 7.4), and the indicated concentration of lauric acid ([1-^{14}C]-lauric acid, usually added as an aqueous 10 mM stock solution of sodium laurate) in a final volume of 0.25 ml. b_5 was included because it stimulates the catalytic activity (60).

Following temperature equilibration to 37 °C for 5 min, reactions were initiated by the addition of an NADPH-regenerating system consisting of 0.5 mM $NADP^+$, 10 mM glucose 6-phosphate, and 1 IU ml^{-1} yeast glucose 6-phosphate dehydrogenase (188). Reactions generally proceeded at 37 °C for 2 min and were terminated with 1.0 ml of ethyl acetate containing 0.1% CH_3CO_2H (v/v) and, following mixing with a vortex device, the mixtures were centrifuged ($10^3 \times g$ for 10 min). A 0.8 ml aliquot of the ethyl acetate layer (upper phase) was transferred to a clean tube, and the solvent was removed under an N_2 stream.

The dried extracts were dissolved in 200 μl of 1:1 mixture of H_2O:CH_3CN containing 0.1% CH_3CO_2H (v/v) and 10 μM butylated hydroxytoluene, and aliquots were analyzed on a reversed-phase (octadecylsilane, C_{18}) HPLC column (5 μm, 2.1 mm × 100 mm (Waters, Milford, MA)) coupled with a radioactivity detector (IN/US Systems β-RAM, Tampa, FL). Reaction products and substrate were eluted at a flow rate of 0.6 ml min^{-1} using an increasing linear gradient of CH_3CN (including 0.1% (v/v) HCO_2H) from 35 to 95% (v/v) over 30 min.

2.6.2. Other P450s

Assays with P450s other than P450 4A11 were performed as described previously, with the modification of either preincubation with DTT (1 mM) for 10 min or not (the DTT remained in the reactions): P450 2C8–paclitaxel as substrate (189), P450 2C9—tolbutamide as substrate (190), P450 2D6—bufuralol as substrate (186), P450 3A4—nifedipine as substrate (191), P450 19A1—testosterone as substrate (63), P450 21A2—progesterone as substrate (192), P450 2A6—coumarin as substrate (52), and P450s 1B1, 1A1, and 1A2–7-ethoxyresorufin as substrate (193).

Assays with P450s were performed as described previously with P450 2C8–paclitaxel as substrate (185,189), P450 2D6—dextromethorphan as substrate (186,194), P450 3A4—testosterone as substrate (191), and P450 1A2—phenacetin as substrate (193). b_5 was only used in the P450 3A4 incubations.

2.7. Protein Oxidation

2.7.1. Rationale

Optimizing conditions for sufficient oxidation was determined empirically. Considering that P450s require oxygen for catalysis, oxidation of the protein by H_2O_2 could not be done in a completely anaerobic environment which is ideal when determining concentration-dependent effects of oxidation. To overcome this, protein was oxidized initially in an anaerobic environment and, instead of removing H_2O_2 via buffer exchange, catalase was added in excess to remove H_2O_2. For activity assays, P450 was diluted in buffer that was not anaerobic to ensure sufficient oxygenation for the catalytic reaction.

Dilution of the P450 to 500 nM during oxidation was required to obtain a reproducible inhibition.

2.7.2. Method

Purified recombinant P450 (0.4 ml of a 10 μM stock solution, stored at -80 °C in 50 mM potassium phosphate buffer (pH 7.4) containing 20% glycerol, 1 mM DTT, and 0.1 mM EDTA) was thawed on ice and reduced for 30 minutes by the addition of 1 mM TCEP at 4 °C. A Zeba Spin Desalting Column (Thermo) pre-equilibrated with “oxidation buffer” (100 mM potassium phosphate buffer (pH 7.4) containing 0.1 mM EDTA and sparged with Ar) was used to remove reducing agents. Reduced protein was then diluted to a concentration of 500 nM using oxidation buffer. Aliquots were treated with varying

amounts of H_2O_2 or TCEP. Aliquots for the activity assay (175 pmol, described above) were incubated with H_2O_2 or TCEP for 15 minutes at 37 °C. Human erythrocyte catalase (10 units, Sigma, catalog #C3556) was added and incubations proceeded at 23 °C for 5 minutes to remove H_2O_2. These samples were used to measure catalytic activity as described above.

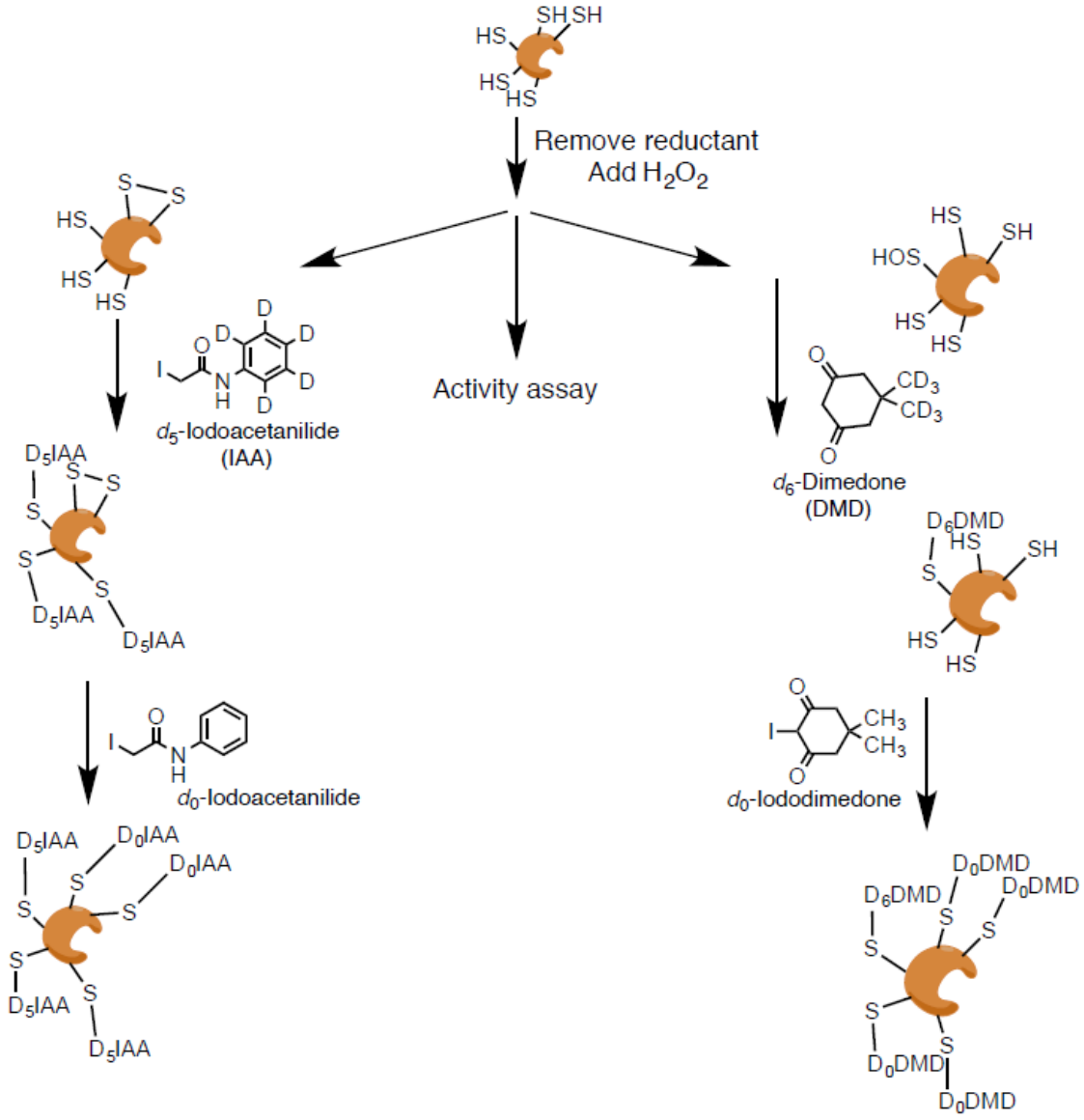

Figure 10. **Scheme for Analysis of Sulfenic Acids and Disulfides of P450 Enzymes.**

2.8. Chemical Proteomic Labeling Techniques

2.8.1. Rationale

Chemical proteomic labeling can be visualized in Figure 10. These chemical labeling techniques required multiple iterations of optimization to prove effective. For isotope-coded dimedone/iododimedone (ICDID) labeling, the rate of alkylation for dimedone with sulfenic acid is ~20 M^{-1} s^{-1}, which is very slow. A 10,000-fold molar excess of dimedone co-incubated with oxidant (H_2O_2) for 2 hours with the target protein is required to achieve sufficient labeling as determined empirically. Labeling may also be slowed due to solvent accessibility of the target cysteine. Newer reagents have been synthesized recently that are more efficient at alkylating sulfenic acids (195). ICDID labeling was selected because it was the most straightforward method to measure relative sulfenylation of cysteines over a variety of peroxide concentrations.

Isotope-coded affinity tag (ICAT) labeling with iodoacetanilide for disulfide bond determination also proved to be challenging. If left at a neutral pH, disulfide bonds tend to rearrange readily and quickly (196). There are two strategies to avoid this: (1) acidification to protonate all free thiols and denature and precipitate protein or (2) rapid alkylation. A hybrid approach was used to take advantage of both strategies. Acidification with trichloroacetic acid (TCA) allowed for the rapid quenching of thiols and subsequent precipitation of proteins. Resuspension of the protein precipitate in pH 8 buffer with SDS and “heavy” alkylating agent exposes all free thiols for fast alkylation. Reprecipitation of the protein removes the “heavy” reagent. Subsequent resuspension in reducing agent and the “light” alkylating agent alkylates the remaining thiols presumably in disulfide bonds.

Precipitating protein twice reduced alkylated protein yields, however, using recombinant protein ensures sufficient amounts of starting protein.

After chemoproteomic labeling was complete (either ICDID or ICAT) samples were loaded on onto an SDS-PAGE gel to remove reagents. This process allowed for separation of aggregated and multimeric protein by band excision of the monomeric protein band. Coomassie Brilliant Blue R staining of the gel provided an estimate of protein recovery in relation to a loading control lane.

2.8.2. ICDID Labeling for Sulfenic Acid Identification

Additional aliquots of oxidized protein (100 pmol) were incubated with 5 mM d_6-dimedone (from a 50 mM stock suspended in 100 mM sodium 3-[4-(2-hydroxyethyl)-1-piperazinyl]propanesulfonate (HEPPS) buffer (pH 8.0) containing 5% NaCl (w/v)) for 2 hours at 37 °C. Trichloroacetic acid was then added to a final concentration of 10% (w/v) and the samples were incubated on ice for 15 minutes. The enzymes in the samples were pelleted by centrifugation (12,000 $\times$ *g,* 15 min, 4 °C). The supernatant was removed from each sample, and the pellet was washed with ice cold CH_3CN. The pellet was resuspended in 20 μl of 100 mM HEPPS buffer (pH 8.0) containing 2% (w/v) SDS and 1 mM TCEP, and reduction proceeded for 30 minutes at 37 °C. (d_0)-Iododimedone (100 mM, in DMSO) was added to a final concentration of 10 mM, and incubation was done at 23 °C in the dark for 30 minutes. Samples were subjected to SDS-polyacrylamide gel electrophoresis (10% Bis-Tris, NuPAGE, Invitrogen) separation and stained with SimplyBlue SafeStain (Invitrogen). The M_r region corresponding to each P450 was excised, digested with trypsin (8 ng/μl) for 16 hours in 25 mM NH_4HCO_3 buffer (pH 7.8) at 37 °C, and subjected to LC-MS/MS analysis.

2.8.3. ICAT Labeling for Disulfide Bond Identification

Additional aliquots of reduced, buffer exchanged protein (from above, 100 pmol) were incubated with H_2O_2 or TCEP for 15 minutes. Human erythrocyte catalase (10 units) was added and incubations proceeded at 23 °C for 5 minutes to remove H_2O_2. Trichloroacetic acid was then added to a final concentration of 10% (v/v) and the samples were incubated on ice for 15 minutes. The enzymes in the samples were pelleted by centrifugation (12,000 × *g,* 15 min, 4 °C). The supernatant was removed from each sample, and the pellet was washed with ice cold CH_3CN. The pellet was resuspended in 50 μl of 100 mM HEPPS buffer (pH 8.0) containing 2% (w/v) SDS and 10 mM d_5-iodoacetanilide, and alkylation proceeded for 30 minutes at 23 °C, shaking in the dark. Protein was precipitated again using the same method as above to remove heavy reagent. The pellet was resuspended in 20 μl of 100 mM HEPPS buffer (pH 8.0) containing 2% (w/v) SDS and 1 mM TCEP, and reduction proceeded for 30 minutes at 50 °C. d_0-Iodoacetanilide (100 mM, in acetone) was added to a final concentration of 10 mM, and incubation was done at 23 °C in the dark for 30 minutes, shaking. Samples were subjected to SDS-PAGE (10% Bis-Tris, NuPAGE, Invitrogen) separation and stained with SimplyBlue SafeStain (Invitrogen). The M_r region corresponding to P450 4A11 was excised, digested with trypsin (8 ng/μl) for 16 hours in 25 mM NH_4HCO_3 buffer (pH 7.8) at 37 °C and subjected to LC-MS/MS analysis.

2.9. Preparation of Microsomes

2.9.1. Rationale

When analyzing specific proteins in a complex mixture, an enrichment strategy is optimal. To enrich for ER proteins, microsomes were prepared by differential centrifugation followed by SDS-PAGE separation. Since P450s are all approximately 50 kDa in molecular weight, excising the "P450 region" from the gel provided sufficient enrichment to quantify dimedone-labeled (sulfenylated) peptides. Mouse microsomes were digested with chymotrypsin to produce peptides unique to the heme-thiolate containing peptide sequence in 4a/4A enzymes (Fig. 11).

2.9.2. Microsomal Preparation

Microsomes from human and mouse tissues were prepared with slight modifications of published methods (188). For ICDID labeling studies, Buffer A (0.10 M Tris-acetate buffer (pH 7.4) containing 0.10 M KCl, 1.0 mM EDTA, and 20 μM butylated hydroxytoluene) was sparged with Ar before use. Tissue samples were homogenized in buffer A using a Teflon®-glass Potter-Elvehjem device and centrifuged at $10^4 \times g$ for 20 min. at 4 °C. Post-mitochondrial supernatants were then treated as described (188), and the final microsomal pellets were resuspended in 100 mM HEPPS buffer (pH 8.0) containing 1.0 mM EDTA. Aliquots of these samples were incubated with 10 mM d_6-dimedone for 1 hour at 37 °C. Aliquots were reduced with 1.0 mM TCEP at 37 °C for 30 minutes and then 10 mM (d_0)-iododimedone was added. The protein concentrations of microsomes were estimated using a bicinchoninic acid (BCA) assay (Pierce). Alkylated microsomes (60 μg protein) were subjected to SDS-polyacrylamide gel electrophoresis (10% acrylamide gel, *vide supra*), and the P450 region (M_r 40-60 kDa) was excised,

digested with trypsin (8 ng/μl) for 16 hours in 25 mM NH_4HCO_3 buffer (pH 8.0) at 37 °C, and subjected to LC/MS/MS analysis as described below.

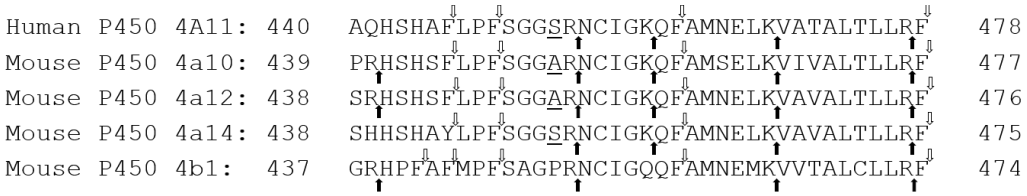

Figure 11. **Cleavage Sites of P450 Subfamily 4A Enzymes.** Closed upward arrows denote tryptic cleavage sites and open downward arrows denote chymotryptic cleavage sites.

2.10. LC-MS/MS Peptide Identification

Extracted peptides from mouse microsomes or recombinant P450s were analyzed on a nanoLC Ultra system (Eksigent Technologies, Dublin, CA) interfaced with an LTQ Orbitrap XL mass spectrometer (Thermo Scientific, San Jose, CA). Approximately 2.5 μg (microsomes) or 10 pmol (recombinant P450) of peptides was reconstituted in 0.1% HCO_2H (v/v) and pressure-loaded (1.5 μl min^{-1}) onto a 360 μm outer diameter × 100 μm inner diameter microcapillary analytical column packed with Jupiter octadecylsilane (C18) (3 μm, 300 Å, Phenomenex) and equipped with an integrated electrospray emitter tip. Peptides were then separated with a linear gradient formed with 0.1% HCO_2H in H_2O (solvent A) and 0.1% HCO_2H in CH_3CN (solvent B) (all v/v) by increasing from 2-45% B (v/v) over a period of 0-45 minutes at a flow rate of 500 nl min^{-1}. The spray voltage was set to 2.3 kV and the heated capillary temperature to 200 °C. Higher energy collisional dissociation (HCD) and collision-induced dissociation (CID) MS/MS spectra were recorded in the data-dependent mode using a Top 2 method for each fragmentation mode. MS1 spectra were measured with a resolution of 70,000, an automatic gain control (AGC) target of 1e6, and a mass range from *m/z* 300 to 1,500. HCD MS/MS spectra were acquired with a resolution of 7,500, an AGC target of 1e5, and a normalized collision energy of 35. CID MS/MS spectra were acquired with normalized collision energy of 35 with a 50 ms max injection time. Peptide *m/z* values that triggered MS/MS scans were dynamically excluded from further MS/MS scans for 20 s, with a repeat count of 1.

For samples produced with human microsomes, an analytical column was packed with 20 cm of C18 reverse phase material (Jupiter, 3 μm beads, 300 Å, Phenomenex) directly into a laser-pulled emitter tip. Peptides (500 ng) were loaded on the capillary

reverse phase analytical column (360 μm O.D. $\times$ 100 μm I.D.) using a Dionex Ultimate 3000 nanoLC and autosampler. The mobile phase solvents consisted of 0.1% HCO_2H, 99.9% H_2O (solvent A) and 0.1% HCO_2H, 99.9% CH_3CN (solvent B). Peptides were eluted at a flow rate of 400 nl/min. The 90-minute gradient consisted of the following: 1-3min, 2% B (sample loading from autosampler); 3-70 min, 2-40% B; 70-78 min, 40-95% B; 78-79 min, 95% B; 79-80 min, 95-2% B; 80-90 min (column re-equilibration), 2% B (all v/v). A Q-Exactive mass spectrometer (Thermo Scientific), equipped with a nanoelectrospray ionization source, was used to mass analyze the eluting peptides. The instrument method consisted of MS1 using an MS AGC target value of 1e6, followed by up to 20 MS/MS scans of the most abundant ions detected in the preceding MS scan. A maximum MS/MS ion time of 100 ms was used with a MS2 AGC target of 1e5 and an intensity threshold of 5e4. Dynamic exclusion was set to 15 seconds, HCD collision energy was set to 27 normalized collision energy (NCE), and peptide match and isotope exclusion were enabled.

2.11. Proteomic Data Analysis

2.11.1. Rationale

MS^1 precursor quantitation was selected because this is a robust method for quantitation of peptides, especially when using a recombinant protein when the sample is not complex. This method was extended to quantitation of peptides in human liver and kidney microsomes. This was done for two reasons, (1) precursor quantitation of heavy/light-paired peptides allows for a seemingly unlimited amount of peptides to be quantified in a single run in a similar fashion to stable isotope labeling of amino acids in cell culture (SILAC) quantitation and (2) MS^2 quantitation would require multiple runs per

sample including pilot runs to determine peptide elution time and positive peptide identification to schedule either MRM, PRM, or DIA methods.

2.11.2. Method

Raw data files were analyzed using MyriMatch software (Version 2.2.140) (197), and in the case of the mouse microsomes, also MS-GF+ (v2016.12.12) (198), against a decoy protein database consisting of a forward and reversed human Uniprot/Swissprot database with only reviewed proteins included (Version 20170202–20,165 entries). For mouse microsomes, a mouse Uniprot/Swissprot database with only reviewed proteins included was used (Version 20150825–16,718 entries). Trypsin (human microsomes and recombinant P450) or chymotrypsin (mouse microsomes) with fully specific digestion was used as the enzyme search parameter. Chymotrypsin was used with the mouse samples in order discern between mouse P450 4a12 and 4a14 (Fig. 11). The number of missed cleavages permitted was two. Precursor ion mass tolerance was set at 10 ppm, and the fragmentation tolerance was 20 ppm for the database search. Methionine oxidation (15.9949 Da, dynamic) and cysteine modifications by d_6-and d_0-dimedone (i.e., derived from iododimedone) (144.1057 and 138.0681 Da, respectively, dynamic) were included as variable search modifications. For the mouse microsomes and recombinant P450 assays, an additional low-resolution search was performed with the same databases where precursor ion mass tolerance was set at 10 ppm, and fragmentation tolerance set at 0.5 *m/z*. The maximum Q values of peptide spectrum matches were adjusted to achieve a peptide false discovery rate ≤5%, using IDPicker software (Version 3.1.642.0) (199). A spectral library of peptides was then created with IDPicker and loaded into Skyline Software for confident identification and quantitation of precursors pertaining to cysteine-

containing peptides. MS^1 precursor quantitation was performed as described previously (200,201). The retention time of the identified peptide was used to position a retention time window (± 2.0 min) across the run lacking the same peptide identification. Second, the resolution for extracting the MS1 filtering chromatogram of the target precursor ions with both light and heavy labeled peptides was set to 60,000 at 400 Th. Then extracted ion chromatograms for the top three isotopic peaks were manually inspected for proper peak picking of MS1 filtered peptides and those with isotopic dot product scores lower than 0.8 were rejected. Additional criteria were used to further ensure the high accuracy and precision of quantification: S/N> 3.0 and baseline separation was required between the isotopic peaks of a quantifiable peptide and unknown isobaric interference. The ratios of peptide areas of light peptides to their heavy isotopes (RL:H) were calculated automatically. Quantification results were obtained from five biological replicates for human microsomes, four biological replicates for mouse microsomes, and two biological replicates for recombinant protein.

2.12. Spectroscopic Techniques

2.12.1. Rationale

This method was chosen to take advantage of the inherent properties of P450 enzymes which show strong absorbance at 450 nm when the heme iron is reduced to its ferrous form and bound to CO. A P450 concentration of 1 μM was used instead of 500 nM for this experiment to increase spectroscopic signal. Deaeration in conjunction with the use of protocatechuate dioxygenase greatly reduces the amount of molecular oxygen in the sample to decrease futile cycling of the reductase enzyme.

2.12.2. Method

P450s were oxidized with H_2O_2 as above but the procedure was adapted slightly for spectroscopic assays. The enzyme was diluted with oxidation buffer to 1.0 μM prior to introduction of 1.0 mM TCEP or 500 μM H_2O_2. After oxidation, 30 units of catalase was added, and each sample was incubated at 23 °C for five minutes. To this solution, final concentrations of 1.0 μM NADPH-P450 reductase, 150 μM DLPC, and 0.1 unit/ml protocatechuate dioxygenase (Sigma) were added to an anaerobic cuvette, with NADPH (300 nmol, in aqueous solution) in a sidearm of the cuvette. Samples were degassed, 20 μM 3,4-dihydroxybenzoate (Sigma, substrate for protocatechuate dioxygenase) was added to remove oxygen (202), and samples were further degassed using a manifold attached to both vacuum and purified Ar (203,204), and placed under an anaerobic CO atmosphere. The valves of the cuvettes were sealed, and multiple UV-visible absorbance spectra were recorded using an OLIS/Hewlett Packard 8452 diode array spectrophotometer (On-Line Instrument Systems, Bogart, GA). Spectra were collected from 380 to 600 nm before and after the addition of NADPH and then sodium dithionite (112).

Chapter III

3. Heme-Thiolate Sulfenylation of Human Cytochrome P450 4A11 as a Redox Switch for Catalytic Inhibition

3.1. Introduction

As discussed in Chapter I, P450 4A11 was the first P450 enzyme shown to exhibit redox sensitivity. In this chapter, the steps to identify and verify this sensitivity are described using methods developed which are included in Chapter II.

Since the main enzymatic product catalyzed by P450 4A11, 20-hydroxyeicosatetraenoic acid) 20-HETE, is a molecule with opposing physiological activities depending on its site of production related to blood pressure regulation, this enzyme is of interest as a potential drug target for anti-hypertensive research.

In this chapter, I used a combination of chemoproteomic and spectroscopic techniques to investigate the mechanism behind the redox sensitivity observed in P450 4A11. The aims for this chapter were to prove the hypothesis that 4A11 is redox regulated through sulfenylation of the heme-thiolate ligand.

3.2. Results

3.2.1. Stimulation of P450 4A11 *ω*-Hydroxylation Activity by Reducing Agents

In previous work the rates of *ω*-hydroxylation of lauric acid varied considerably, from 9-21 min^{-1}, under varying conditions (60). When P450 4A11 was pretreated with either DTT or TCEP reagents in the preliminary experiments performed by Donghak Kim (Fig. 12), *ω*-hydroxylation activity was routinely increased two- to four-fold. Similar results were found with reduced GSH (results not presented). The ratio of the two major products, 11- and 12-hydroxy lauric acid, remained constant with this activation, performed by

Donghak Kim (Fig. 13). These results indicated that P450 4A11 has a thiol-dependent redox sensitivity, which was investigated further. Redox-dependent activation was also reflected in the increase in k_{cat} values for both the wild-type and F434S (*rs1126742*) (162) variants of P450 4A11 (2.1-fold) (Figs. 14*A,* 14*B*). The K_m values with and without DTT remained constant between the wild type enzyme (63 ± 10 *μ*M and 62 ± 15 *μ*M, respectively) and the F434S variant (67 ± 7 *μ*M and 58 ± 10 *μ*M, respectively) (Figs. 14*A,* 14*B*). Collectively, these results indicate that both wild-type and F434S variant P450 4A11 are activated in a reducing environment, which may have biological relevance *in vivo*.

Ten other human P450 enzymes were tested for thiol-dependent activation with their relevant substrates (Table 3). The highest stimulation observed among these was P450 2C9, with only a 33% increase. The reductive activation of P450 4A11 was unique among human P450 enzymes examined here. These analyses were performed by Leslie Nagy and Fred P. Guengerich.

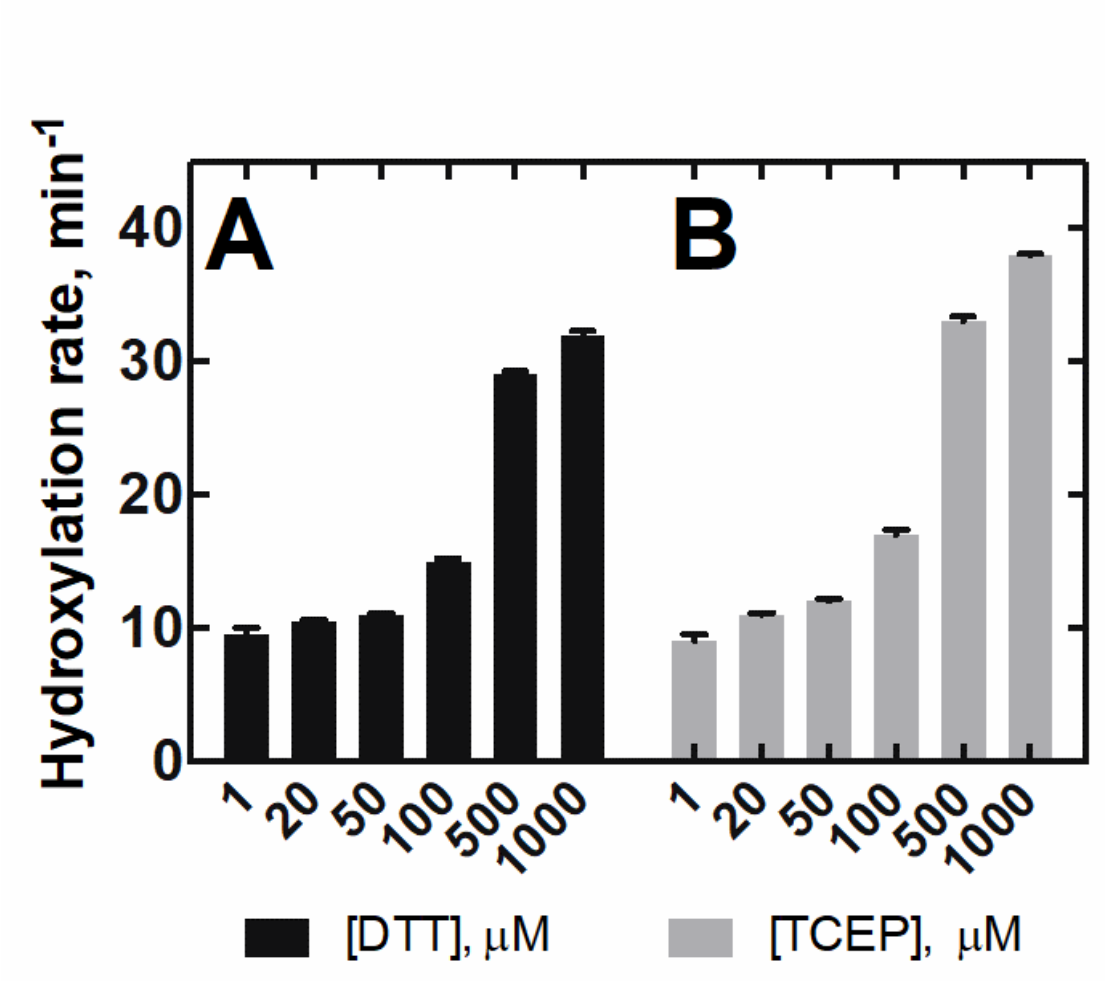

Figure 12. **Stimulation of Lauric Acid *ω*-Hydroxylation Activity by DTT and TCEP.** P450 4A11 was pre-incubated with varying concentrations of either (A) DTT or (B) TCEP and rates of lauric acid *ω*-hydroxylation were measured.

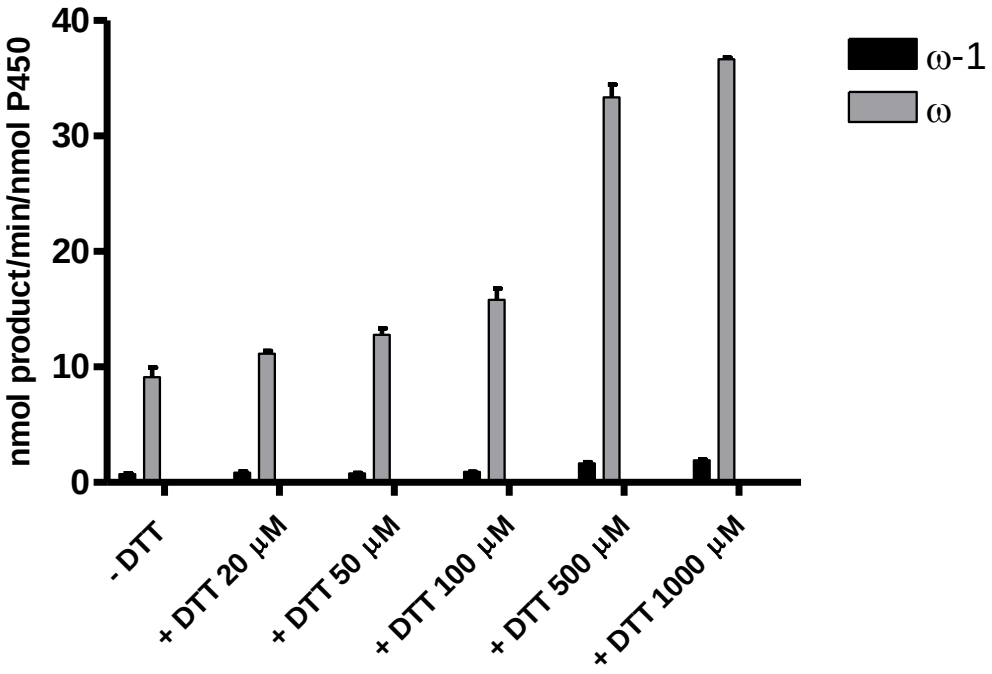

Figure 13. ***ω/ω*-1 Ratios with Stimulation of Lauric Acid *ω*-Hydroxylation Activity by DTT.** P450 4A11 was pre-incubated with varying concentrations of DTT and rates of lauric acid ω- and ω-1 hydroxylation were measured.

Human P450	Substrate	Reaction	Catalytic activity, nmol product/min/nmol P450 -DTT	+DTT (1 mM)	% increase
4A11	Lauric acid	12-OH	9.0 ± 1.1	38 ± 1	+ 420
2C8	Paclitaxel	6-OH	1.8 ± 0.1	1.9 ± 0.1	+ 7
2C9	Tolbutamide	1´-OH	1.1 ± 0.1	1.5 ± 0.2	+ 33
2D6	Bufuralol	4´-OH	2.9 ± 0.1	3.2 ± 0.1	+ 9
3A4	Nifedipine	Desaturation	2.0 ± 0.6	1.8 ± 0.5	- 10
19A1	Testosterone	Estrone formation	10.8 ± 0.2	10.9 ± 0.9	+ 1
21A2	Progesterone	21-OH	51 ± 10	68 ± 6	+ 30
2A6	Coumarin	6-OH	[a]	[a]	- 14
1A1	Ethoxyresorufin	(resorufin)	[a]	[a]	+ 8
1A2	Ethoxyresorufin	(resorufin)	[a]	[a]	+ 26
1B1	Ethoxyresorufin	(resorufin)	[a]	[a]	- 4

Position of hydroxylation (OH) or product indicated.

[a] Assayed using fluorescence methods but absolute amounts of product not calibrated.

Table 3. **Effects of DTT on Catalytic Activities of P450 4A11 and Other Human P450s**

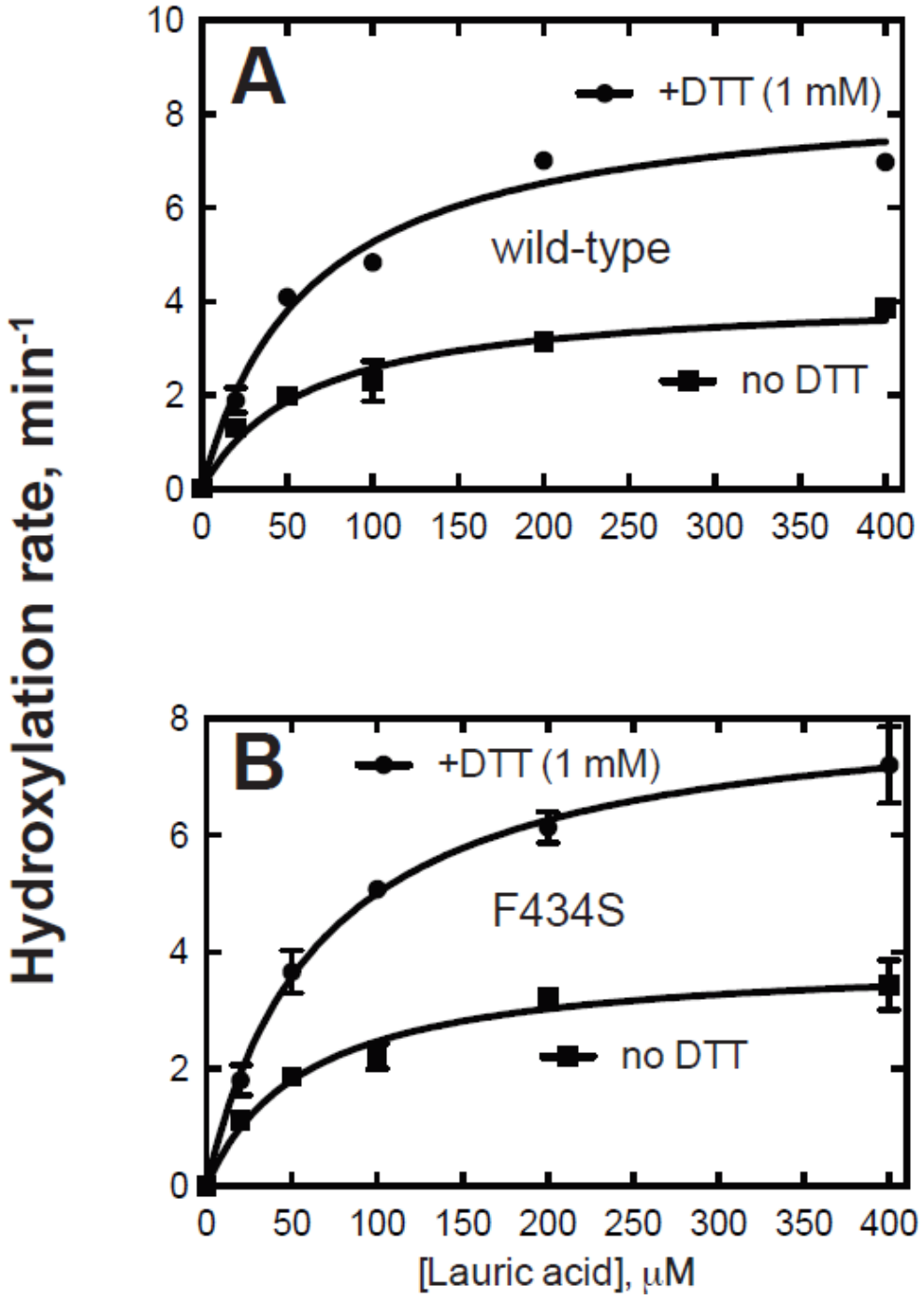

Figure 14. **Stimulation of P450 4A11 Variants of Lauric Acid *ω*-Hydroxylation Activity by DTT**. A, wild-type P450 4A11 (CYP4A11*1); B, F434S variant (rs1126742).

3.2.2. Oxidative Inhibition of P450 4A11

P450 4A11 hydroxylation activity was inhibited by H_2O_2. This inhibition occurred in a time-dependent manner with an 80% loss in activity occurring within 15 minutes (Fig. 15), a rate much higher than reported for uncatalyzed sulfenylation of thiols (27). Fifty percent activity loss occurred at a concentration of 140 μM H_2O_2 (Fig. 16).

3.2.3. Site-directed Mutagenesis

P450 4A11 encodes eight cysteinyl residues in the translated protein, and five of these cysteines were mutated to serine. Cys-457 corresponds to the proximal heme ligand and could not be changed (28), and neither C347S nor C375S produced protein with the typical P450 difference spectrum (29). Steady-state kinetic assays were done with the remaining five cysteine mutants, both with and without DTT pretreatment (Fig. 17). The response to DTT was qualitatively the same as the wild-type P450 4A11 (Fig. 14A), except for C200S (Fig. 17C) and possibly C513S (Figs. 17A, 17E), but these analyses did not implicate any of these five cysteines as being involved in the modulation of hydroxylation activity observed in the wild-type enzyme. The major conclusion was that none of these five cysteines are critical to the normal activity of P450 450 4A11, leaving only the non-mutated Cys-347, Cys-375, and Cys-457 as candidates for the oxidation-reduction phenomenon. These analyses were performed by Donghak Kim.

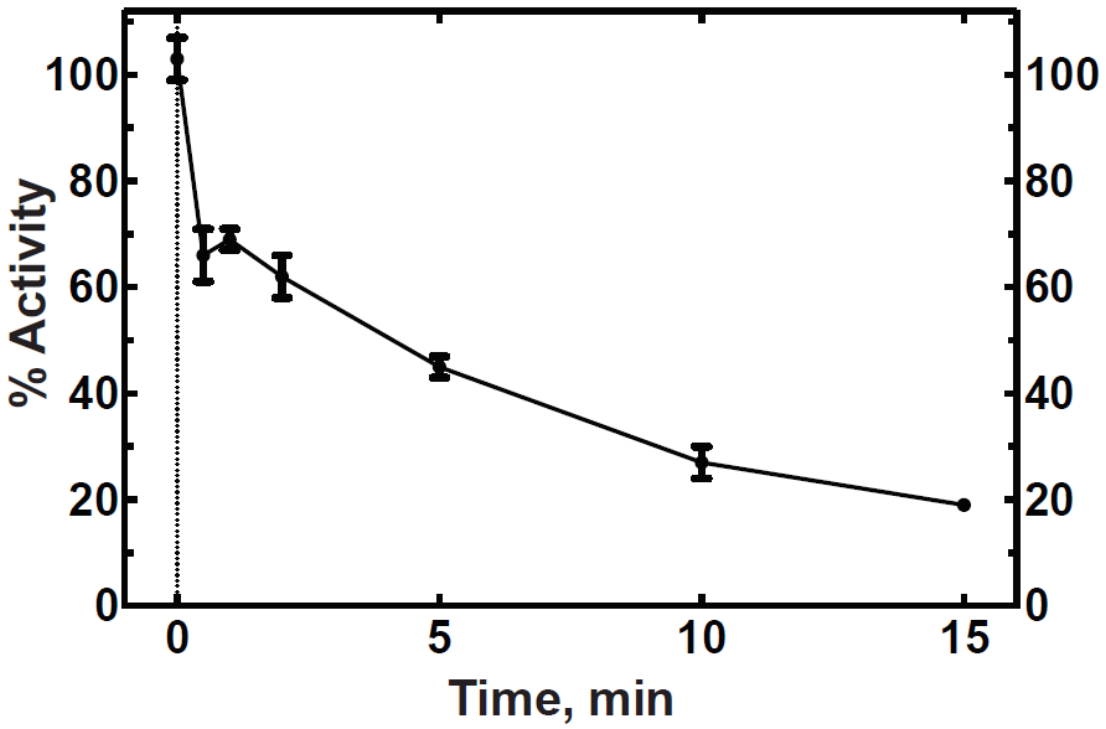

Figure 15. **Kinetics of Loss of Lauric Acid *ω*-Hydroxylation Activity of P450 4A11 in the Presence of H_2O_2.** P450 4A11 (500 nM) was incubated with 500 µM H_2O_2 in "oxidation buffer" (Chapter II) (pH 8.0) for the indicated times. Residual H_2O_2 was removed by treatment with human erythrocyte catalase (50 units/ml) for 10 minutes, and lauric acid *ω*-hydroxylation activity was measured in a reconstituted enzyme system. The initial (uninhibited) rate was 26.9 nmol *ω*-hydroxylation activity lauric acid formed min^{-1} (nmol P450)$^{-1}$.

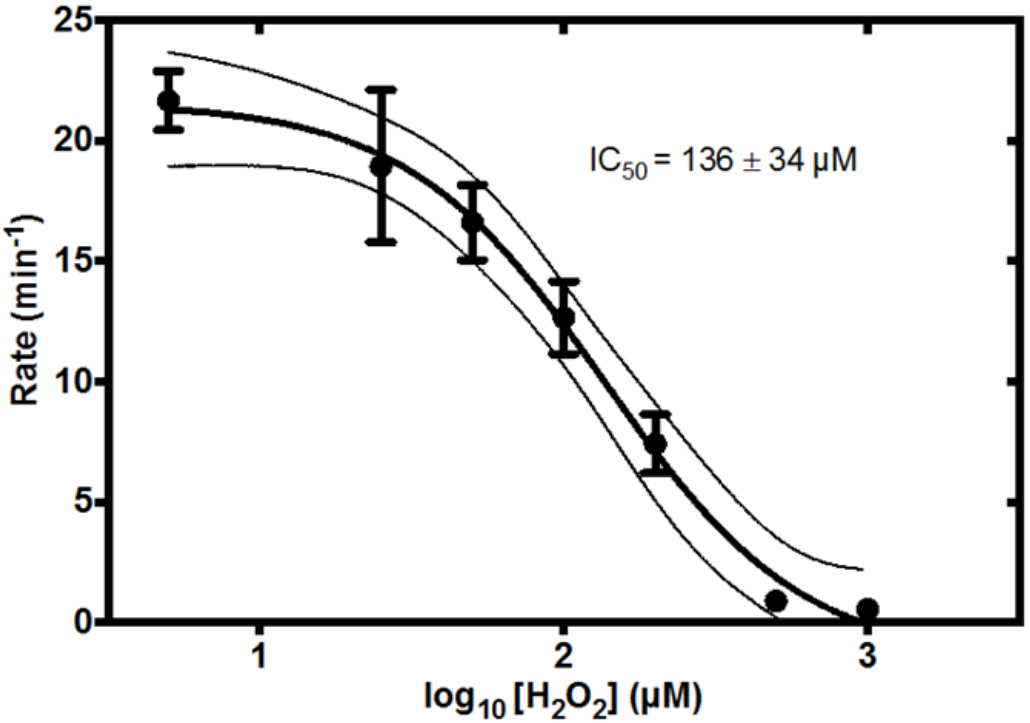

Figure 16. **Loss of P450 4A11 Lauric Acid *ω*-Hydroxylation Activity as a Function of H_2O_2.** P450 4A11 (500 nM) was incubated with varying concentrations of H2O2 for 15 min at 37 °C in oxidation buffer (pH 8.0). Catalase (10 units/ml) was added to quench the residual H2O2 (for 10 min at 25 °C), and the remaining P450 4A11 was reconstituted and used to measure lauric acid *ω*-hydroxylation activity. Results are presented as means ± SD of triplicate experiments. The outer lines indicate 95% confidence intervals.

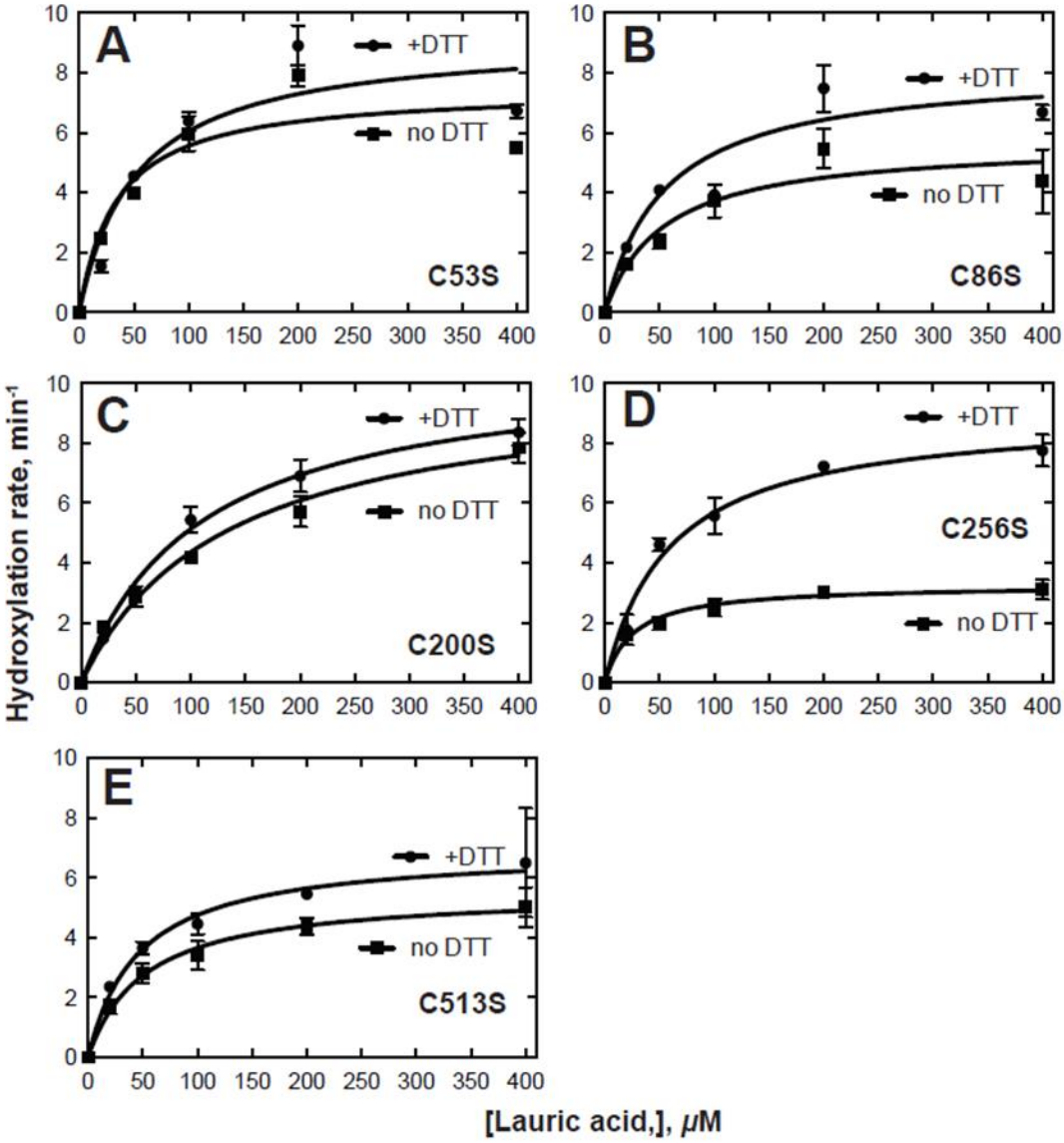

Figure 17. **Lauric Acid *ω*-Hydroxylation Activity of Cys→Ser Mutants of P450 4A11.** For experiments done at the same time with wild-type P450 4A11, see Fig. 2*A*. Assays were done in the absence (■) and presence (●) of 1 mM DTT, as indicated. *A*, C43S; *B*, C86S; *C*, C200S; *D*, C255S; *E*, C513S.

3.2.4. Identification of a Sulfenic Acid

A portion of oxidized P450 4A11 treated with each of several different concentrations of H_2O_2 was treated with d_6-dimedone (co-incubation) and subsequently counter-alkylated with (d_0-) iododimedone (30) (Fig. 10). The alkylated protein was digested with trypsin and analyzed by LC-MS/MS; integrated areas of extracted ion chromatograms for the heavy (sulfenic acid-modified) and light (free thiol) were compared using the program Skyline (31). The peptide containing Cys-457 was found to be sulfenylated. (Fig. 18). Sulfenylation of (the heme-thiolate ligand) Cys-457 coincided with the attenuation of enzymatic activity observed with increasing concentrations of H_2O_2 (Fig. 19). Oxidation of the heme-thiolate ligand would lead to an inability of the heme iron to effectively activate oxygen and carry out catalysis.

Additionally, cysteines other than Cys-457 were found to be sulfenylated, but overall were less modified, in general, than the heme-thiolate ligand (Fig. 20). These peptides were positively identified by MS/MS fragmentation (Fig. 21).

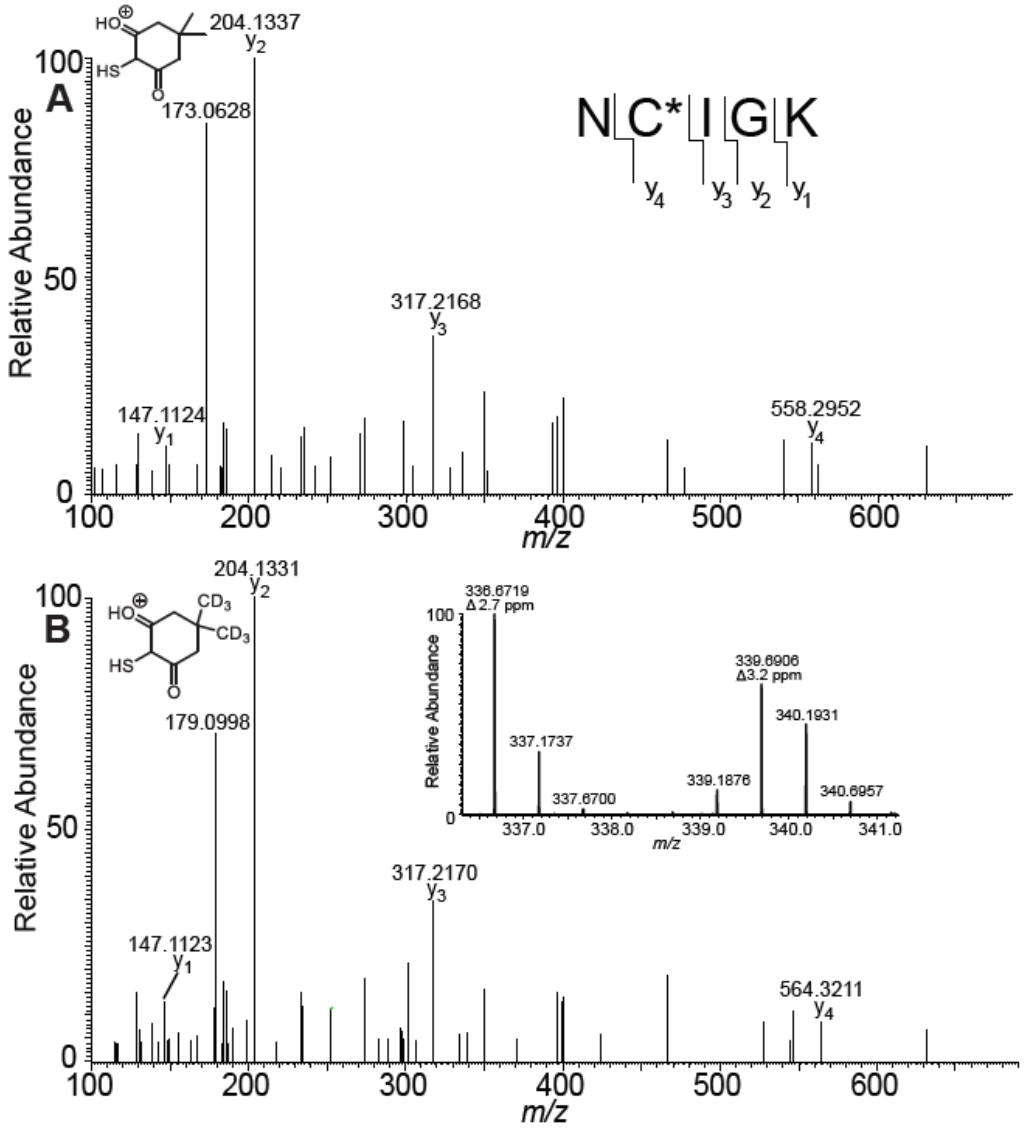

Figure 18. **MS/MS Fragmentation of Cys-457 Containing Peptide of 4A11.** Annotated HCD MS/MS of the heme-thiolate containing peptide (456-NCIGK-460) alkylated with d_0-dimedone (*A*) or d_6-dimedone (*B*).

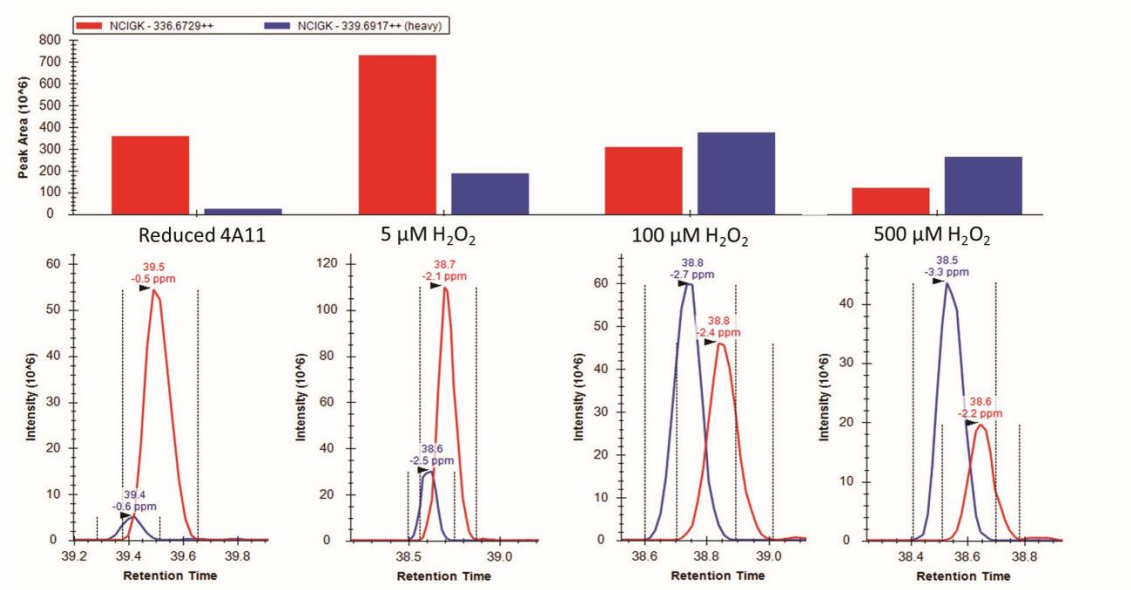

Figure 19. **Formation of a Sulfenic Acid in Cys-457 (Heme Thiol Group) as a Function of H_2O_2 Concentration.** P450 4A11 samples were labeled with d_6-dimedone and counter-alkylated with d_0-iododimedone at varying concentrations of H_2O_2. Labeled protein was then subject to trypsin digestion and LC/MS/MS analysis. Masses corresponding to Cys-457 deuterated and non-deuterated peptides were extracted, and the resulting areas were integrated using Skyline software. *A*, bar graphs of comparisons of peak areas for CySH peptide (red) and Cys-OH peptide (blue); raw peaks for CySH peptide (red) and Cys-OH peptide (blue) (not normalized in each case).

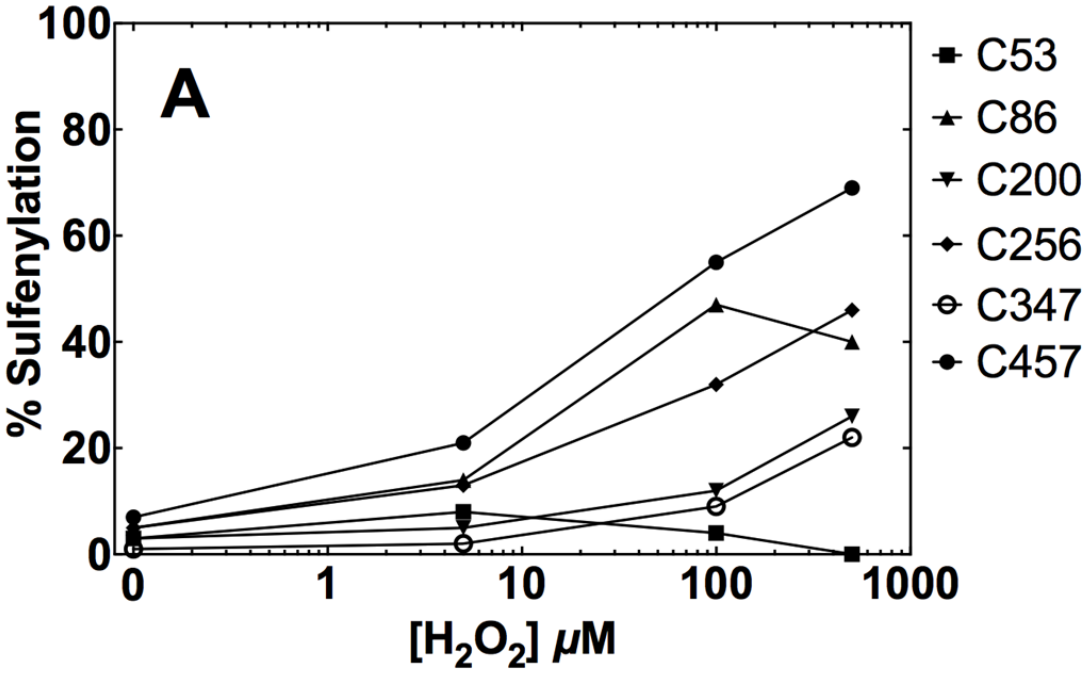

Figure 20. **Quantitation of Sulfenylated Cysteines of P450 4A11.** Graph of quantitated peptides containing P450 4A11 pre-incubated with H_2O_2 with ratios of sulfenylation

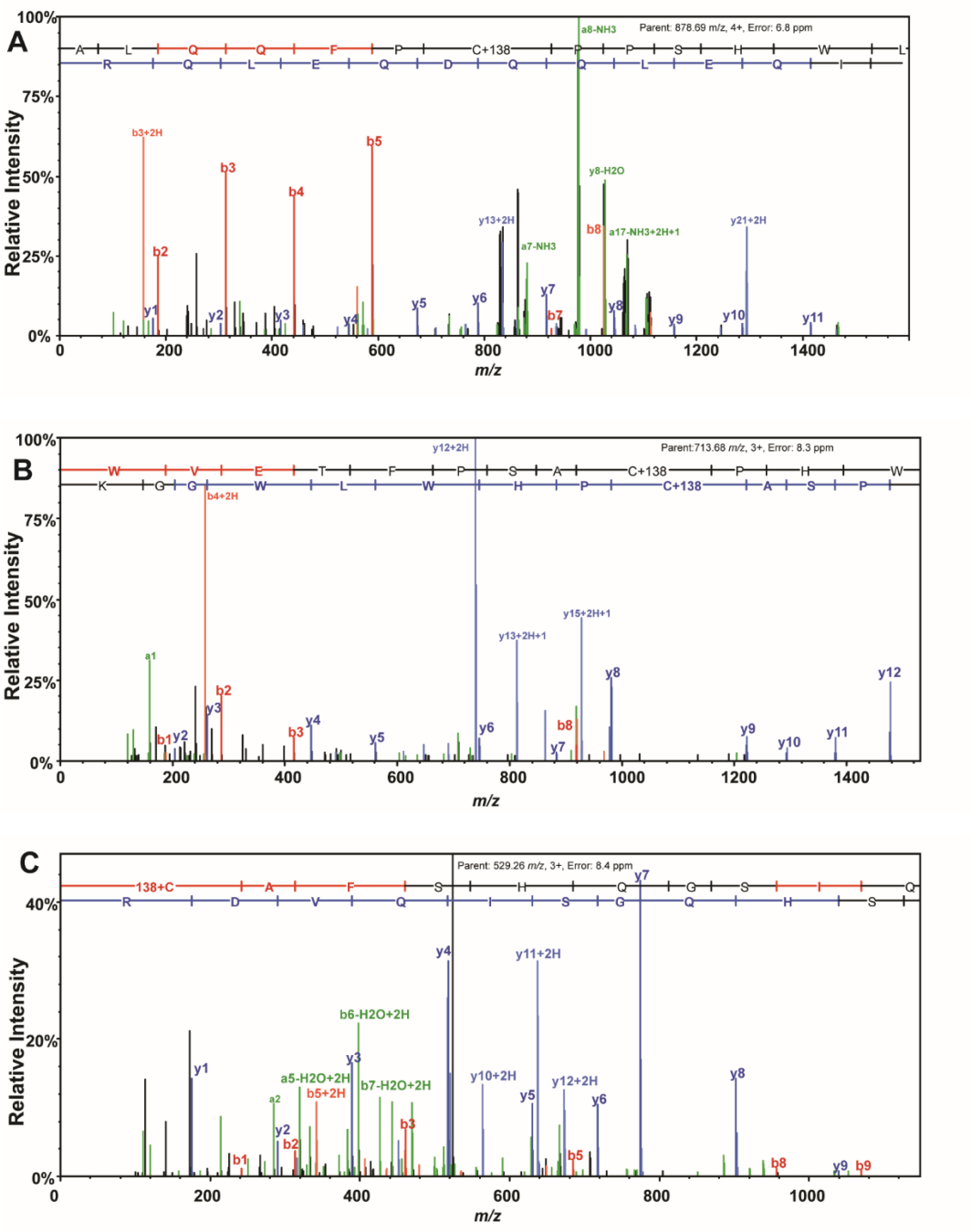
A
Parent: 878.69 m/z, 4+, Error: 6.8 ppm
a8-NH3
A L Q Q F P C+138 P P S H W L
R Q L E Q D Q Q L E Q I
b3+2H
b5
b3
b4
y8-H2O
y13+2H
b8
a17-NH3+2H+1
y21+2H
b2
a7-NH3
y7
y1
y2
y3
y4
y5
y6
b7
y8
y9
y10
y11
Relative Intensity
100%
75%
50%
25%
0%
0
200
400
600
800
1000
1200
1400
m/z
B
Parent:713.68 m/z, 3+, Error: 8.3 ppm
y12+2H
W V E T F P S A C+138 P H W
K G G W L W H P C+138 A S P
b4+2H
y15+2H+1
y13+2H+1
a1
y8
y12
b2
y3
y4
b1
y2
b3
y5
y6
b8
y7
y9
y10
y11
Relative Intensity
100%
75%
50%
25%
0%
0
200
400
600
800
1000
1200
1400
m/z
C
Parent: 529.26 m/z, 3+, Error: 8.4 ppm
y7
138+C A F S H Q G S Q
R D V Q S G Q H S
y4
y11+2H
b6-H2O+2H
y3
y1
a5-H2O+2H
b5+2H
b7-H2O+2H
y10+2H
y12+2H
y8
a2
y5
y6
y2
b3
b2
b1
b5
b8
y9
b9
Relative Intensity
40%
20%
0%
0
200
400
600
800
1000
m/z

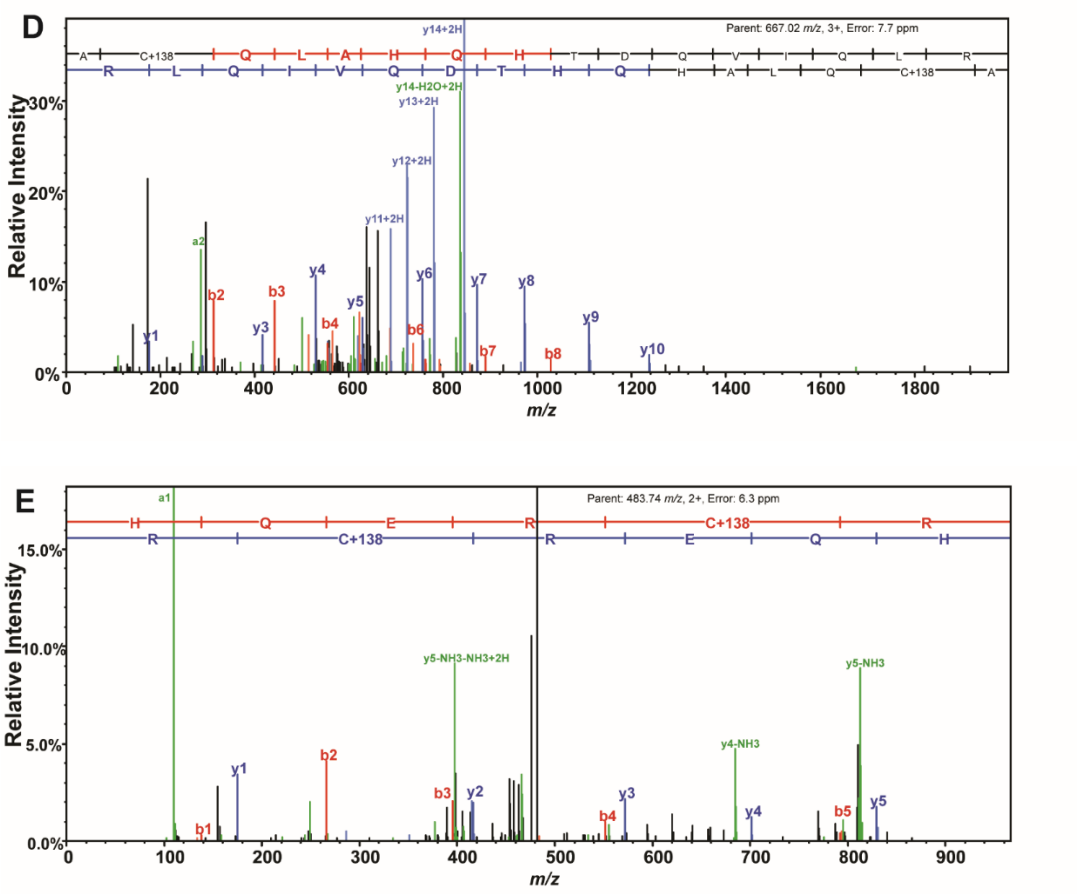

Figure 21. **Iododimedone-labeled Peptides of P450 4A11.** Annotated spectra of tryptic peptides. *A*, Cys-53; *B*, Cys-86; *C,* Cys-200, *D*, Cys-255; *E*, Cys-347. Peaks are annotated with: b- (red) and y-series (blue) ions; neutral losses and a-series ions (green). Spectra were annotated using Scaffold (205).

This sulfenylation, however, did not exclude the possibility for thiol oxidation to occur in the form of intra- or intermolecular disulfide bonds for other P450 4A11 thiols. An ICAT approach was developed using d_5/d_0-iodoacetanilide (206,207) (Fig. 10). Briefly, samples were treated with varying concentrations of H_2O_2 and thiols were then trapped using a trichloroacetic acid precipitation (208). Protein was then pelleted by centrifugation, resuspended, and treated with d_5-iodoacetanilide to alkylate free thiols (209). The protein was then precipitated and resuspended in reducing buffer to reduce disulfide bonds (and any unreacted sulfenic acids) and alkylated with d_0-iodoacetanilide. Tryptic peptides were analyzed via LC-MS/MS and the area ratios of alkylated deuterated/non-deuterated thiol containing peptides were analyzed. This experiment showed no differences in ratios between a reduced P450 4A11 protein control and up to 1 mM H_2O_2 (Fig. 22). Seven of the eight cysteines in P450 4A11 maintained at least 60% reduction (i.e. >60% d_0 labeling) with only Cys-513, the carboxy-terminal cysteine, being oxidized further with increasing H_2O_2.

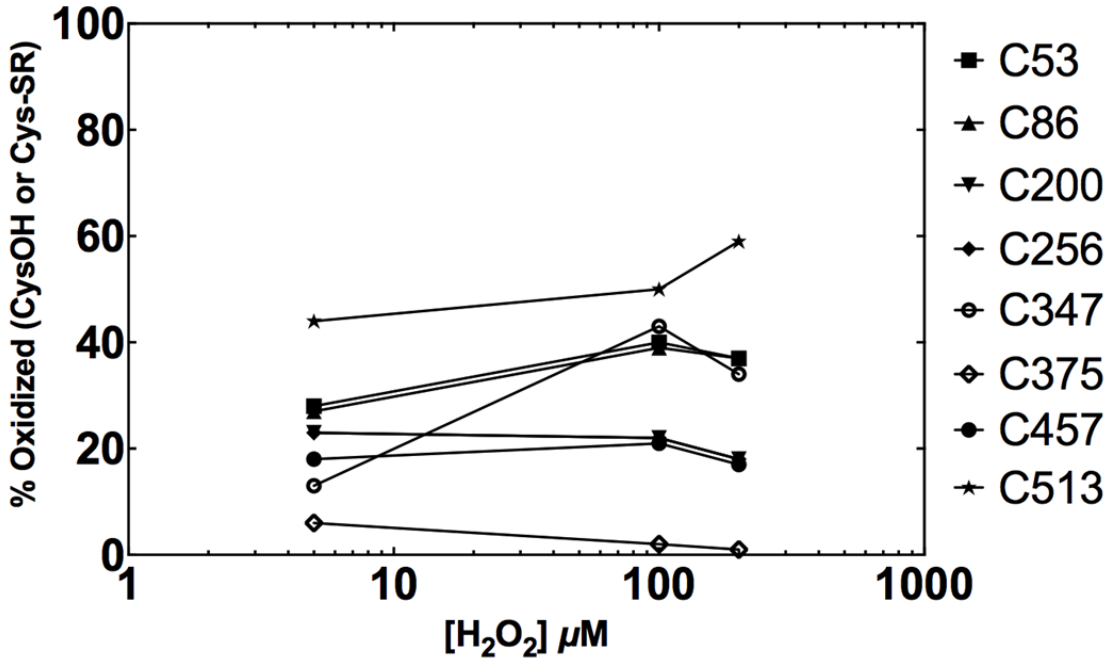

Figure 22. **Quantitation of Oxidized Cysteines of P450 4A11.** Graph of quantitated peptides containing P450 4A11 pre-incubated with H_2O_2 with ratios of iodoacetanilide labeling.

3.2.5. Spectral Analysis of Heme-thiolate Oxidation

Spectral properties of P450 4A11 were used to further address the proteomic results, i.e. to confirm the hypothesis that the sulfenic acid moiety is disrupting the iron coordination of the heme, TCEP-treated P450 4A11 was treated with H_2O_2, reconstituted with NADPH-P450 reductase, deaerated, and placed under an anaerobic atmosphere of CO. Following the addition of NADPH, spectra were recorded for TCEP-reduced (Fig. 9*A*) and H_2O_2-oxidized (Fig. 23) P450 4A11. The H_2O_2-oxidized protein showed increased absorbance at 420 nm for the CO-bound form. Sodium dithionite was added to these samples, which increased the absorbance of the oxidized enzyme at 450 nm and decreased the absorbance at 420 nm. NADPH-P450 reductase is able to reduce ferric heme to the ferrous state (allowing CO binding) but cannot reduce the sulfenic acid, leading to an inactive protein due to the loss of the thiolate axial coordination. However, dithionite is able to reduce a sulfenic acid (210), allowing for the reduced thiolate to re-ligand with the heme-iron (Fig. 6).

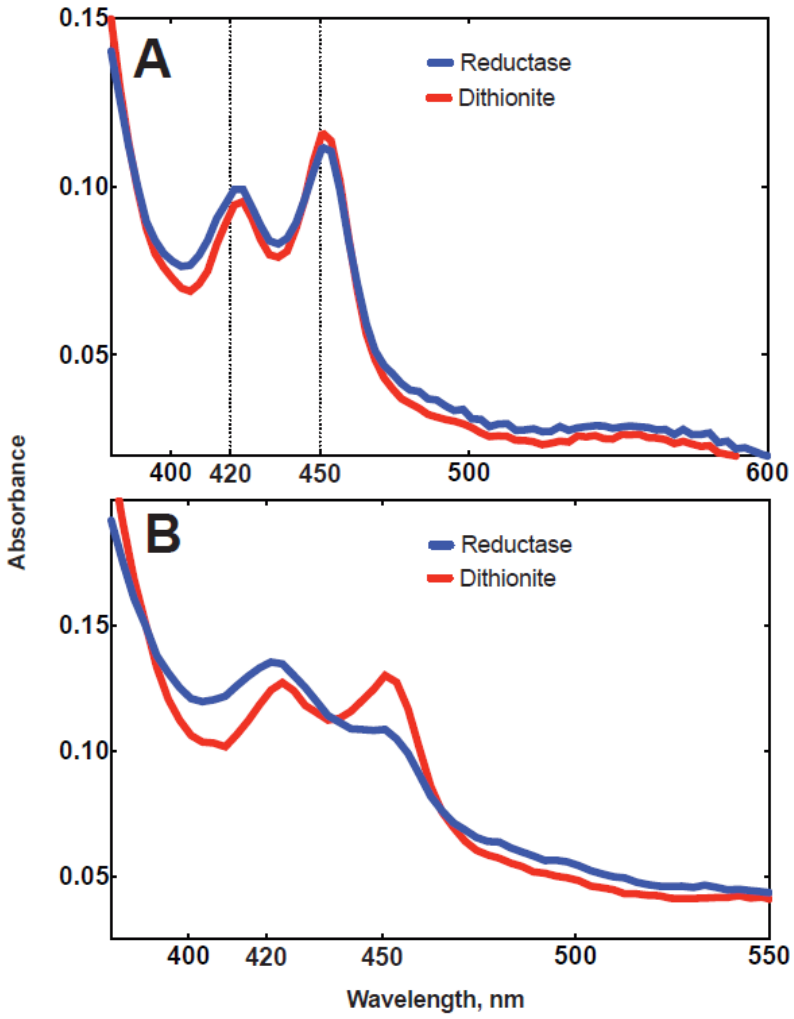

Figure 23. **Reduction of P450 4A11 by NADPH-P450 Reductase and Sodium Dithionite in the Presence of CO.** Reduced protein (A) and protein oxidized with 500 μM H_2O_2 (B) was deaerated and placed under an anaerobic CO atmosphere. NADPH was then added, and absorbance spectra was recorded (blue). Dithionite was then added (red).

3.2.6. Sulfenylation of Family 4 P450 Enzymes in a CYP4A11*tg* Mouse Model

To determine if this oxidative modification of P450 4A11 occurs *in vivo*, a *CYP4A11* transgenic mouse model was used (174). Liver and kidney tissues from four male mice were harvested and subcellular fractionation was done immediately. Microsomes were obtained within three hours of tissue harvesting via differential centrifugation and, as with the recombinant protein, incubated with either buffer, d_6-dimedone, or d_6-dimedone supplemented with 500 μM H_2O_2 (Fig. 10). These labeled samples were then treated with catalase, reduced, counter-alkylated with (d_0-) iododimedone, and digested with chymotrypsin. Chymotrypsin was used to produce peptides containing the heme-ligand cysteine unique to both P450s 4A11 and 4a12 in kidneys of male mice (Fig. 11) (211). The microsomal chymotryptic peptides were analyzed via LC-MS/MS and the resulting peak area ratios were quantitated.

The heme-thiolate Cys-457 of P450 4A11 showed ~ 75% dimedone labeling (sulfenylation) in both the dimedone and H_2O_2-supplemented samples in the kidney microsomes of three mice and ~40% labeling in the liver microsomes (Figs. 24*A,* 24*B*, 25*)*. One mouse was considerably younger (age of six weeks at time of harvest) and the expression of P450 4A11 was greatly diminished compared to the older mice (3 months (2) and 7 months). Interestingly, mouse P450s 4a12 (Fig. 24*C,* 24*D*, 26) and 4b1 (Fig. 24*E*, 27) also showed significant sulfenylation of the respective heme-thiol ligands.

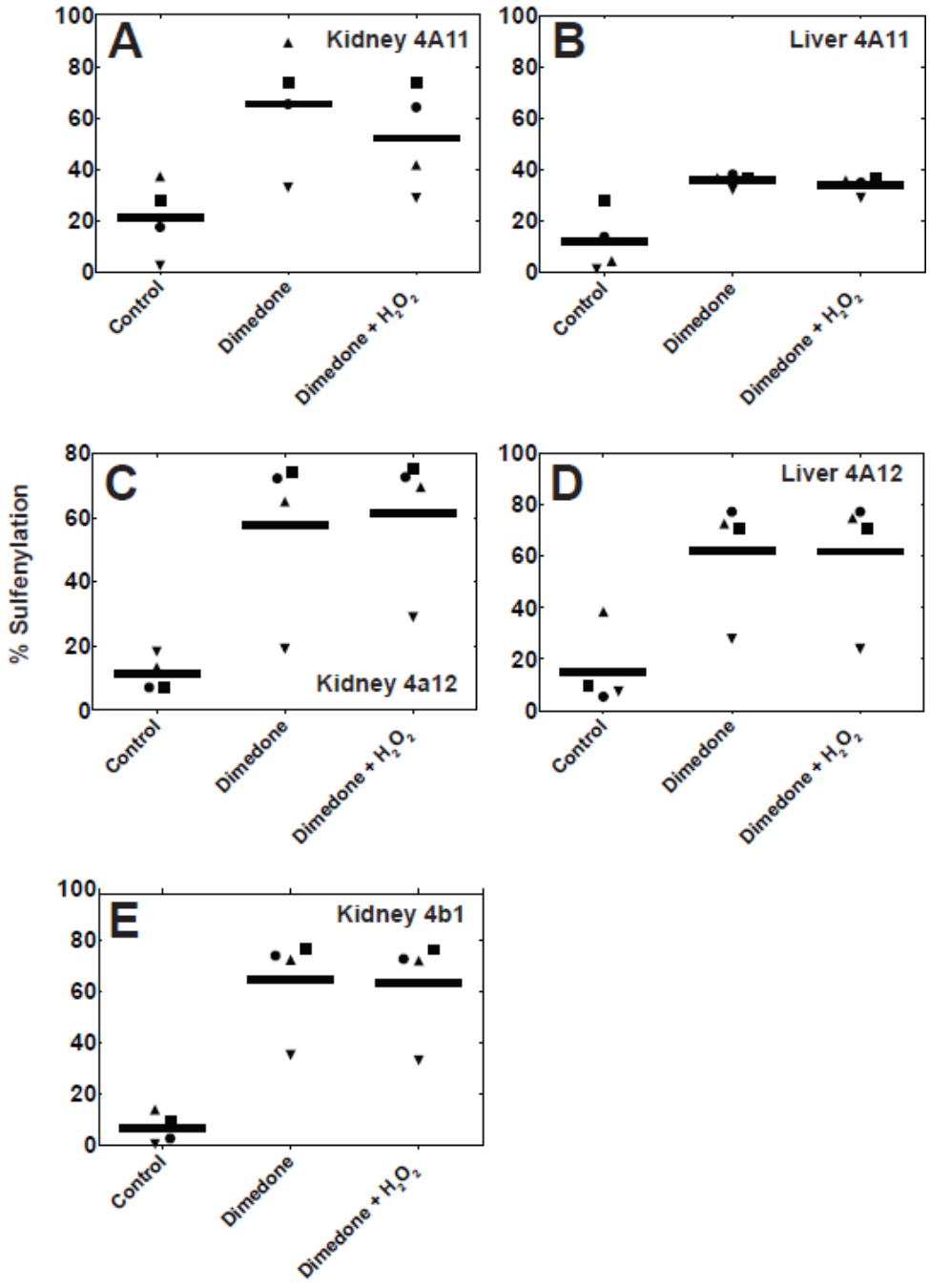

Figure 24. **Analysis of Human and Mouse P450 Peptides in *tg*4A11 Mice.**

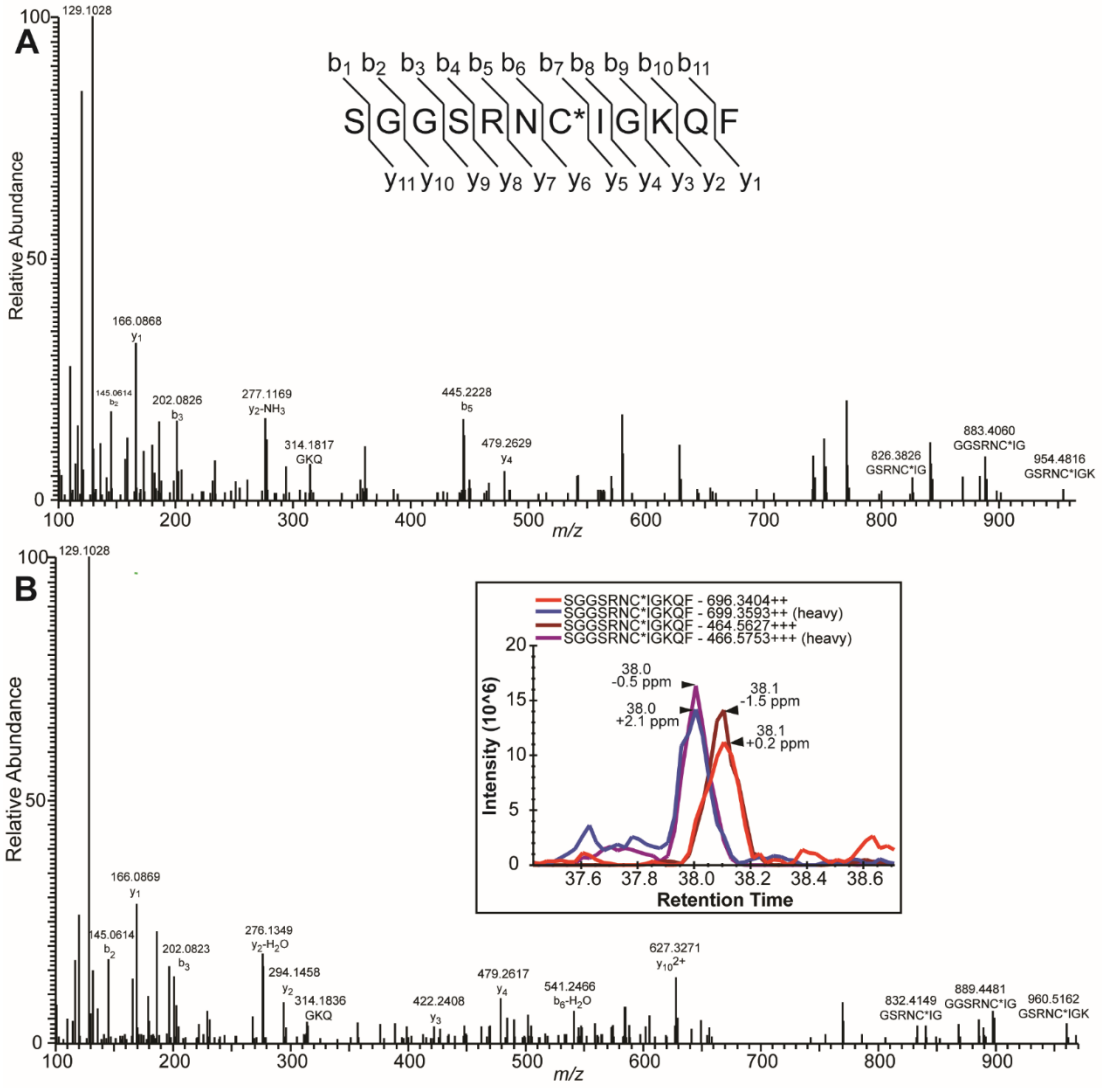

Figure 25. **Iododimedone-labeled Peptide of P450 4A11 in Mouse Tissue Sample.** Annotated spectra of the chymotryptic peptide containing Cys-457 alkylated with d_0-iododimedone (*A*) and d_6-dimedone (B) from mouse tissue. A representative extracted ion chromatogram showing the [M+2H] and [M+3H] ion species used for MS1 precursor quantitation in Skyline (*B*, Inset). HCD fragmentation produced doubly dissociated internal fragments which were considered to be diagnostic. Spectra were annotated using Protein Prospector MS-Product (http://prospector.ucsf.edu) (212). All annotated fragments have *m/z* values <10 Δppm from predicted fragment.

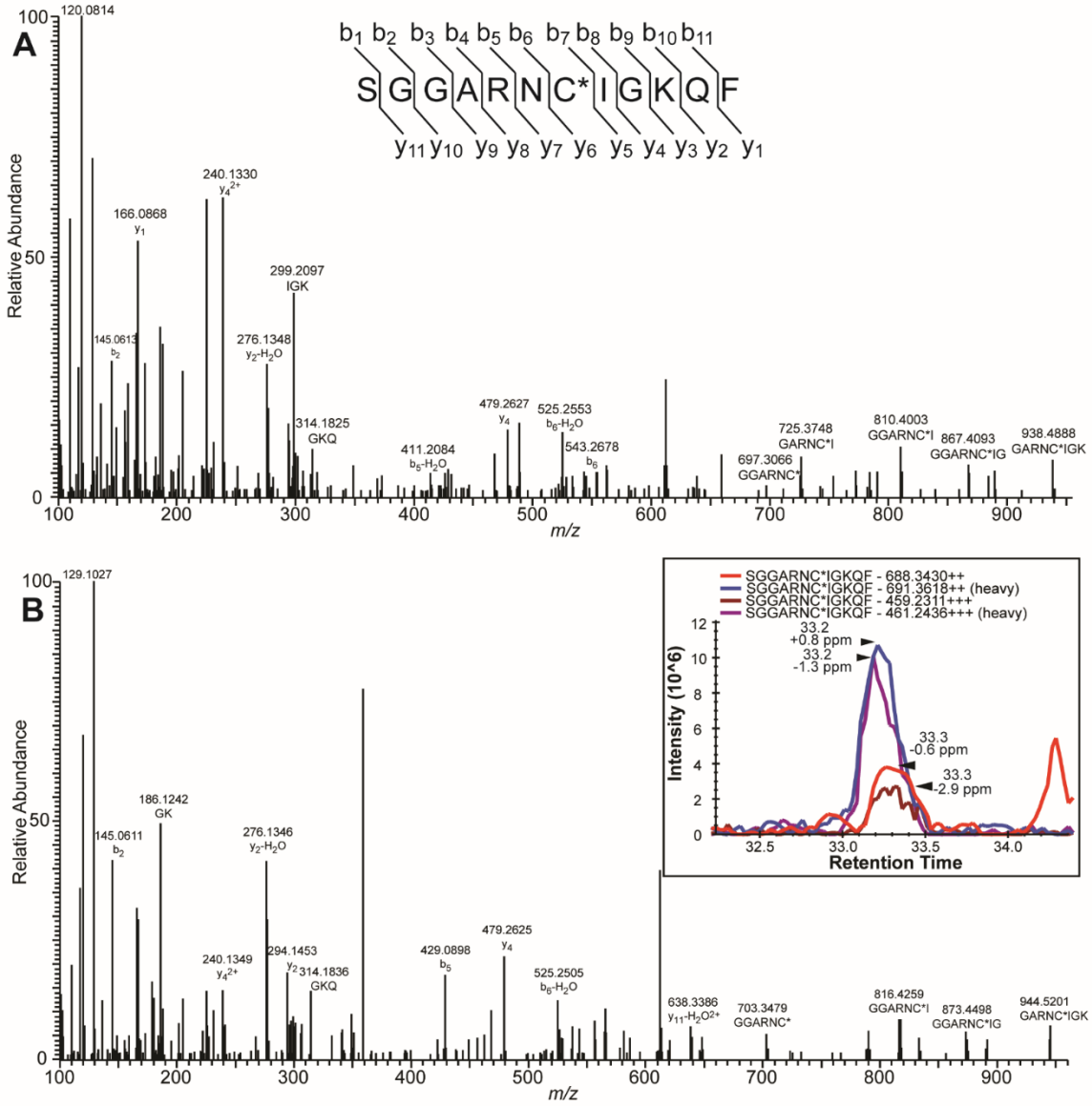

Figure 26. **Evidence of P450 4a12 Sulfenylation of Heme-Thiolate Ligand**. Annotated spectra of the chymotryptic peptide containing Cys-455 alkylated with d_0-iododimedone (*A*) and d_6-dimedone (B) from mouse tissue. A representative extracted ion chromatogram showing the [M+2H] and [M+3H] ion species used for MS1 precursor quantitation in Skyline (*B*, Inset). HCD fragmentation produced doubly dissociated internal fragments which were considered to be diagnostic. Spectra were annotated using Protein Prospector MS-Product (http://prospector.ucsf.edu) (212). All annotated fragments have *m/z* values <10 Δppm from predicted fragment.

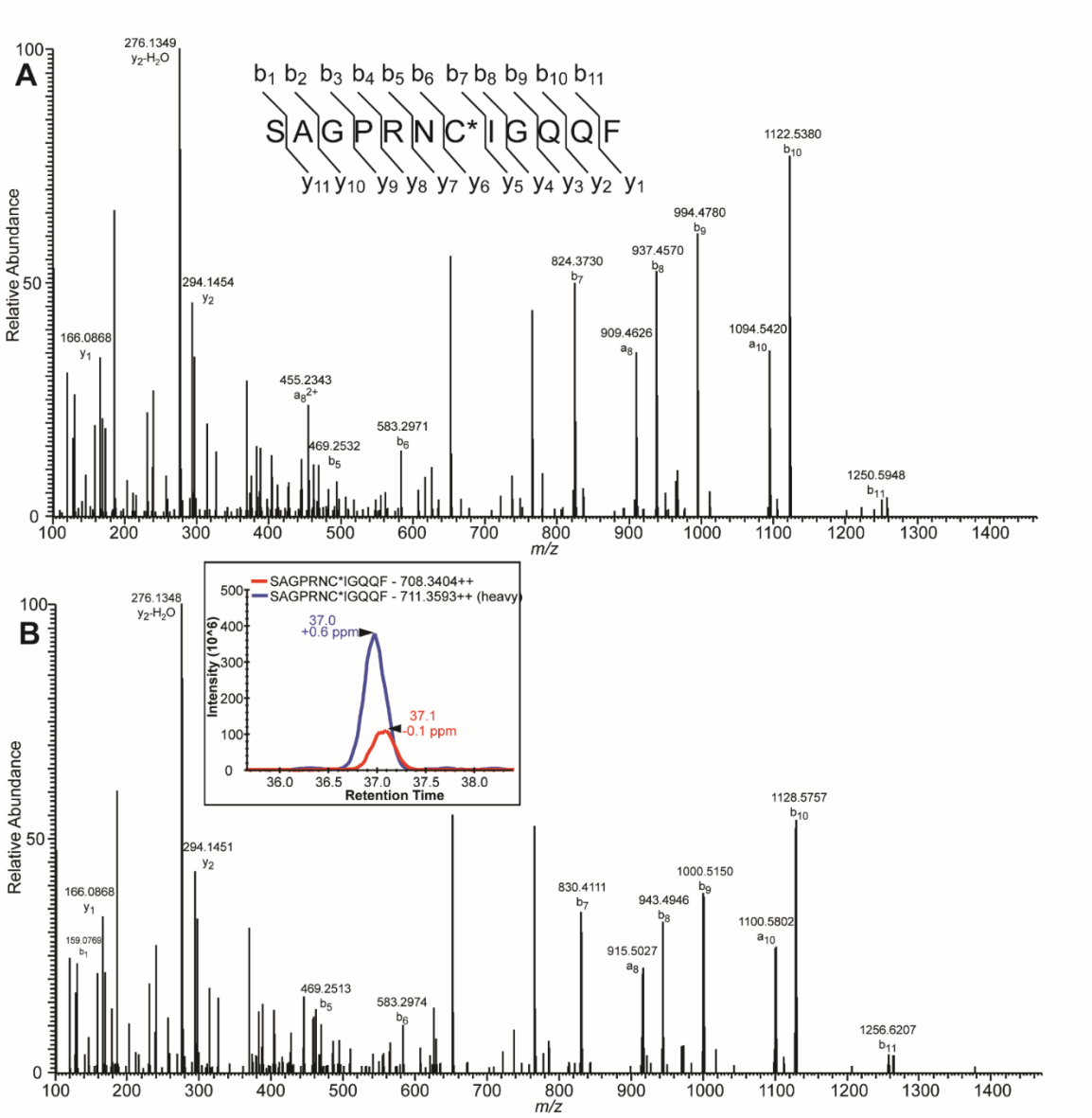

Figure 27. **Evidence of P450 4b1 Sulfenylation of Heme-Thiolate Ligand.** Annotated spectra of the chymotryptic peptide containing Cys-452 alkylated with d_0-iododimedone (*A*) and d_6-dimedone (B) from mouse tissue. A representative extracted ion chromatogram showing the [M+2H] ion species used for MS1 precursor quantitation in Skyline (*B*, Inset). Spectra were annotated using Protein Prospector MS-Product (http://prospector.ucsf.edu) (212). All annotated fragments have m/z values <10 Δppm from predicted fragment.

3.3. Discussion

I have shown that H_2O_2 reacts with the heme-thiolate cysteine of P450 4A11 to form a sulfenic acid and disrupt the iron-sulfur coordination. Five of the eight Cys residues in the protein were shown not to be essential for activity (Fig. 17), and the heme proximal ligand Cys-457 was identified as the major site of oxidation by modification and proteomic analysis (Figs. 18, 19). It is well-established that breaking this bond will also convert P450 to an inactive form, cytochrome P420 (213,214). The accessibility of the heme thiolate ligand has been established in studies with mercurials, as well as the conversion to the inactive cytochrome P420 (215,216).

The concentration of H_2O_2 required to inhibit P450 4A11 (Fig. 16) is within a physiological range (217) and was shown to be reversible via reduction by thiols (Fig. 12, 13, 14). P450 enzymes are known to produce H_2O_2 in conjunction with NADPH-P450 reductase and NADPH, with or without substrate present (218). H_2O_2 production was measured (218) for a typical reaction containing 0.2 μM P450 4A11, 0.4 μM NADPH-P450 reductase, the NADPH-generating system, and 100 μM lauric acid and determined to be 5 μM min^{-1}, i.e. 25 nmol H_2O_2 produced min^{-1} (nmol P450 4A11)$^{-1}$(Fig. 28). Typical incubations with lauric acid or arachidonic acid are conducted for two to five minutes, and the concentration of H_2O_2 produced should be negligible in proportion to the amount needed to inhibit the enzyme (Fig. 16).

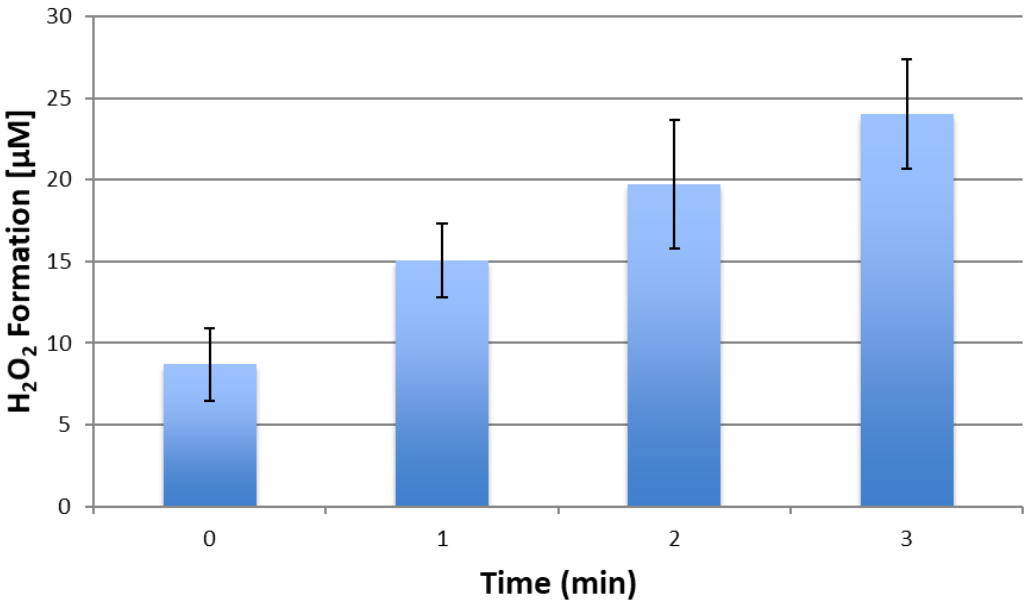

Figure 28. **Rate of H_2O_2 Formation by P450 4A11.** Rate of Formation (Background Subtracted) = 5.1 µM/min^{-1}. Adjusted for P450 concentration (200 nM) = 25 min^{-1}

Thiol activation is common in *in vitro* (219). The activation seen in the case of P450 4A11 was considerably higher than with any other P450s tested (Table 3), indicating that this redox sensitivity is rather unique among the human P450s tested. Although numerous P450 purification protocols include dithiothreitol or *β*-mercaptoethanol (220,221), it is not clear that this is necessary in most cases.

Oxidation of P450 4A11 with H_2O_2 led to an attenuation of enzymatic activity (Figs. 12, 13, 14). This loss of activity was correlated with an increased observation of dimedone alkylation (sulfenylation) at Cys-457, the heme-thiolate ligand (Figs. 18, 19). Sulfenic acid modifications have been directly implicated in the regulation of numerous enzymatic processes including GAPDH, peroxiredoxin, EGFR, and others (222). However, sulfenic acid formation involving disruption of heme-iron coordination is unprecedented to our knowledge. Choudhury et al. (223) mutated the cytochrome *c* peroxidase distal histidine ligand to a cysteine and observed a cysteic acid (cysteine sulfonic acid) in a crystal structure of the cysteine mutant, with a sulfonate oxygen coordinated to the heme. They observed activity but it was markedly lower than that of the unmodified enzyme. These results were interpreted as the heme iron itself oxidizing the cysteine, as a substrate. This is an appropriate conclusion, in that peroxidases generally have non-Cys heme ligands (224,225). Nitrile hydratase enzymes are known to coordinate iron or cobalt with both sulfenylated and sulfinylated thiols; additionally, the sulfenic acid is essential for the formation of the carbamate product (226). Our results do not discern whether the sulfenylated thiol is still (weakly) coordinated to the heme or if the coordination completely disrupted in P450 4A11. Dimedone, however, can react with sulfenamides as well as sulfenic acids (227) which would provide similar results in these experiments as sulfenic

acid. If a sulfenamide was indeed the cause of this redox modulation, generally thiol oxidation to sulfenic acid would occur first followed by subsequent condensation with a backbone nitrogen to form the sulfenamide (227).

ICAT analysis with iodoacetanilide did not provide evidence for a disulfide bond. *α*-Haloketones react with sulfenic acids to form sulfoxides (133), so these peptides would not be quantified in a direct analysis between d_0/d_5-alkylated peptides because the *m/z* value would increase by 16, the mass of oxygen. Inaccuracy could also be due to further di- and tri-oxidation (SO_2 and SO_3 respectively) of cysteines. Cys-513 appeared to be the only thiol oxidized to a large extent in our analysis, although the exact nature is unknown. Additionally, Cys-347 and Cys-375 appear to have proximity to each other in the homology model (Fig. 29). The inability to express the mutated forms of these two cysteines indicates that they are important for structural and/or conformational integrity, but our ICAT analysis did not indicate that either thiol is oxidized. This may suggest slight structural differences between human P450 4A11 and rabbit P450 4B1.

Taken together the mutant analysis, dimedone labeling, and ICAT labeling methods show that cysteines other than Cys-457 are oxidized in P450 4A11 but do not appear to directly inactivate the protein or are correlated with the loss of activity. The oxidation or mutation of these ancillary cysteines could produce slight conformational changes, but these changes would not produce the spectral change at 450 nm that sulfenylation of Cys-457 does.

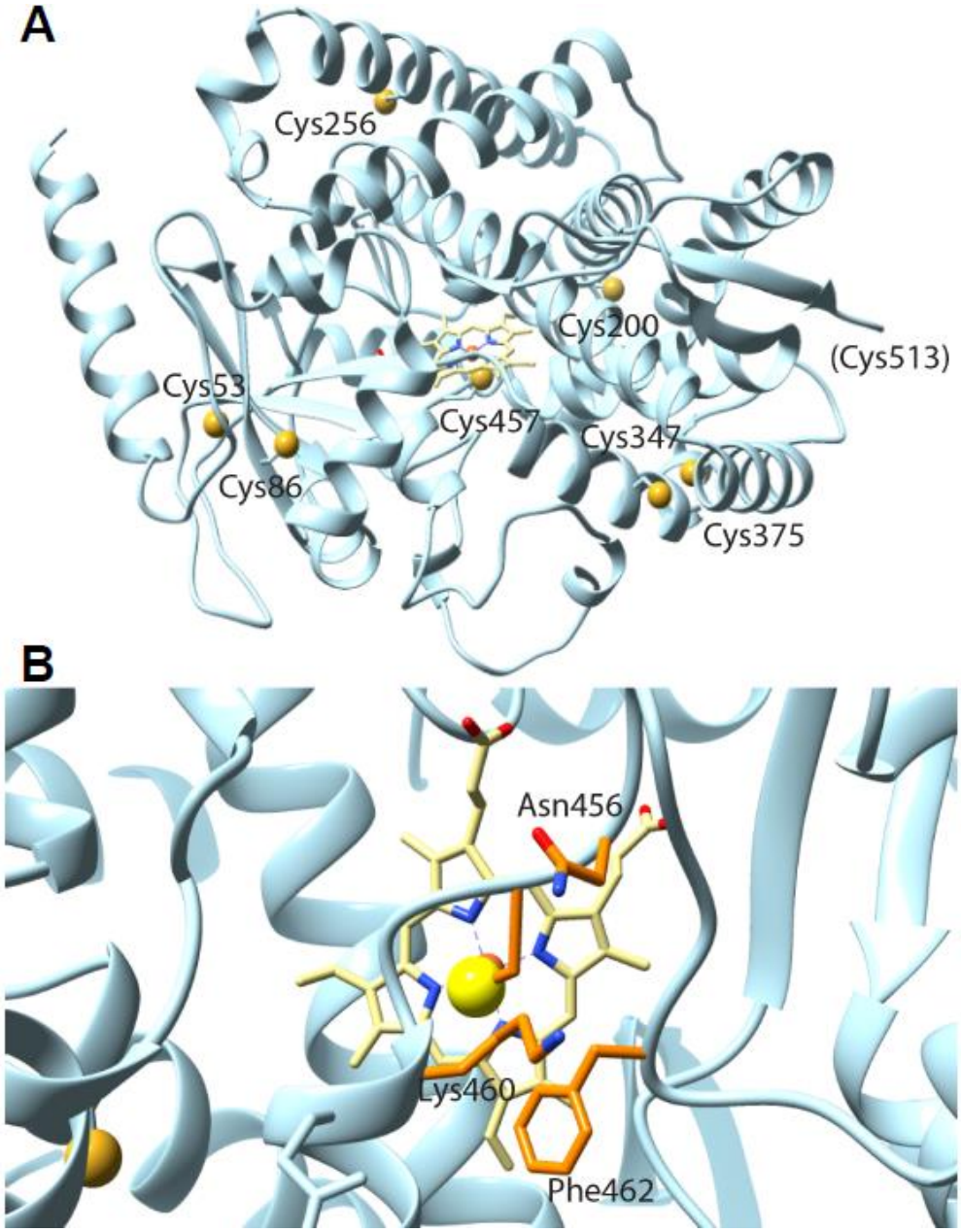

Figure 29. **Homology Model of P450 4A11 Based on Crystal Structure of Rabbit P450 4B1.** (228). Cys residues are shown, as are Asn-456, Lys-460 and Phe-462.

Detection of sulfenylation in mouse kidneys and livers provides a physiological context for this modification. The high percentage of dimedone alkylation seen in the P450 4A11, 4a12, and 4b1 heme peptides was surprising in that this would imply that a large percentage of the Family 4 P450 enzymes is constitutively inactive in the kidney. One possible explanation could be that, since 20-HETE is a very potent vasoconstrictor with submicromolar activity (229,230), these enzymes are very tightly regulated and sulfenylated enzymes could act as a reserve mechanism. Conversely, if an increase in vascular tone is required quickly, Family 4 P450 enzymes could be reduced quickly and be available for production of 20-HETE. P450 4A11 sulfenylation was observed to a lesser degree in liver. This may be due to the larger reducing potential in GSH stores the liver has compared to the kidney (231).

One unique feature of Subfamily 4A P450 enzymes is the covalent binding of the heme prosthetic group to the enzyme through a conserved glutamic acid residue (232,233). This unique feature may allow for easier re-coordination of the reduced thiol with an immobilized heme iron. In recombinant P450 4A11 it is reported that approximately 25% of the enzyme has covalently bound heme (233), but the fraction has not been determined in human samples. Rodent Subfamily 4A P450 enzymes have higher percentages of heme covalently bound to the enzyme (233). LeBrun et al. (233) have suggested that this covalent binding may contribute to differences in substrate binding rates and enzymatic regioselectivity.

A recent crystal structure of recombinant rabbit P450 4B1 shows complete adduction of the heme through a bond between a heme methyl group and Glu-310 (analogous to Glu-321 in P450 4A11) (228). In examining the alignment of mouse P450

4b1 and rabbit P450 4B1 (uniport.org), these two enzymes share 86% identity and 95% similarity. A modeled structure shows a relatively open conformation on the proximal side of the protein (Fig. 29). Cysteines that were mutated in this study are located in the peripheries of the protein, away from the proposed active site, and likely do not influence enzyme function.

Disruption of the iron-sulfur coordination would alter the absorbance properties of P450 4A11 (Fig. 23). Under an anaerobic CO atmosphere, NADPH-P450 reductase can reduce ferric heme to its ferrous state, allowing CO to bind. This CO-bound state has absorbance with λ_{max} at 450 nm if the heme-thiolate ligand is intact. When this coordination is disrupted (via sulfenylation in this case), the CO-binding spectrum was shifted to a λ_{max} at 420 nm (Fig. 23). Interestingly, the addition of dithionite after reduction with NADPH-P450 oxidoreductase reduces the sulfenic acid (210) and allows for re-coordination of the thiolate-heme complex. The observation of a sulfenylated heme-thiolate ligand has probably been overlooked previously because of the common laboratory practice of determining P450 concentration using dithionite as the reducing agent for obtaining P450 difference spectra.

In summary, P450 4A11 seems to show a unique activation under reducing conditions compared to other P450 enzymes tested. Conversely, H_2O_2 inhibits the enzymatic activity of the enzyme. Sulfenic acid formation of the heme thiolate ligand was detected by labeling and LC-MS analysis (Figs. 18, 19) and was verified spectrally (Fig. 23). The physiological relevance of the modification was demonstrated with the identification of sulfenylated P450s in freshly isolated mouse kidneys and livers. This modification is a potentially important observation that may have implications in other

P450s, as shown by our results with the mouse P450 4a and 4b enzymes. Sulfenylation could provide for biological regulation of P450 4A11 and its production of the potent vasoconstrictor 20-HETE. As mentioned previously, 20-HETE has been shown to induce ROS formation as well as play an important role in blood pressure control, which is known to be mediated by ROS production (157). The extent of sulfenylation of 4A/a P450 enzymes in tissues may provide a mechanism to greatly reduce the production of 20-HETE.

This finding led to the hypothesis that other P450s are also redox regulated and this sensitivity may function to regulate xenobiotic metabolism. I began testing this hypothesis and those results can be found in Chapter IV.

Chapter IV

4. Sulfenylation of Human Liver and Kidney Microsomal Cytochromes P450 and Other Drug Metabolizing Enzymes as a Response to Redox Alteration

4.1. Introduction

Following the results, I acquired in Chapter III, I decided to further investigate these LC-MS/MS DDA data which indicated that P450s in other subfamilies were also sulfenylated in a similar fashion to the P450 4 family (Table 4). This result required further testing which resulted in another body of work. Initially, I repeated the dimedone-labeling experiment in human liver and kidney microsomes. The results from this study indicated that human P450 enzymes were also sulfenylated in a similar fashion as one found in mice. Interestingly, many other drug metabolizing enzymes showed sulfenic acid formation, suggesting redox regulation.

I decided to focus on drug metabolizing P450 enzymes specifically in the P450 Subfamilies 1A, 2C, 2D, and 3A. Enzymes in these classes are involved in the metabolism of the majority of xenobiotic compounds the human body is exposed to. These enzymes were readily available in this laboratory for testing.

I performed identical experiments with these enzymes as I had done in Chapter III (see Chapter II for methods). The results from the P450 subfamilies mentioned above indicated that P450s likely have three separate redox classes: (1) redox insensitive, (2) heme-thiolate sensitive, and (3) ancillary thiol sensitive. This differential redox sensitivity likely translates to a phenotype previously observed *in vivo* in which the mechanism has not been elucidated.

Description	Gene Name	Modification
Carboxylesterase 3B	Ces3b	C434 (L)
Cytochrome P450 1a2	Cyp1a2	C404 (L)
Cytochrome P450 2c29	Cyp2c29	C435 (L)[1], C216 (L), C226 (L), C372 (L)
Cytochrome P450 2c50	Cyp2c50	C435 (L)[1]
Cytochrome P450 2c54	Cyp2c54	C435 (L)[1]
Cytochrome P450 2d10	Cyp2d10	C462 (L), C496 (L)
Cytochrome P450 2d26	Cyp2d26	C462 (L/K)[2], C496 (L)
Cytochrome P450 2d9	Cyp2d9	C462 (L/K)[2], C496 (L)
Cytochrome P450 2e1	Cyp2e1	C488 (L/K)
Cytochrome P450 2f2	Cyp2f2	C487 (L)
Cytochrome P450 3a11	Cyp3a11	C64 (L), C443(L), C98(L), C239(L)
Cytochrome P450 4a12A	Cyp4a12a	C373 (L/K)
Cytochrome P450 4b1	Cyp4b1	C453 (K), C369 (K), C373 (K)
Leukotriene-B_4 ω-hydroxylase 2	Cyp4f3	C384 (L)
Dimethylaniline monooxygenase, *N*-oxide-forming 2	Fmo2	C146 (K)
Dimethylaniline monooxygenase, *N*-oxide-forming 5	Fmo5	C248 (L), C468 (L)
Epoxide hydrolase 1	Ephx1	C312 (L)

Shared peptide sequences: [1]STGKRICAGEGLARMELF, [2] LFFTCLLQRF

Table 4. **Sulfenylated Mouse Microsomal Proteins.** Proteins with respective gene names identified in microsomes of mouse livers and kidneys at 5% peptide FDR. Modifications are presented as cysteine (C) and sequence location. Tissue location is denoted as liver (L) or kidney (K) by the modification.

4.2. Results

4.2.1. Identification of Sulfenylated P450s in Mouse Microsomes

Following my report that identified oxidation of P450 Subfamily 4a enzymes in mouse kidney and liver microsomes (112), further analysis led to the identification of other sulfenylated cysteines in other P450s in Subfamilies 2, 3, and 26 (Table 4). Of these, the mouse P450 3a, 2c, 2d, and 2e proteins are known drug metabolizing enzymes in mice (234). These results indicate that many P450s may be inhibited by oxidative posttranslational modification of cysteines.

4.2.2. Identification of Sulfenylated Drug Metabolizing Enzymes in Human Kidney and Liver Microsomes

The mouse results (Table 4) led to the expansion of the proteomic study to human microsomes. Frozen human kidney and liver tissues from five individuals were rapidly fractionated into microsomal fractions in deaerated buffer and labeled using an isotope-coded ICDID strategy for relative quantitation (Fig. 10) (32). After excising the 40-60 kDa P450 region and digesting the proteins with trypsin, I identified 347 modified proteins in the kidney microsomes at a 5% peptide false discovery rate (FDR) (Table 5, Fig. 30). In addition, 380 modified proteins were identified in the liver microsomal fractions (5% peptide FDR, Table 5, Fig. 30). Of these proteins, 11 P450s were sulfenylated in the kidney microsomes and 24 P450s in liver microsomes. The identified P450s included enzymes that are important in the metabolism of both endogenous and xenobiotic substrates.

In addition to the P450 enzymes, other modified proteins were identified that are important in drug metabolism, including UDP-glucuronosyltransferases (UGT), epoxide

hydrolase, flavin-containing monooxygenases (FMO), monoamine oxidases (MAO), and carboxylesterases. Other previously known sulfenylated proteins were also identified including protein disulfide isomerases (33) and aldehyde dehydrogenases (34). MS1 precursor intensities for peptides were quantified using Skyline software (26).

Table 5. **Sulfenylated Human Microsomal Proteins.** Proteins with respective gene names identified in microsomes prepared from human livers and kidneys, at 5% peptide FDR. Modifications are presented as cysteine (C) and sequence location.

Description	Gene Name	Modifications Found in Liver				Modifications Found in Kidney	
Arylacetamide deacetylase	AADAC	C340 (28±5%)				--	
Alcohol dehydrogenase 1A	ADH1A	C133[1] (32±2%) C112[2] (35±4%) C241[3] (37±3%)	C328 (31±6%) C98 (29±8%) C196	C171[4] C175[4]	C212 C47	--	
Alcohol dehydrogenase 1B	ADH1B	C47 (27±3%) C98[5] (34±2%) C133[1]	C112[2] C241[3] C171[4]	C175[4] C196[6] C212[6]		--	
Alcohol dehydrogenase 1C	ADH1C	C112[2]	C98[5]	C196[7]	C241[3]	--	
Alcohol dehydrogenase 4	ADH4	C246 (28±2%) C274 (39±5%) C47 (35±3%)	C23 (37±4%) C99 (32±4%) C105	C287 C201[6] C217[6]		--	
Alcohol dehydrogenase 6	ADH6	C196[7]				--	
Aldehyde dehydrogenase family 16 member A1	ALDH16A1	C350				C496	
Aldehyde dehydrogenase family 1 member A3	ALDH1A3	--				C196	C197
Aldehyde dehydrogenase, mitochondrial	ALDH2	C386 (33±3%)	C66	C472		C66	C472
Aldehyde oxidase	AOX1	--				C386 (23±13%)	C179
Liver carboxylesterase 1	CES1	C285 (40±3%) C274 (37±5%)	C390 (37±1%)	C116 (37±3%)		C390	
Steroid 17-α-hydroxylase/17,20 lyase	CYP17A1	--				C442	
P450 1A2	CYP1A2	C504 (42±5%)	C159 (44±5%)			--	
P450 26A1	CYP26A1	--				C170	
Sterol 26-hydroxylase, mitochondrial	CYP27A1	C228 (36±6%)	C427 (43±1%)			C228	
P450 2A6	CYP2A6	C82 (34±4%)	C439 (36±3%)			--	
P450 2B6	CYP2B6	C436 (32±3%)	C180 (27±7%)	C152 (46±2%)	C79	--	
P450 2C18	CYP2C18	C338[8] (42±2%) C151[9] (38±2%)	C216 (38±4%)	C486	C266[10]	--	
P450 2C19	CYP2C19	C338[8] C435	C372 (40±4%) C266[10]	C216 C179	C151[9]	--	

Description	Gene Name	Modifications Found in Liver				Modifications Found in Kidney	
P450 2C8	CYP2C8	C435 (37±3%) C151[9] (41±3%) C51 (34±2%)	C266[10] (39±3%) C486 (37±4%) C338[8]	C216 C225 C179	C172 C175 C164	C266[10]	
P450 2C9	CYP2C9	C372 (38±1%) C486 (38±2%) C266 (41±5%)	C216 (38±3%) C172	C164 C179	C338[8] C151[9]	C151[9]	C216
P450 2D6	CYP2D6	C443 (45±7%)	C191 (39±4%)	C57 (27±7%)		--	
P450 2E1	CYP2E1	C261 (39±6%) C437 (37±3%)	C488 (34±2%) C268 (42±2%)	C480 (39±4%)		--	
P450 3A4	CYP3A4	C98[11] (33±1%)	C468[12] (40±2%)	C58		--	
P450 3A5/3A7	CYP3A5/A7	C98[11]	C467[12]			--	
P450 4A11	CYP4A11	C256[13] (40±2%) C53 (36±5%)	C200 (33±4%) C86 (36±4%)	C513[14]	C375	C256[13] (41±5%) C200 (38±6%)	C86 C513[14]
P450 4A22	CYP4A22	C256[13]	C513[14]			C256[13]	C513[14]
P450 4F11	CYP4F11	C354 (36±2%) C50[16]	C468[17] (43±6%) C102 (84±5%)	C384[18]* C276	C260	C384[18]*	
P450 4F12	CYP4F12	C354[15]	C468[17]	C384	C50[16]	--	
P450 4F2	CYP4F2	C102 (37±2%) C384 (43±13%)	C50[19] (36±6%)	C354[15]	C468	C354[15] (43±5%)	C102
P450 4F22	CYP4F22	C58[19]				--	
P450 4F3	CYP4F3	C354[15] C50 (38±2%)	C402	C384[18]*	C468[17]	C354[15]	C384[18]*
P450 4F8	CYP4F8	--				C354[15]	C384[18]*
P450 4V2	CYP4V2	C282 (37±5%)	C383 (37±5%)	C483 (40±4%)	C406	--	
P45051A1	CYP51A1	C337	C345	C366 (31±6%)	C449	--	
Epoxide hydrolase 1	EPHX1	C80 (39±1%) C182 (38±1%)	C304 (38±7%)	C232 (39±2%)		C80 (43±4%) C182 (41±3%)	C304 (46±14%) C232
Dimethylaniline monooxygenase [*N*-oxide-forming] 1	FMO1	--				C63 (43±4%) C423	C111 (33±3%)
Dimethylaniline monooxygenase [*N*-oxide-forming] 3	FMO3	C170 (38±1%) C397 (36±1%) C146 (36±4%)	C466 (43±4%) C197 (41±2%)	C68 (37±3%) C294 (36±9%)	C21 C30	C294	

Description	Gene Name	Modifications Found in Liver	Modifications Found in Kidney
Dimethylaniline monooxygenase [*N*-oxide-forming] 5	FMO5	C112 (35±4%) C468 (29±10%) C147 C22 C248 (28±0%) C31	--
Amine oxidase [flavin-containing] A	MAOA	C374[21]* (39±2%) C165 (32±1%) C306 (31±2%) C266 C201[20] (35±1%)	C201[20] (40±4%) C165 C266 C374[21]*(42±4%)
Amine oxidase [flavin-containing] B	MAOB	C156 (36±1%) C297 (37±1%) C365[21]* C192[20]	C297 (37±1%) C192[20] C156 (41±3%) C365[21]*
Serum paraoxonase/arylesterase 1	PON1	C42 (29±2%) C284	--
Serum paraoxonase/lactonase 3	PON3	C42 (38±7%)	--
UDP-glucuronosyltransferase 1-4	UGT1A4	C187 (37±4%)	--
UDP-glucuronyltransferase 1-6	UGT1A6	C176	C176
UDP-glucuronyltransferase 1-7	UGT1A7	--	C174
UDP-glucuronyltransferase 1-9	UGT1A9	--	C153
UDP-glucuronyltransferase 2A3	UGT2A3	--	C31
UDP-glucuronyltransferase 2B10	UGT2B10	C281[22] (40±4%)	--
UDP-glucuronyltransferase 2B15	UGT2B15	C283[22]	--
UDP-glucuronyltransferase 2B17	UGT2B17	C283[22]	--
UDP-glucuronyltransferase 2B4	UGT2B4	C127 (28±6%) C514	--
UDP-glucuronyltransferase 2B7	UGT2B7	C282 (35±5%)	--

Shared peptide sequences: [1]RFTCR, [2]NPESNYCLK, [3]ELGATECINPQDYK, [4]VCLIGCGFSTGYGSAVNVAK, [5]VIPLFTPQCGK, [6]VTPGSTCAVFGLGGVGLSAVMGCK, [7]VTPGSTCAVFGLGGVGLSVVMGCK, [8] SPCMQDR, [9] CLVEELRK, [10]DFIDCFLIK, [11]ECYSVFTNR, [12]VLQNFSFKPCK, [13]ACQLAHQHTDQVIQLR, [14]RLPNPCEDKDQL, [15]HPEYQEQCR, [16]LQCFPQPPK, [17]NCIGQAFAMAEMK, [18]EIEWDDLAQLPFLTMCI(/L)K, [19]LRCFPQPPR, [20]QCGGTTR, [21]I(/L)CELYAK, [22]PFLPNVDFVGGLHCK.

* Single amino acid variation (leucine/isoleucine) in peptide sequences that cannot be determined from MS/MS fragmentation.

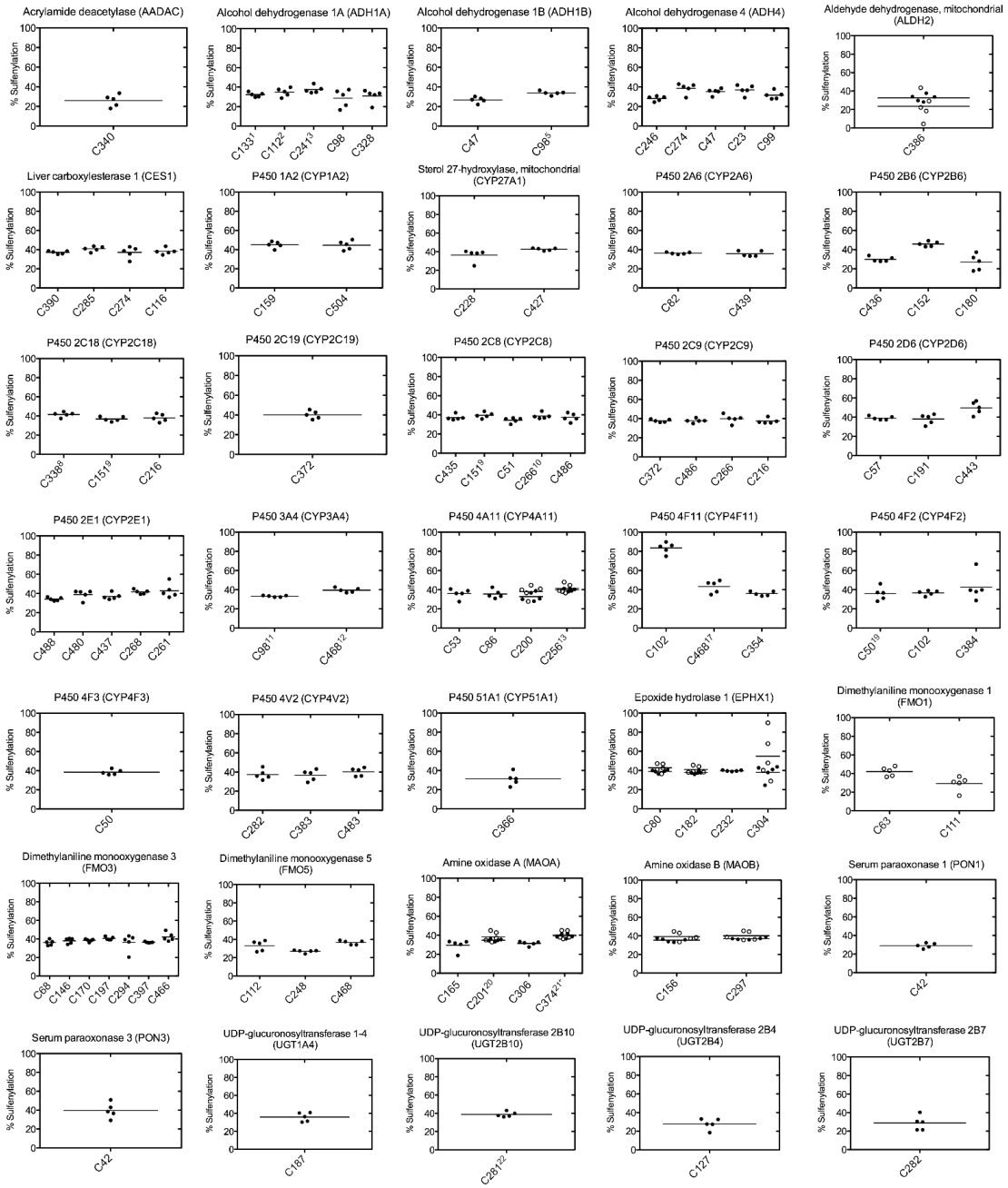

Figure 30. **Quantitation of Sulfenylated Human Microsomal Proteins.** Percent sulfenylation of cysteine (C) containing peptides for each protein in liver samples (closed circle) and kidney samples (open circle) represented with mean value (black line). Superscripts denote shared peptide sequences: [1]RFTCR, [2]NPESNYCLK, [3]ELGATECINPQDYK, [4]VCLIGCGFSTGYGSAVNVAK, [5]VIPLFTPQCGK, [6]VTPGSTCAVFGLGGVGLSAVMGCK, [7]VTPGSTCAVFGLGGVGLSVVMGCK, [8] SPCMQDR, [9] CLVEELRK, [10]DFIDCFLIK, [11]ECYSVFTNR, [12]VLQNFSFKPCK,

[13]ACQLAHQHTDQVIQLR, [14]RLPNPCEDKDQL, [15]HPEYQEQCR, [16]LQCFPQPPK, [17]NCIGQAFAMAEMK, [18]EIEWDDLAQLPFLTMCI(/L)K, [19]LRCFPQPPR, [20]QCGGTTR, [21]I(/L)CELYAK, [22]PFLPNVDFVGGLHCK. * denotes a single amino acid variation (leucine/isoleucine) in peptide sequences that cannot be determined from MS/MS fragmentation.

4.2.3. Spectral Analysis of Recombinant P450s for Thiol Sensitivity to H_2O_2

P450s 1A2, 2C8, 2D6, and 3A4 were selected for further analysis. To confirm that these P450 enzymes were affected by sulfenylation, we utilized their spectral properties to determine if heme coordination or interaction with NADPH-P450 reductase was disrupted. In the presence of CO, disruption of the heme thiol ligation either prevents reduction of the heme or yields the inactive form, cytochrome P420 (the five-coordinate ferrous-CO complex of which has a maximal absorbance at P420 nm) so that a characteristic 450 nm spectrum is not observed (35). TCEP-pretreated P450s were treated with 500 μM H_2O_2 and (after the removal of residual H_2O_2 by catalase) reconstituted with NADPH-P450 reductase, deaerated, and placed under an anaerobic atmosphere of CO. Following the addition of NADPH, spectra were recorded for the TCEP-reduced (Fig. 31, left column) and H_2O_2-oxidized (Fig. 31, right column) samples. Sodium dithionite, which reduces both sulfenic acids and the heme iron, was subsequently added to both samples (Fig. 6). P450 1A2 was very insensitive to H_2O_2, with only a slight increase in 450 nm absorbance after dithionite addition (Fig. 31A). P450s 2D6 (Fig. 31B) and 2C8 (Fig. 31C) both exhibited sensitivity to H_2O_2-dependent oxidation, with a noted decrease in 420 nm absorbance (indicative of the inactive form, cytochrome P420) and an increase in 450 nm absorbance indicative of reestablishment of the heme-thiol ligand. P450 3A4 (Fig. 31D) exhibited a complete loss of 450 nm absorbance in the oxidized sample, which was not reversible upon addition of dithionite and increased absorbance at 420 nm.

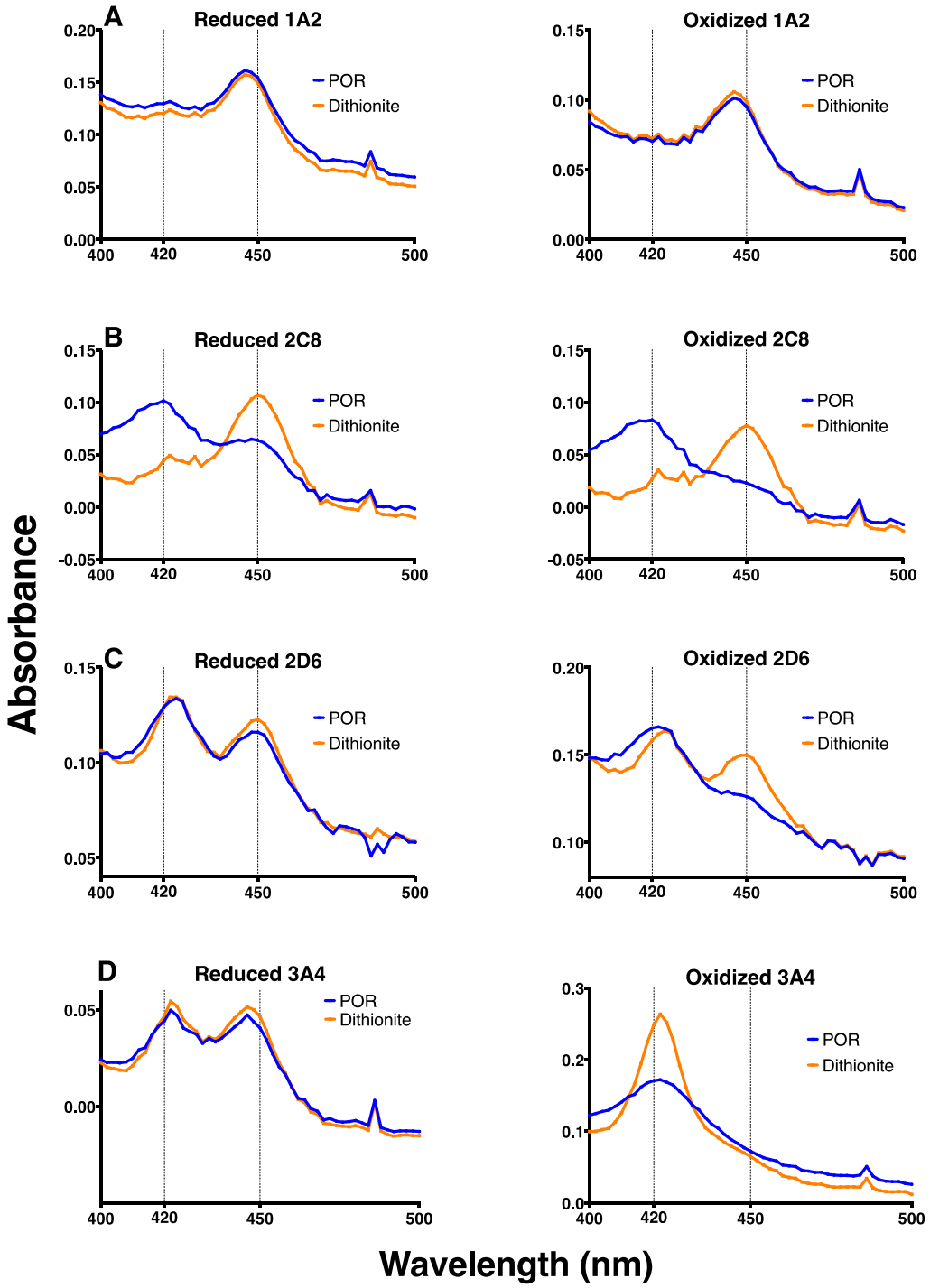

Figure 31. **Spectral Analysis of Oxidized P450s.** Analysis was performed for P450s 1A2 (A), 2C8 (B), 2D6 (C), and 3A4 (D). POR; P450 Oxidoreductase

4.2.4. Oxidative Inhibition of P450 1A2, 2C8, 2D6, and 3A4 Catalytic Activities

The enzymatic activity of P450 1A2 was largely uninhibited with preincubation of up to 1 mM H_2O_2, using phenacetin O-deethylation as a reaction, consistent with the spectral results (Fig. 32A). P450 2C8 showed sensitivity to H_2O_2, with an approximate IC_{50} value of 150 µM and a loss of 87% activity at 1 mM H_2O_2, using taxol as a substrate (Fig. 32B). P450 2D6 was also inhibited by H_2O_2, with an estimated IC_{50} value of ~300 µM (Fig. 32C) and loss of 70% activity at 1 mM H2O2, using dextromethorphan as a substrate. An IC_{50} value of ~300 µM H_2O_2 was determined for P450 3A4, using testosterone as a substrate (Fig. 32D), with a loss of 95% of activity at 1 mM H_2O_2.

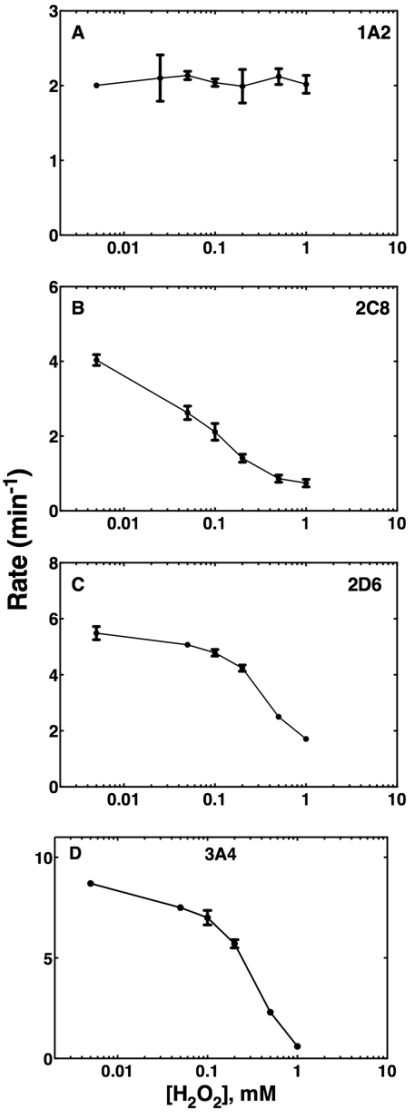

Figure 32. **Oxidative Inhibition of P450 Catalytic Activity.** A, P450 1A2 was incubated with the substrate phenacetin, and acetaminophen was monitored as the product. The reduced control enzymatic rate was 1.85 ± 0.01 min-1. B, P450 2C8 was incubated with taxol, and 6α-hydroxytaxol was monitored as the product. The reduced control enzymatic rate was calculated as 5.5 ± 0.4 min-1. C, P450 2D6 was incubated with dextromethorphan and dextrorphan was monitored as the product. The reduced control enzymatic rate was 5.6 ± 0.1 min-1. D, P450 3A4 was incubated with testosterone and 6β-hydroxytestosterone was monitored as the product. The reduced control enzymatic rate was 11.3 ± 0.3 min-1. Samples were acquired in biological duplicate and presented as means ± SD (range).

4.2.5. Sulfenylation of P450s 1A2, 2C8, 2D6, 3A4

P450s 1A2, 2C8, 2D6, and 3A4 were subjected to ICDID labeling followed by LC-MS/MS analysis of tryptic peptides (Fig. 10). For P450 1A2, this assay allowed three of the seven cysteines to be quantified (Fig. 33A, APPENDIX A1). Cys-458 (heme-thiol ligand) and Cys-504 showed low levels of sulfenylation up to 1 mM H_2O_2. Additionally, Cys-159 showed very high levels of oxidation, but this did not impair the enzymatic activity of P450 1A2 (Fig. 32A,33A), indicating that P450 1A2 is insensitive to thiol oxidation.

Five thiol-containing peptides were quantified for P450 2C8 (Fig. 33B, APPENDIX A2). Cys-338, Cys-51, Cys-151 and Cys-435 (heme-thiol ligand) were sulfenylated in a H_2O_2-dependent manner, while Cys-266 was oxidation insensitive.

Two peptides of P450 2D6 could be quantified (Fig. 33C, APPENDIX A3). Cys-443 (heme-thiol ligand) showed a H_2O_2-dependent increase in sulfenylation compared to the reduced control.

P450 3A4 ICDID labeling allowed for the quantitation of four of the seven cysteines (Fig. 33D, APPENDIX A4). The heme-thiol cysteine (Cys-442) showed a significant H_2O_2-dependent increase in sulfenylation. Cys-468 also showed a H_2O_2-dependent increase in sulfenylation, but peptides containing the di- and trioxidized cysteine sulfinic (SO_2^-) and sulfonic (SO_3^-) acids (respectively) were also found (Fig. 34, APPENDIX A5), suggesting that Cys-468 is very sensitive to oxidation.

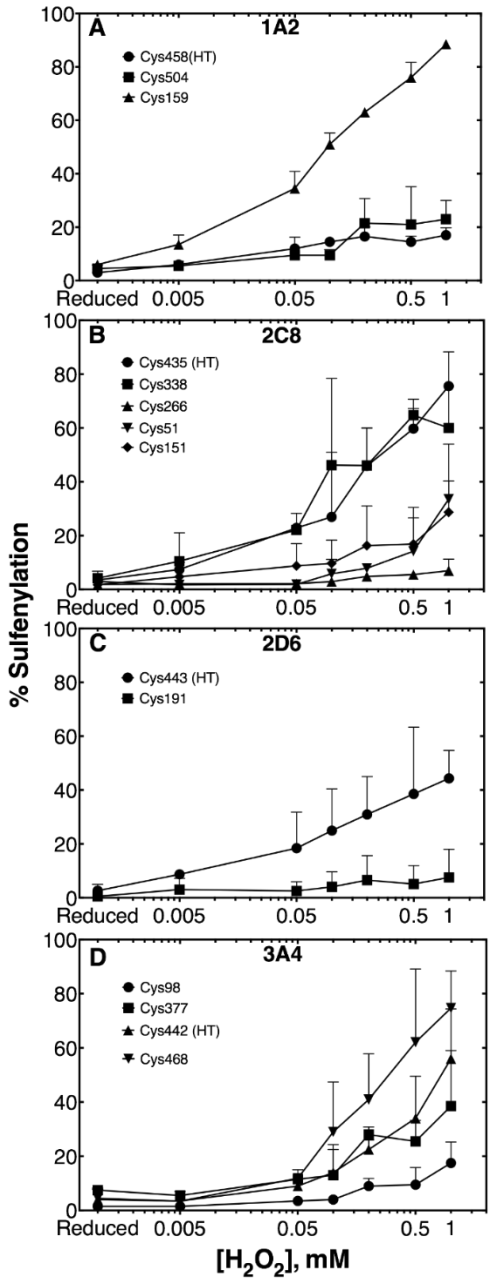

Figure 33. **Sulfenylation of P450 Enzymes.** Prereduced enzyme was coincubated with d_6-dimedone and varying concentrations of H_2O_2 or TCEP. Proteins were then reduced, and counter alkylated with d_0-iododimedone. Labeled samples were then subjected to LC-MS/MS analysis and heavy/light ratios were quantified as described in the experimental procedures. Peptides for P450 1A2 (*A*), 2C8 (*B*), 2D6 (*C*), and 3A4 (*D*) were acquired in biological duplicate and presented as means ± SD.

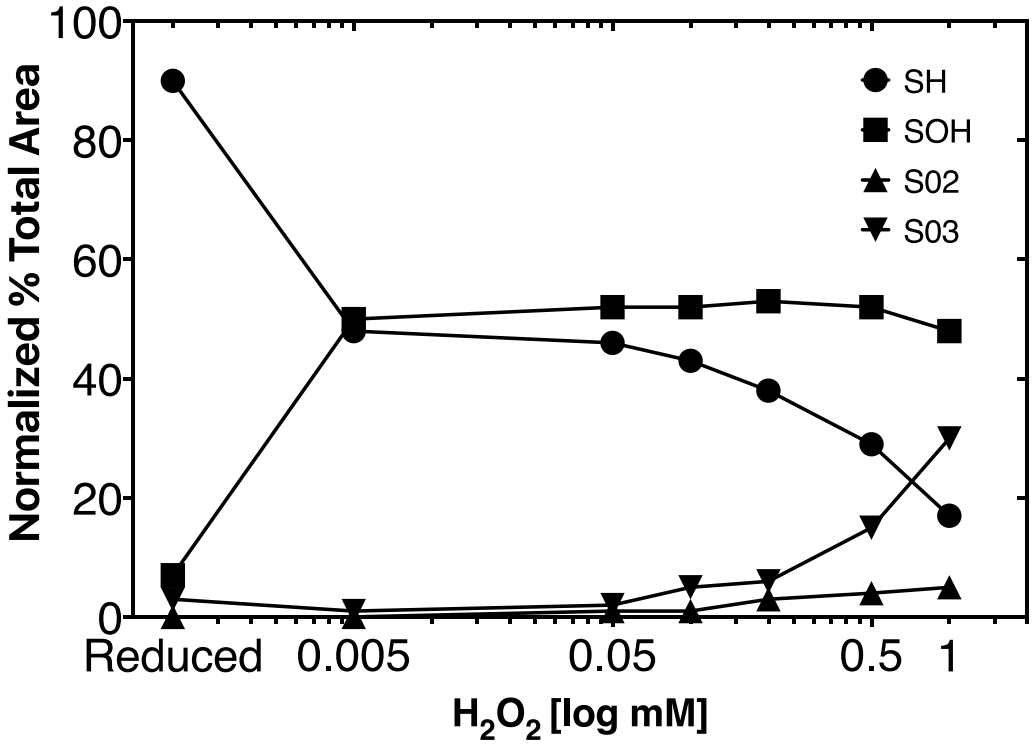

Figure 34. **Hyperoxidation of P450 3A4 Cys467.** Areas for cysteine-containing peptide VLQNFSFKP**C**K modified with d_0-iododimedone (SH), d_6-dimedone (SOH), sulfinic acid ($SO2^-$), and sulfonic acid ($SO3^-$) were normalized to areas for a proteotypic 3A4 peptide and each area is reported as a percentage of the summed total of the four modified peptides.

4.3. Discussion

ICDID labeling of mouse liver and kidney microsomes provided the interesting finding that P450s other than the Family 4 enzymes previously described (112) also contained oxidatively modified cysteines. This result may seem inconsistent with previous activation studies involving other P450s and DTT, which found no significant differences in enzymatic rates (112). However, this is probably because it is a regular practice to dialyze against buffer containing dithiothreitol when removing imidazole after His_6-nitrilotriacetic acid/nickel (NTA-Ni^{2+}) purification and storage. P450 4A11 is unusual in its ability to readily oxidize in the presence of air, at least under these conditions. This labeling strategy was then expanded to human liver and kidney microsomes. Many other P450s were found to be sulfenylated in these samples (Table 4). While our knowledge of transcriptional regulation, sequence variation, and inhibition is extensive for many P450s (9), information about post-translational regulation of P450s is limited, with research mostly focused on glycosylation, phosphorylation, ubiquitination, and nitration (198,235). Cysteine oxidation may play a role in physiological post-translational regulation as well.

Cysteine sulfenylation was found in a total of 57 drug metabolizing enzymes. The group includes UGTs, FMOs, and carboxylesterases, suggesting that many microsomal enzymes are modified by oxidation. These results seem reasonable, in that many enzymes have been found to be regulated by oxidation to form cysteine sulfenic acids (123,236). Additionally, a comparison of the results presented here and a recent study on sulfenylated proteins (127) revealed that 21% (kidney microsomes) and 14% (liver microsomes) of proteins were identified in both datasets. This comparison may indicate that the RKO adenocarcinoma cell line studied by Gupta *et al.* (38) likely has similar basal

proteins that are oxidized. More in-depth studies of the non-P450 enzymes will be required to further verify sensitivity of catalytic activity to oxidation and effects that oxidation may have on activity and regulation.

Relative quantitation of the modified cysteines (Table 4, Fig. 30) yielded similar levels of d_6-dimedone labeling, which may be due in part to the one-hour incubation time with microsomes. While dimedone has been shown to be selective, the low reactivity of dimedone with sulfenic acids requires extended incubation times to achieve sufficient labeling (rate of 0.8 min^{-1} under the reported conditions) (146,195). The modified cysteines identified are likely sensitive to oxidation, but the amount of labeling observed may be representative of the equilibrium of a saturated system. Overall, 35% and 33% of all cysteine-containing peptides identified were modified with d_6-dimedone in kidney and liver microsomes, respectively. Since more than half of the peptides identified were not sulfenylated, the likelihood that this observation is an artifact would seem to be low. Furthermore, a control experiment was performed in which kidney and liver tissues were homogenized in 5 mM TCEP, fractionated into microsomes, labeled, and subjected to LC-MS/MS analysis as described in Experimental Procedures. Approximately 6% of all cysteine-containing peptides from both the kidney and liver samples were modified with d_6-dimedone suggesting that some sulfenylated cysteines may have been inaccessible to the TCEP reducing agent (Fig. 35). Also, the fractionation and labeling protocol may have introduced a slightly oxidative environment that modified highly susceptible cysteines. Nevertheless, this experiment serves as a control for the positive results.

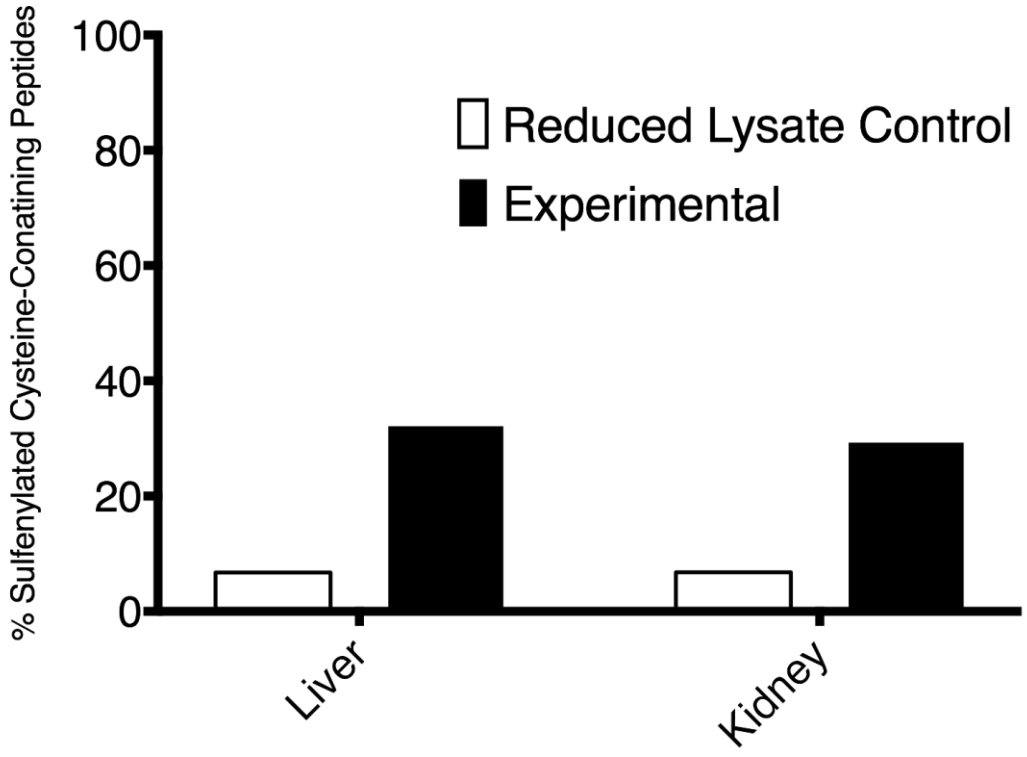

Figure 35. **Reduced Lysate Control Experiment of Human Microsomes.** Kidney and liver tissue were homogenized in 5 mM TCEP, fractionated into microsomes, labeled, and subjected to LC-MS/MS analysis as described in Experimental Procedures. The number of d_6-dimedone-labeled cysteine-containing peptides was taken as a percentage of total cysteine-containing peptides identified at 5% FDR. Reduced lysate control samples were acquired using a 30-minute gradient.

Four drug metabolizing P450s were chosen for more in-depth oxidative inhibition studies. Interestingly, P450 1A2 was resistant to oxidation, as established by spectral, inhibition, and dimedone labeling studies (Figs. 31A, 32A, and 33A, respectively). Of note was the hyperoxidation of Cys-159, which did not affect the catalytic activity of P450 1A2 (Fig. 33A). This ancillary cysteine is positioned away from the active site, and its modification has a negligible effect on function (Fig. 36A). The resistance to oxidation is proposed to be related to access of oxidants or to stabilization of the heme-thiol system due to either the surrounding amino acid residues or the overall structure of the protein. This resistance may also allow for P450 1A2 to have such a high degree of enzymatic uncoupling and production of H_2O_2 when compared to other P450s (Table 3).

P450 2C8 showed an 87% loss of catalytic activity at 1 mM H_2O_2, compared to the reduced control (Fig. 32B). This inhibition may seem surprising in light of the large number of cysteines contained in P450 2C8 (Fig. 37), but the heme thiol peptide was still modified. Despite the gradual loss of activity, the spectral and ICDID labeling studies (Figs. 31B and 33B) showed a high loss and recovery of the heme-thiol ligand spectrally and significant sulfenic acid labeling (Cys-435). Only four of the 16 thiols were quantified because of the clustering of thiols in the sequence; i.e., some tryptic peptides contained up to four cysteines and spanned >25 amino acids.

P450 2D6 showed less loss of activity (70%) than P450 2C8 but still exhibited inhibition after treatment with H_2O_2 (Fig. 32C) and the ability of the heme-thiol to re-ligand the heme iron in the spectral analysis (Fig 31C). This diminished response was reflected in ICDID analysis, which showed lower amounts of sulfenylation of the heme-thiol Cys-443 and also Cys-191 (Fig. 33C).

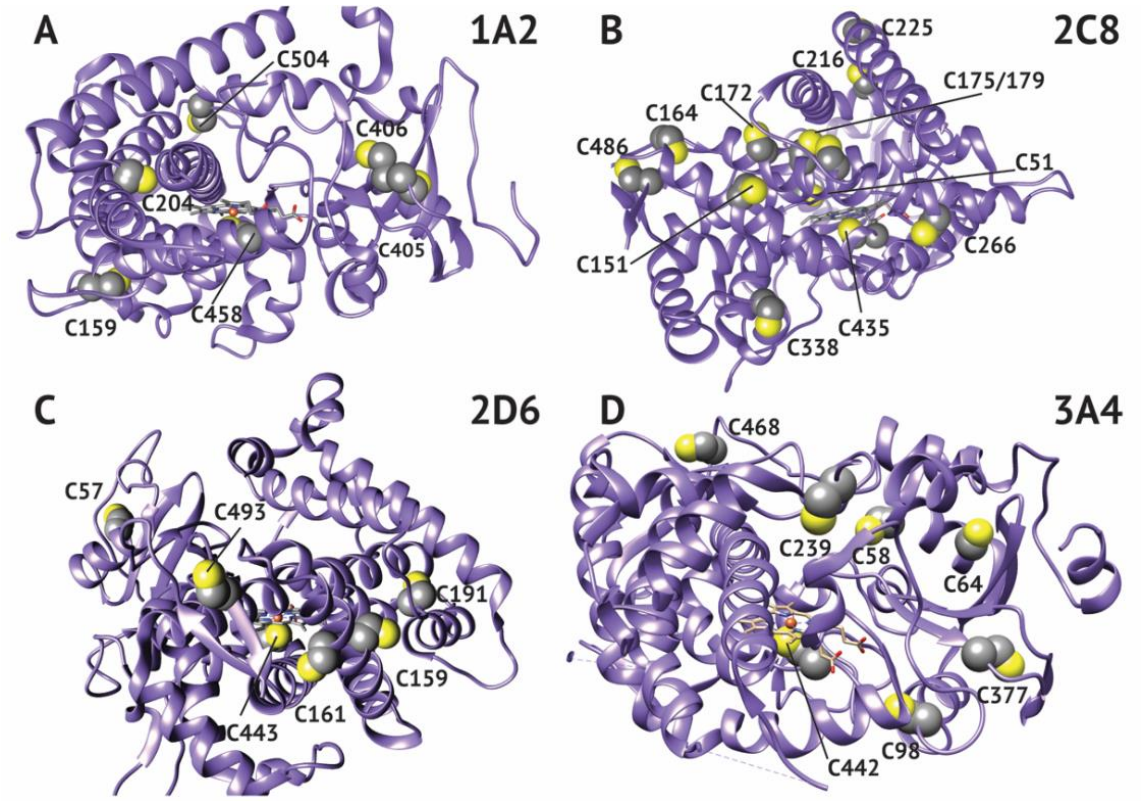

Figure 36. **Crystal Structure of P450s Highlighting Positions of Cysteine.** Crystal structures for 1A2 (A), 2C8 (B), 2D6 (C), and 3A4 (D) were adapted from the RCSB Protein Data Bank (rcsb.org). The Accession numbers used were 2HI4, 2NNJ, 5TFT, and 5G5J, respectively.

Oxidized P450 3A4 showed an inability of the heme-thiol to re-ligand to the heme-iron (after dithionite reduction), as judged by the spectra (Fig. 31D). This irreversible inactivation is proposed to be related to stabilization of the oxidized thiol by surrounding residues and is a unique feature among P450s tested. ICDID labeling showed high amounts of sulfenylation on several cysteine thiols, including the heme-thiol Cys-442, indicating a high susceptibility to oxidation. This sensitivity of the non-heme thiols can be considered in light of the report that a cysteine-depleted variant of P450 3A4 has increased activity compared to the wild-type enzyme (113). We concur that the cysteine residues are not essential but that the presence of the (non-heme peptide) sulfenic acids appears to be inhibitory to catalytic activity, through an unknown mechanism.

There has been difficulty designing probes that can directly measure local bursts of H_2O_2 and not just a cumulative or average amount over time, especially in prominent production areas such as the plasma membrane, endoplasmic reticulum, and peroxisomes (237). When looking at redox issues, one mainly focuses on a concentration of H_2O_2 for which the effect can be reversed. This is the case for three of the four P450s tested spectrally, suggesting that this treatment does not irreversibly destroy the protein.

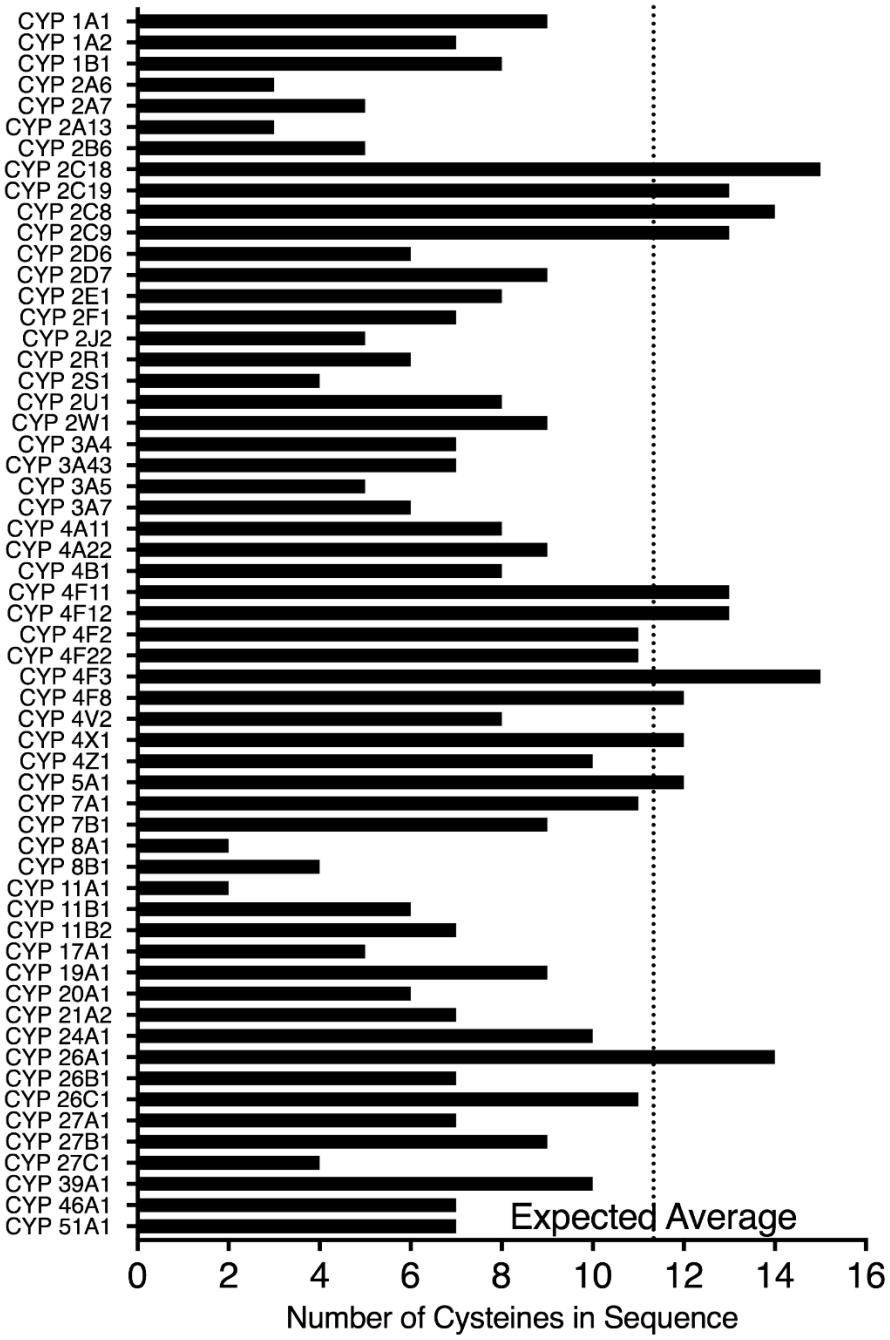

Figure 37. **Number of Cysteines Found in Human P450 Enzymes.** Cysteines of P450 sequences obtained from Uniprot (uniport.org) were counted. The average number of cysteines in the human proteome (49) was applied to the average length of human P450s (501 amino acids) to determine the expected number of cysteines to be 11.3 (dotted vertical line).

These spectral studies have been challenging to interpret because the proper conditions have not yet been identified to produce a homogenous sample of stable sulfenylated heme-thiol cysteine P450 protein in large quantities. The spectral studies in conjunction, with the observation that sulfenylated cysteines cause enzymatic inhibition, lead us to believe this phenomenon is blocking steps in the P450 catalytic cycle. This blocked step may be reduction of the heme iron. This could be occurring directly (most likely) or through a peripheral oxidation that limits reductase binding. It may also reduce the ability for the heme iron to bind oxygen (or carbon monoxide in the case of the inhibitory or spectral studies, respectively). The spectral studies also require physical changes (i.e., vacuum and slight bubbling) to remove the existing oxygen in the sample. These manipulation conditions likely affect some protein irreversibly, accounting at least in part for the cytochrome P420 seen in the pre-reduced samples. What is most relevant is the change in the amount of P450 seen between the reductase- and dithionite -reduced spectra (Fig. 31).

It has been known that some P450s can catalyze reactions with the use of H_2O_2 alone for quite some time (238-241). Also, mutating residues around the proximal heme ligand allows for alterations in both the heme redox potential and reactivity (242). P450s are also known to produce H_2O_2 as a byproduct of catalysis (32). CYP4A11 H_2O_2 production was measured to be 5 μM min^{-1}, which would be 25 nmol H_2O_2 min^{-1} under our experimental conditions (112). Typical incubation times would likely not produce enough H_2O_2 to produce an inhibitory effect. These data point to the significance of H_2O_2 in the catalytic cycle of P450s and of the residues surrounding the heme-thiol ligand. The presence of a biological mechanism that limits potentially harmful H_2O_2 shunting in certain

mammalian P450s but is not present in others (e.g. P450 1A2), seems reasonable but more studies are needed to evaluate the significance of this phenomenon.

Our finding of both thiol-sensitive and insensitive P450s expands the knowledge of potential post-translational modifications found in drug metabolizing enzymes. In general, cysteines are reactive, underrepresented in the proteome, and conserved among proteomes (243). In an accounting of all human P450s, the number of cysteines varies from two to 15 (Fig. 37). Using the average length of all human P450s (501 amino acids) and the overall percent of cysteines found in the human proteome (2.3% (243)), the expected number of cysteines in human P450s would be 11. Due to the deviation from this number, these cysteines may play important roles other than heme coordination and further investigation in cellular systems may be of interest.

The drug metabolizing enzymes found to be sulfenylated in our proteomic screen and the subsequent validation of the inhibitory nature of this oxidative modification in P450s pose many new questions and potentially provide insight into the biological regulation of P450s. In further studies, a major goal is to determine the biological role of heme-thiolate sulfenylation and its relevance to oxidative stress.

Chapter V

5. Conclusions and Future Directions

5.1. A New Model of P450 Regulation

Using methods, I developed which are outlined in Chapter II, I was able to propose a mechanism of oxidative inhibition in most P450s discussed in Chapters III and IV. This method centers around the concept that sulfenylation can occur on the heme-thiolate cysteine of the enzyme (Fig. 6). This phenomenon was observed in P450s 2C8, 2D6, 3A4, and 4A11 but not P450 1A2. Although this idea had been proposed by Hrycay and O'Brien in the 1970s, it was never tested to my knowledge (84).

ICDID labeling of human and mouse liver and kidney microsomes revealed that many P450s and other drug metabolizing enzymes are sulfenylated. This finding, as well as *in vitro* results with recombinant enzymes, warrants further investigation. Determining how sulfenylation plays a role in drug metabolism *in vivo* may be important an important discovery because of the known interplay between drug AUCs and inflammatory diseases where an increase in ROS leads to longer drug half-lives(118). This question is difficult to answer because of the pleiotropic effects ROS have in cells. Targeting P450 enzymes directly with a specific form of oxidant (i.e. ROS) would be extremely difficult, and proper controls would have to be in place for meaningful results.

One of the more important questions is how would oxidation of some P450 enzymes confer a biological advantage through heme-thiolate sulfenylation? There are currently several theories postulated:

(1) Limitation of futile cycling. Without substrate present P450 enzymes are still able to be reduced allowing the ferrous heme to bind oxygen. The activated oxygen will

likely be released as superoxide if no substrate is present. The heme-thiolate ligand provides sufficient electronegativity to allow for this oxygen binding, by attracting electron density to the thiolate cysteine. It follows then, that the lack of this fifth ligand would prevent oxygen binding. This could be beneficial for the cell because it limits oxygen and NADPH consumption while reducing the amount of harmful ROS produced. This theory could be tested in cells (primary hepatocytes) by examining the amount of heme-thiolate sulfenylation present in P450s with or without substrate available. If this theory were proven, then presumably, sulfenylation would be high before adding substrate. After incubation of cells with substrate, a decrease in heme-thiolate sulfenylation would be correlative with enzymatic activity.

(2) Inactivation during an oxidative insult. In times of oxidative stress, cells require reducing equivalents in the forms of GSH and NAD(P)H to counteract and survive the stress. P450s that are mainly xenobiotic metabolizing enzymes (e.g. P450s 3A4 and 2D6) are not necessary for survival and can therefore be inactivated until the redox environment reaches homeostasis. This would allow NADPH to be diverted to enzymes devoted to combating oxidative stress, e.g. glutathione reductase and thioredoxin reductase. Testing this hypothesis would involve exposing cells (primary hepatocytes) to an oxidative insult such as paraquat or H_2O_2 and measuring the enzymatic activity, sulfenylation, and NADPH levels. In this case, a decrease in NADPH levels would lead to a loss in enzymatic activity and a concomitant increase in heme-thiolate sulfenylation would be observed.

(3) Oxidative modification as a degradation signal. Oxidation of cysteine thiols has been shown to signal proteins for degradation. This is likely a protective mechanism as oxidation can modify other amino acids, inactivating proteins. Since cysteines are the most

easily oxidized amino acids in proteins, this process serves as a chemosensor for damage. Downregulation of P450s due as response to inflammation has been reported (118). Oxidation of thiols of P450s may be an acute response to inflammatory insults. With the goal of removing (in)active P450 enzyme before P450 genes are transcriptionally downregulated. To test this hypothesis, a proteasome inhibitor such as carfilzomib could be used in conjunction with an oxidative insult to cells (primary hepatocytes). Presumably a buildup of sulfenylated protein would be observed compared to the control sample with no oxidative stress.

(4) Another reason for this modification would be the one originally proposed by Hrycay and O'Brien (110). They postulated that formation of a sulfenic acid on the heme-thiolate ligand would alter the spin state of the iron, allowing the enzyme to more easily catalyze peroxidatic reactions with H_2O_2 being a co-substrate, donating oxygen. This could be possible because P450 enzymes can utilize oxygen from peroxides and peracids as co-substrates. During oxidative stress events, highly reactive lipid peroxides and isoprostanes are produced. This P450 sulfenylation may allow for more facile metabolism of these damaging oxidative byproducts. This can be first tested *in vitro* by oxidizing recombinant P450, removing H_2O_2 and adding an organic peroxide such as cumene-peroxide with a peroxidatic substrate such as *N, N, N', N',* tetramethyl-p-phenylenediamine. This would provide a spectroscopic signal to measure the relative activities of oxidized and reduced protein. Testing this hypothesis in cells would be markedly more difficult. Using a cell line devoid of P450 expression, P450 enzymes (and reductase if necessary) could be stably transfected and the amount of total peroxides or

isoprostanes could be measured after an oxidative insult. This measurement of peroxides in conjunction with sulfenylation could verify that this mechanism is possible.

```
1A2:  FGMGKRRCIGEVLA
2C8:  FSAGKRICAGEGLA
2D6:  FSAGRRACLGEPLA
3A4:  FGSGPRNCIGMRFA
4A11: FSGGSRNCIGKQFA
```

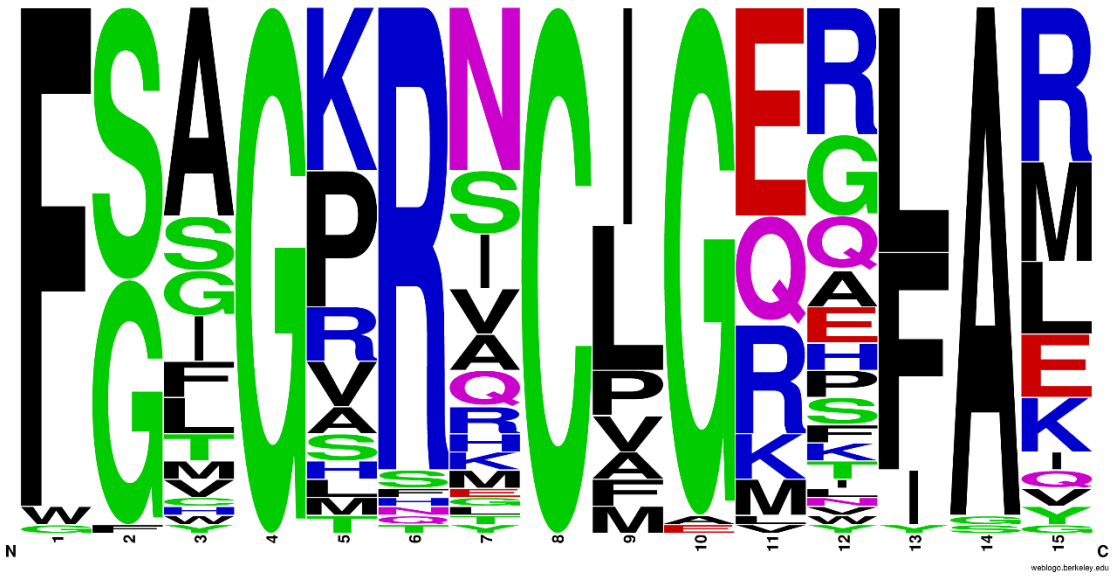

Figure 38. **Sequence Alignment of Surrounding Heme-thiolate Amino Acids.** Alignment of P450s tested (Top). Probability matrix of amino acids surrounding the heme-thiolate ligand generated from sequences of all 57 human P450s (Bottom). Bottom matrix generated through WebLogo (244).

5.2. P450s Have Three Classes of Redox Sensitivity

As mentioned in Chapter IV, P450 enzymes seem to fall into three classes following oxidative stress: (1) Redox Insensitive (1A2), (2) heme-thiolate sensitive (2C8, 2D6, 4A11), and (3) ancillary thiol sensitive (3A4). These results were a surprising discovery. From the proteomic screen of sulfenylation in human liver and kidney microsomes (Table 5), I hypothesized that all P450s would share a similar sensitivity to H_2O_2. However, *in vitro* results with recombinant enzymes show that this is not the case.

Regarding heme-thiolate sulfenylation, I believe the differences in susceptibility observed arise from a combination of several factors. From only testing five P450s thus far, data is limited for general inferences. However, there are differences in the amino acid sequence surrounding the heme-thiolate cysteine (Fig. 38). P450 1A2 has three positive charges in close proximity to the cysteine ligand possibly adding a stabilizing the thiol-iron interaction. This surrounding amino acid sequence is known to favor the stability of the thiolate coordination to the heme iron. The known consensus sequence for the heme thiolate cysteine is Phe-x-x-Gly-x-Arg-x-Cys-x-Gly (245). As “x” indicates a variable amino acid, this region is not well conserved and there are likely differences in the strength and stability of the heme-thiolate ligand among P450s (Fig. 38). These potential disparities among P450s could lead to differences in liganding ability of the thiol to the heme-iron yielding breakage of the thiol-iron coordination and exposing the thiol to potential oxidation by H_2O_2.This may happen more frequently with P450 4A11 (and other Subfamily 4A P450s), because the heme is covalently linked to the protein. Therefore, movement of the heme would be more limited than if it were free, potentially allowing the heme-thiol to recoordinate without having to “find” the iron. This heme thiolate coordination is much

likely weaker when the sixth ligand is water coordinated to ferric heme compared to molecular oxygen or CO bound to ferrous heme. This ferrous bound form has much higher electronegativity which pulls the thiolate closer, strengthening the bond.

Ancillary cysteines are likely to have surrounding microenvironments that stabilize the thiolate and allow for interaction with ROS such as H_2O_2. Oxidation of these cysteines may disrupt the P450 interaction with its substrate or redox partner, inhibiting its catalytic activity.

5.3. Future Directions

There are five major questions that need to be addressed to increase the understanding of H_2O_2-dependent inhibition of P450s through sulfenic acid formation of the heme-thiolate ligand:

(1) How do other P450 enzymes respond to H_2O_2 preincubation? As noted previously in Section 5.2, the results I have acquired are limited in consideration of the number of P450 enzymes currently known. By measuring redox sensitivity of more enzymes, we should be able to build an inference model to predict enzyme sensitivity. This could be a powerful tool that one could use to putatively predict redox classes of P450s without testing them *in vitro*.

(2) Is this modification biologically relevant and, if so, what is the function of this modification? Biological relevance of a posttranslational modification on an amino acid required for catalytic activity is inherently difficult to test because, in this case, the cysteine cannot be mutated without compromising the enzyme. I have highlighted several possible biological reasons for heme-thiolate sulfenylation in Section 5.1, and testing these in

primary hepatocytes would provide a biological context and give more insight into the biological mechanism of the modification.

(3) Is heme-thiolate sulfenylation reversible enzymatically *in vitro* and *in vivo*? Results from studies with microsomes (*in situ*) indicate that this modification likely occurs *in vivo*. Since sulfenic acids can easily be further oxidized to sulfonic acids or disulfide bonds a mechanism likely exists to reduce the sulfenic acid to a thiolate, allowing for recoordination with the heme iron. This can be performed using classical biochemical methods, e.g. preincubating the P450 with H_2O_2 and adding back both active and inactive (heat treated) cytosolic and microsomal cellular fractions. Reversibility could be measured by a cellular fraction concentration-dependent increase in activity relative to the control. Reversibility could then be followed through chromatographic separations of either the cytosol or microsomes. Finally, proteomic analysis followed by recombinant expression of candidate proteins could be utilized to determine the protein with the reversible activity.

(4) How stable is the heme-thiolate sulfenic acid? From my experiments, it seems that the sulfenic acid is stable enough to survive through several manipulations (e.g. preparation of microsomes, and *in vitro* spectroscopic and activity assays), but the mechanism behind this stability is not known. Molecular dynamics (MD) simulations of P450 with a heme-thiolate sulfenic acid present may provide some insight into this phenomenon. Using the knowledge gained from MD, mutations could be made to the enzyme and tested *in vitro* for either resistance or susceptibility to redox modification. These experiments, in conjunction with question (1), can help define the amino acids required for sulfenic acid formation and stability.

(5) How are the electronics of the heme-iron affected by heme-thiolate sulfenylation? Understanding the changes conferred to the heme iron by sulfenic acid formation would help to further understand the catalytic competency of the oxidized enzyme. There are some limitations in studying this, however. Instruments to study this type of electronic change to the iron such as Mössbauer spectroscopy or electron paramagnetic resonance (EPR) require large quantities of homogenously oxidized protein in high concentration. Currently I have not been able to oxidize high concentrations of P450 consistently. The main issue with producing homogenously oxidized P450 is the concern that the oxidation will aggregate the protein at high concentrations.

In summary, a novel oxidative regulatory method for P450 enzymes has been discovered. By showing that P450s have differential sensitivity to H_2O_2, I have raised more questions than I currently have answers for in the field of drug metabolism. I hope that determining the *in vivo* relevance of heme-thiolate sulfenylation will help to provide more context in the future.

PUBLICATIONS

Albertolle, M.E., Guengerich, F.P. (2018) The Relationships Between Cytochromes P450 and H_2O_2: Production, Reaction, and Inhibition. *J. Inorg. Biochem.* 186, 228-234 (Review)

Albertolle, M. E., Phan, T. T. N., Pozzi, A., Guengerich, F. P. (2018) Sulfenylation of Human Microsomal Liver and Kidney Cytochromes P450 and Other Drug Metabolizing Enzymes as a Response to Redox Alteration. *Mol. Cell. Proteomics.* 17, 889-900

Johnson, K. M., Phan, T. T. N., **Albertolle, M. E.,** and Guengerich, F. P. (2017) Human mitochondrial cytochrome P450 27C1 is localized in skin and preferentially desaturates trans-retinol to 3,4-dehydroretinol. *J. Biol. Chem.* 292, 13672-13687

Albertolle, M. E., Kim, D., Nagy, L. D., Yun, C. H., Pozzi, A., Savas, U., Johnson, E. F., and Guengerich, F. P. (2017) Heme-thiolate sulfenylation of human cytochrome P450 4A11 functions as a redox switch for catalytic inhibition. *J. Biol. Chem.* 292, 11230-11242

Federspiel, J. D., Codreanu, S. G., Goyal, S., **Albertolle, M. E.,** Lowe, E., Teague, J., Wong, H., Guengerich, F. P., and Liebler, D. C. (2016) Specificity of Protein Covalent Modification by the Electrophilic Proteasome Inhibitor Carfilzomib in Human Cells. *Mol. Cell. Proteomics.* **15**, 3233-3242

LITERATURE CITED

1. Omura, T., and Sato, R. (1964) The carbon monoxide-binding pigment of liver microsomes. I. evidence for its hemoprotein nature. *J Biol Chem* **239**, 2370-2378
2. Beaune, P., Dansette, P., Flinois, J. P., Columelli, S., Mansuy, D., and Leroux, J. P. (1979) Partial purification of human liver cytochrome P 450. *Biochem Biophys Res Commun* **88**, 826-832
3. Kaschnitz, R. M., and Coon, M. J. (1975) Drug and fatty acid hydroxylation by solubilized human liver microsomal cytochrome P-450-phospholipid requirement. *Biochem Pharmacol* **24**, 295-297
4. Wang, P., Mason, P. S., and Guengerich, F. P. (1980) Purification of human liver cytochrome P-450 and comparison to the enzyme isolated from rat liver. *Arch Biochem Biophys* **199**, 206-219
5. Nelson, D. R. (2009) The cytochrome p450 homepage. *Hum Genomics* **4**, 59-65
6. Fewell, S. W., Travers, K. J., Weissman, J. S., and Brodsky, J. L. (2001) The action of molecular chaperones in the early secretory pathway. *Annu Rev Genet* **35**, 149-191
7. Saaranen, M. J., Karala, A. R., Lappi, A. K., and Ruddock, L. W. (2010) The role of dehydroascorbate in disulfide bond formation. *Antioxid Redox Signal* **12**, 15-25
8. Tavender, T. J., Springate, J. J., and Bulleid, N. J. (2010) Recycling of peroxiredoxin IV provides a novel pathway for disulphide formation in the endoplasmic reticulum. *EMBO J* **29**, 4185-4197
9. Guengerich, F. P. (2015) Human cytochrome P450 enzymes. in *Cytochrome P450: Structure, Mechanism, and Biochemistry* (Ortiz de Montellano, P. R. ed.), 4th Ed., Springer, New York. pp 523-785
10. Gotoh, S., Ohno, M., Yoshinari, K., Negishi, M., and Kawajiri, K. (2015) Nuclear receptor-mediated regulation of cytochrome P450 genes. in *Cytochrome P450: Structure, Mechanism, and Biochemistry* (Ortiz de Montellano, P. R. ed.), 4th Ed., Springer, New York. pp 787-811
11. Zeeshan, H. M., Lee, G. H., Kim, H. R., and Chae, H. J. (2016) Endoplasmic reticulum stress and associated ROS. *Int J Mol Sci* **17**, 327
12. Ohyama, Y., and Yamasaki, T. (2004) Eight cytochrome P450s catalyze vitamin D metabolism. *Front Biosci* **9**, 3007-3018
13. Raner, G. M., Vaz, A. D., and Coon, M. J. (1996) Metabolism of all-*trans*, 9-*cis*, and 13-*cis* isomers of retinal by purified isozymes of microsomal cytochrome P450 and mechanism-based inhibition of retinoid oxidation by citral. *Mol Pharmacol* **49**, 515-522
14. Ingelman-Sundberg, M., Sim, S. C., Gomez, A., and Rodriguez-Antona, C. (2007) Influence of cytochrome P450 polymorphisms on drug therapies: pharmacogenetic, pharmacoepigenetic and clinical aspects. *Pharmacol Ther* **116**, 496-526
15. Lee, C. R., Goldstein, J. A., and Pieper, J. A. (2002) Cytochrome P450 2C9 polymorphisms: a comprehensive review of the in-vitro and human data. *Pharmacogenetics* **12**, 251-263
16. Zordoky, B. N., and El-Kadi, A. O. (2010) Effect of cytochrome P450 polymorphism on arachidonic acid metabolism and their impact on cardiovascular diseases. *Pharmacol Ther* **125**, 446-463

17. Rendic, S., and Guengerich, F. P. (2015) Survey of human oxidoreductases and cytochrome P450 enzymes involved in the metabolism of xenobiotic and natural chemicals. *Chem Res Toxicol* **28**, 38-42
18. Saravanakumar, A., Sadighi, A., Ryu, R., and Akhlaghi, F. (2018) Contribution of cytochrome P450 and other enzymes to the metabolism of FDA approved drugs between 2005–2016. *Drug Metabolism and Pharmacokinetics* **33**, S36
19. Schuler, M. A. (2015) P450s in plants, insects, and their fungal pathogens. in *Cytochrome P450: Structure, Mechanism, and Biochemistry* (Ortiz de Montellano, P. R. ed.), Springer International Publishing, Cham. pp 409-449
20. Khmelevtsova, L. E., Sazykin, I. S., Sazykina, M. A., and Seliverstova, E. Y. (2017) Prokaryotic cytochromes P450. *Applied Biochemistry and Microbiology* **53**, 401-409
21. Girvan, H. M., and Munro, A. W. (2016) Applications of microbial cytochrome P450 enzymes in biotechnology and synthetic biology. *Curr Opin Chem Biol* **31**, 136-145
22. Hrycay, E. G., and Bandiera, S. M. (2015) Monooxygenase, peroxidase and peroxygenase properties and reaction mechanisms of cytochrome P450 enzymes. in *Monooxygenase, Peroxidase and Peroxygenase Properties and Mechanisms of Cytochrome P450* (Hrycay, E. G., and Bandiera, S. M. eds.), Springer International Publishing, Cham. pp 1-61
23. Hassan, F., Mohammed, G., Mahdi, S., Mahdy, S., Win, Y.-F., Mohammed, S., and Yousif, E. (2016) Cytochrome P450s in breast cancer. *Res. J. Pharm., Biol. Chem. Sci.* **7**, 248-256
24. Kenaan, C., Zhang, H., Shea, E. V., and Hollenberg, P. F. (2011) Uncovering the role of hydrophobic residues in cytochrome P450-cytochrome P450 reductase interactions. *Biochemistry* **50**, 3957-3967
25. Hamdane, D., Xia, C., Im, S. C., Zhang, H., Kim, J. J., and Waskell, L. (2009) Structure and function of an NADPH-cytochrome P450 oxidoreductase in an open conformation capable of reducing cytochrome P450. *J Biol Chem* **284**, 11374-11384
26. Fenton, H. J. H. (1894) LXXIII.—Oxidation of tartaric acid in presence of iron. *J Chem Soc Trans* **65**, 899-910
27. Walling, C. (1975) Fenton's reagent revisited. *Acc Chem Res* **8**, 125-131
28. Yoshimoto, F. K., Guengerich, F. P. (2018) Formation and cleavage of C–C bonds by enzymatic oxidation–reduction reactions. *Chem Rev*, **118**, 6573-6655.
29. Albertolle, M. E., and Peter Guengerich, F. (2018) The relationships between cytochromes P450 and H_2O_2: Production, reaction, and inhibition. *J Inorg Biochem* **186**, 228-234
30. Gillette, J. R., Brodie, B. B., and La Du, B. N. (1957) The oxidation of drugs by liver microsomes: on the role of TPNH and oxygen. *J Pharmacol Exp Ther* **119**, 532-540
31. Sasame, H. A., Mitchell, J. R., Thorgeirsson, S., and Gillette, J. R. (1973) Relationship between NADH and NADPH oxidation during drug metabolism. *Drug Metab Dispos* **1**, 150-155
32. Nordblom, G. D., and Coon, M. J. (1977) Hydrogen peroxide formation and stoichiometry of hydroxylation reactions catalyzed by highly purified liver microsomal cytochrome P-450. *Arch Biochem Biophys* **180**, 343-347

33. Gorsky, L. D., Koop, D. R., and Coon, M. J. (1984) On the stoichiometry of the oxidase and monooxygenase reactions catalyzed by liver microsomal cytochrome P-450: products of oxygen reduction. *J Biol Chem* **259**, 6812-6817
34. Aust, S. D., Roerig, D. L., and Pederson, T. C. (1972) Evidence for superoxide generation by NADPH-cytochrome C reductase of rat liver microsomes. *Biochem Biophys Res Commun* **47**, 1133-1137
35. Sligar, S. G., Lipscomb, J. D., Debrunner, P. G., and Gunsalus, I. C. (1974) Superoxide anion production by the autoxidation of cytochrome $P450_{cam}$. *Biochem Biophys Res Commun* **61**, 290-296
36. Di Luzio, N. R., and Hartman, A. D. (1967) Role of lipid peroxidation in the pathogenesis of the ethanol-induced fatty liver. *Fed Proc* **26**, 1436-1442
37. Ekstrom, G., and Ingelman-Sundberg, M. (1989) Rat liver microsomal NADPH-supported oxidase activity and lipid peroxidation dependent on ethanol-inducible cytochrome P-450 (P-450IIE1). *Biochem Pharmacol* **38**, 1313-1319
38. Ekstrom, G., von Bahr, C., and Ingelman-Sundberg, M. (1989) Human liver microsomal cytochrome P-450IIE1. Immunological evaluation of its contribution to microsomal ethanol oxidation, carbon tetrachloride reduction and NADPH oxidase activity. *Biochem Pharmacol* **38**, 689-693
39. Cederbaum, A. I. (2017) Chapter 31 - Cytochrome P450 and oxidative stress in the liver. in *Liver Pathophysiology*, Academic Press, Boston. pp 401-419
40. Sharrock, M., Debrunner, P. G., Schulz, C., Lipscomb, J. D., Marshall, V., and Gunsalus, I. C. (1976) Cytochrome $P450_{cam}$ and its complexes. Mossbauer parameters of the heme iron. *Biochim Biophys Acta* **420**, 8-26
41. Harris, D., Loew, G., and Waskell, L. (2001) Calculation of the electronic structure and spectra of model cytochrome P450 compound I. *J Inorg Biochem* **83**, 309-318
42. Denisov, I. G., Grinkova, Y. V., Baas, B. J., and Sligar, S. G. (2006) The ferrous-dioxygen intermediate in human cytochrome P450 3A4. Substrate dependence of formation and decay kinetics. *J Biol Chem* **281**, 23313-23318
43. Eisenstein, L., Debey, P., and Douzou, P. (1977) $P450_{cam}$: oxygenated complexes stabilized at low temperature. *Biochem Biophys Res Commun* **77**, 1377-1383
44. Sevrioukova, I. F., and Peterson, J. A. (1995) Reaction of carbon monoxide and molecular oxygen with $P450_{terp}$ (CYP108) and $P450_{BM-3}$ (CYP102). *Arch Biochem Biophys* **317**, 397-404
45. Yoshioka, S., Tosha, T., Takahashi, S., Ishimori, K., Hori, H., and Morishima, I. (2002) Roles of the proximal hydrogen bonding network in cytochrome P450cam-catalyzed oxygenation. *J Am Chem Soc* **124**, 14571-14579
46. Galinato, M. G., Spolitak, T., Ballou, D. P., and Lehnert, N. (2011) Elucidating the role of the proximal cysteine hydrogen-bonding network in ferric cytochrome P450cam and corresponding mutants using magnetic circular dichroism spectroscopy. *Biochemistry* **50**, 1053-1069
47. Yosca, T. H., Ledray, A. P., Ngo, J., and Green, M. T. (2017) A new look at the role of thiolate ligation in cytochrome P450. *J Biol Inorg Chem* **22**, 209-220
48. Valko, M., Leibfritz, D., Moncol, J., Cronin, M. T., Mazur, M., and Telser, J. (2007) Free radicals and antioxidants in normal physiological functions and human disease. *Int J Biochem Cell Biol* **39**, 44-84

49. Veith, A., and Moorthy, B. (2018) Role of cytochrome P450s In the generation and metabolism of reactive oxygen species. *Curr Opin Toxicol* **7**, 44-51
50. Huang, Q., Deshmukh, R. S., Ericksen, S. S., Tu, Y., and Szklarz, G. D. (2012) Preferred binding orientations of phenacetin in CYP1A1 and CYP1A2 are associated with isoform-selective metabolism. *Drug Metab Dispos* **40**, 2324-2331
51. Mayuzumi, H., Sambongi, C., Hiroya, K., Shimizu, T., Tateishi, T., and Hatano, M. (1993) Effect of mutations of ionic amino acids of cytochrome P450 1A2 on catalytic activities toward 7-ethoxycoumarin and methanol. *Biochemistry* **32**, 5622-5628
52. Yun, C. H., Kim, K. H., Calcutt, M. W., and Guengerich, F. P. (2005) Kinetic analysis of oxidation of coumarins by human cytochrome P450 2A6. *J Biol Chem* **280**, 12279-12291
53. Bumpus, N. N., and Hollenberg, P. F. (2008) Investigation of the mechanisms underlying the differential effects of the K262R mutation of P450 2B6 on catalytic activity. *Mol Pharmacol* **74**, 990-999
54. Mosher, C. M., Hummel, M. A., Tracy, T. S., and Rettie, A. E. (2008) Functional analysis of phenylalanine residues in the active site of cytochrome P450 2C9. *Biochemistry* **47**, 11725-11734
55. Guengerich, F. P., Miller, G. P., Hanna, I. H., Sato, H., and Martin, M. V. (2002) Oxidation of methoxyphenethylamines by cytochrome P450 2D6. Analysis of rate-limiting steps. *J Biol Chem* **277**, 33711-33719
56. Hanna, I. H., Krauser, J. A., Cai, H., Kim, M. S., and Guengerich, F. P. (2001) Diversity in mechanisms of substrate oxidation by cytochrome P450 2D6. Lack of an allosteric role of NADPH-cytochrome P450 reductase in catalytic regioselectivity. *J Biol Chem* **276**, 39553-39561
57. Patten, C. J., and Koch, P. (1995) Baculovirus expression of human P450 2E1 and cytochrome b5: spectral and catalytic properties and effect of b5 on the stoichiometry of P450 2E1-catalyzed reactions. *Arch Biochem Biophys* **317**, 504-513
58. McDougle, D. R., Palaria, A., Magnetta, E., Meling, D. D., and Das, A. (2013) Functional studies of N-terminally modified CYP2J2 epoxygenase in model lipid bilayers. *Protein Sci* **22**, 964-979
59. Grinkova, Y. V., Denisov, I. G., McLean, M. A., and Sligar, S. G. (2013) Oxidase uncoupling in heme monooxygenases: human cytochrome P450 CYP3A4 in Nanodiscs. *Biochem Biophys Res Commun* **430**, 1223-1227
60. Kim, D., Cha, G. S., Nagy, L. D., Yun, C. H., and Guengerich, F. P. (2014) Kinetic analysis of lauric acid hydroxylation by human cytochrome P450 4A11. *Biochemistry* **53**, 6161-6172
61. Peng, H. M., Im, S. C., Pearl, N. M., Turcu, A. F., Rege, J., Waskell, L., and Auchus, R. J. (2016) Cytochrome b5 activates the 17,20-lyase activity of human cytochrome P450 17A1 by increasing the coupling of NADPH consumption to androgen production. *Biochemistry* **55**, 4356-4365
62. Khatri, Y., Gregory, M. C., Grinkova, Y. V., Denisov, I. G., and Sligar, S. G. (2014) Active site proton delivery and the lyase activity of human CYP17A1. *Biochem Biophys Res Commun* **443**, 179-184

63. Sohl, C. D., and Guengerich, F. P. (2010) Kinetic analysis of the three-step steroid aromatase reaction of human cytochrome P450 19A1. *J Biol Chem* **285**, 17734-17743
64. Bansal, S., Anandatheerthavarada, H. K., Prabu, G. K., Milne, G. L., Martin, M. V., Guengerich, F. P., and Avadhani, N. G. (2013) Human cytochrome P450 2E1 mutations that alter mitochondrial targeting efficiency and susceptibility to ethanol-induced toxicity in cellular models. *J Biol Chem* **288**, 12627-12644
65. Bansal, S., Liu, C. P., Sepuri, N. B., Anandatheerthavarada, H. K., Selvaraj, V., Hoek, J., Milne, G. L., Guengerich, F. P., and Avadhani, N. G. (2010) Mitochondria-targeted cytochrome P450 2E1 induces oxidative damage and augments alcohol-mediated oxidative stress. *J Biol Chem* **285**, 24609-24619
66. Imaoka, S., Osada, M., Minamiyama, Y., Yukimura, T., Toyokuni, S., Takemura, S., Hiroi, T., and Funae, Y. (2004) Role of phenobarbital-inducible cytochrome P450s as a source of active oxygen species in DNA-oxidation. *Cancer Lett* **203**, 117-125
67. Puntarulo, S., and Cederbaum, A. I. (1998) Production of reactive oxygen species by microsomes enriched in specific human cytochrome P450 enzymes. *Free Radic Biol Med* **24**, 1324-1330
68. Roberts, B. J., Song, B. J., Soh, Y., Park, S. S., and Shoaf, S. E. (1995) Ethanol induces CYP2E1 by protein stabilization. Role of ubiquitin conjugation in the rapid degradation of CYP2E1. *J Biol Chem* **270**, 29632-29635
69. Sun, X., Ai, M., Wang, Y., Shen, S., Gu, Y., Jin, Y., Zhou, Z., Long, Y., and Yu, Q. (2013) Selective induction of tumor cell apoptosis by a novel P450-mediated reactive oxygen species (ROS) inducer methyl 3-(4-nitrophenyl) propiolate. *J Biol Chem* **288**, 8826-8837
70. Tang, Y., Scheef, E. A., Gurel, Z., Sorenson, C. M., Jefcoate, C. R., and Sheibani, N. (2010) CYP1B1 and endothelial nitric oxide synthase combine to sustain proangiogenic functions of endothelial cells under hyperoxic stress. *Am J Physiol Cell Physiol* **298**, C665-678
71. Dostalek, M., Brooks, J. D., Hardy, K. D., Milne, G. L., Moore, M. M., Sharma, S., Morrow, J. D., and Guengerich, F. P. (2007) In vivo oxidative damage in rats is associated with barbiturate response but not other cytochrome P450 inducers. *Mol Pharmacol* **72**, 1419-1424
72. Dostalek, M., Hardy, K. D., Milne, G. L., Morrow, J. D., Chen, C., Gonzalez, F. J., Gu, J., Ding, X., Johnson, D. A., Johnson, J. A., Martin, M. V., and Guengerich, F. P. (2008) Development of oxidative stress by cytochrome P450 induction in rodents is selective for barbiturates and related to loss of pyridine nucleotide-dependent protective systems. *J Biol Chem* **283**, 17147-17157
73. Couroucli, X. I., Liang, Y. H., Jiang, W., Wang, L., Barrios, R., Yang, P., and Moorthy, B. (2011) Prenatal administration of the cytochrome P4501A inducer, Beta-naphthoflavone (BNF), attenuates hyperoxic lung injury in newborn mice: implications for bronchopulmonary dysplasia (BPD) in premature infants. *Toxicol Appl Pharmacol* **256**, 83-94
74. Maturu, P., Wei-Liang, Y., Jiang, W., Wang, L., Lingappan, K., Barrios, R., Liang, Y., Moorthy, B., and Couroucli, X. I. (2017) Newborn mice lacking the gene for Cyp1a1 are more susceptible to oxygen-mediated lung injury, and are rescued by

postnatal beta-naphthoflavone administration: implications for bronchopulmonary dysplasia in premature infants. *Toxicol Sci* **157**, 260-271
75. Kalyanaraman, B., Darley-Usmar, V., Davies, K. J., Dennery, P. A., Forman, H. J., Grisham, M. B., Mann, G. E., Moore, K., Roberts, L. J., 2nd, and Ischiropoulos, H. (2012) Measuring reactive oxygen and nitrogen species with fluorescent probes: challenges and limitations. *Free Radic Biol Med* **52**, 1-6
76. Kalyanaraman, B., Hardy, M., Podsiadly, R., Cheng, G., and Zielonka, J. (2017) Recent developments in detection of superoxide radical anion and hydrogen peroxide: Opportunities, challenges, and implications in redox signaling. *Arch Biochem Biophys* **617**, 38-47
77. Kadiiska, M. B., Gladen, B. C., Baird, D. D., Graham, L. B., Parker, C. E., Ames, B. N., Basu, S., Fitzgerald, G. A., Lawson, J. A., Marnett, L. J., Morrow, J. D., Murray, D. M., Plastaras, J., Roberts, L. J., 2nd, Rokach, J., Shigenaga, M. K., Sun, J., Walter, P. B., Tomer, K. B., Barrett, J. C., and Mason, R. P. (2005) Biomarkers of oxidative stress study III. Effects of the nonsteroidal anti-inflammatory agents indomethacin and meclofenamic acid on measurements of oxidative products of lipids in CCl_4 poisoning. *Free Radic Biol Med* **38**, 711-718
78. Persson, J. O., Terelius, Y., and Ingelman-Sundberg, M. (1990) Cytochrome P-450-dependent formation of reactive oxygen radicals: isozyme-specific inhibition of P-450-mediated reduction of oxygen and carbon tetrachloride. *Xenobiotica* **20**, 887-900
79. Cederbaum, A. I. (2010) Role of CYP2E1 in ethanol-induced oxidant stress, fatty liver and hepatotoxicity. *Dig Dis* **28**, 802-811
80. Caro, A. A., and Cederbaum, A. I. (2004) Oxidative stress, toxicology, and pharmacology of CYP2E1. *Annu Rev Pharmacol Toxicol* **44**, 27-42
81. Emanuele, S., D'Anneo, A., Calvaruso, G., Cernigliaro, C., Giuliano, M., and Lauricella, M. (2018) The double-edged sword profile of redox signaling: oxidative events as molecular switches in the balance between cell physiology and cancer. *Chem Res Toxicol* **31**, 201-210
82. Morrow, J. D., Awad, J. A., Boss, H. J., Blair, I. A., and Roberts, L. J., II. (1992) Non-cyclooxygenase-derived prostanoids (F_2-isoprostanes) are formed *in situ* on phospholipids. *Proc Natl Acad Sci U.S.A.* **89**, 10721-10725
83. Hollmann, F., and Arends, I. W. (2012) Enzyme initiated radical polymerizations. *Polymers* **4**, 759-793
84. Hrycay, E. G., Gustafsson, J. A., Ingelman-Sundberg, M., and Ernster, L. (1975) Sodium periodate, sodium chlorite, and organic hydroperoxides as hydroxylating agents in hepatic microsomal steroid hydroxylation reactions catalyzed by cytochrome P-450. *FEBS Lett* **56**, 161-165
85. Nordblom, G. D., White, R. E., and Coon, M. J. (1976) Studies on hydroperoxide-dependent substrate hydroxylation by purified liver microsomal cytochrome P-450. *Arch Biochem Biophys* **175**, 524-533
86. Shoji, O., and Watanabe, Y. (2014) Peroxygenase reactions catalyzed by cytochromes P450. *J Biol Inorg Chem* **19**, 529-539
87. Lichtenberger, F., Nastainczyk, W., and Ullrich, V. (1976) Cytochrome P450 as an oxene transferase. *Biochem Biophys Res Commun* **70**, 939-946

88. Hrycay, E. G., Gustafsson, J. A., Ingelman-Sundberg, M., and Ernster, L. (1975) Sodium periodate, sodium chloride, organic hydroperoxides, and H_2O_2 as hydroxylating agents in steroid hydroxylation reactions catalyzed by partially purified cytochrome P-450. *Biochem Biophys Res Commun* **66**, 209-216
89. Rittle, J., and Green, M. T. (2010) Cytochrome P450 compound I: capture, characterization, and C-H bond activation kinetics. *Science* **330**, 933-937
90. O'Brien P, J., and Rahimtula, A. (1975) Involvement of cytochrome P-450 in the intracellular formation of lipid peroxides. *J Agric Food Chem* **23**, 154-158
91. Plastaras, J. P., Guengerich, F. P., Nebert, D. W., and Marnett, L. J. (2000) Xenobiotic-metabolizing cytochromes P450 convert prostaglandin endoperoxide to hydroxyheptadecatrienoic acid and the mutagen, malondialdehyde. *J Biol Chem* **275**, 11784-11790
92. Chefson, A., Zhao, J., and Auclair, K. (2006) Replacement of natural cofactors by selected hydrogen peroxide donors or organic peroxides results in improved activity for CYP3A4 and CYP2D6. *Chembiochem* **7**, 916-919
93. Muindi, J. F., and Young, C. W. (1993) Lipid hydroperoxides greatly increase the rate of oxidative catabolism of all-*trans*-retinoic acid by human cell culture microsomes genetically enriched in specified cytochrome P-450 isoforms. *Cancer Res* **53**, 1226-1229
94. Tan, L., Wang, H. M., and Falardeau, P. (1972) 17-hydroperoxypregnenes. 3. Studies on their role as possible precursors in the biosynthesis of adrenosteroid hormones. *Biochim Biophys Acta* **260**, 731-740
95. van Lier, J. E., Mast, N., and Pikuleva, I. A. (2015) Cholesterol hydroperoxides as substrates for cholesterol-metabolizing cytochrome P450 enzymes and alternative sources of 25-hydroxycholesterol and other oxysterols. *Angew Chem Int Ed* **54**, 11138-11142
96. Ademowo, O. S., Dias, H. K. I., Burton, D. G. A., and Griffiths, H. R. (2017) Lipid (per) oxidation in mitochondria: an emerging target in the ageing process? *Biogerontology* **18**, 859-879
97. Renneberg, R., Scheller, F., Ruckpaul, K., Pirrwitz, J., and Mohr, P. (1978) NADPH and H_2O_2-dependent reactions of cytochrome P-450_{LM} compared with peroxidase catalysis. *FEBS Lett* **96**, 349-353
98. Fujishiro, T., Shoji, O., Nagano, S., Sugimoto, H., Shiro, Y., and Watanabe, Y. (2011) Crystal structure of H_2O_2-dependent cytochrome $P450_{SP\alpha}$ with its bound fatty acid substrate: insight into the regioselective hydroxylation of fatty acids at the alpha position. *J Biol Chem* **286**, 29941-29950
99. Belcher, J., McLean, K. J., Matthews, S., Woodward, L. S., Fisher, K., Rigby, S. E., Nelson, D. R., Potts, D., Baynham, M. T., Parker, D. A., Leys, D., and Munro, A. W. (2014) Structure and biochemical properties of the alkene producing cytochrome P450 $OleT_{JE}$ (CYP152L1) from the *Jeotgalicoccus* sp. 8456 bacterium. *J Biol Chem* **289**, 6535-6550
100. Hsieh, C. H., and Makris, T. M. (2016) Expanding the substrate scope and reactivity of cytochrome P450 OleT. *Biochem Biophys Res Commun* **476**, 462-466
101. Rude, M. A., Baron, T. S., Brubaker, S., Alibhai, M., Del Cardayre, S. B., and Schirmer, A. (2011) Terminal olefin (1-alkene) biosynthesis by a novel P450 fatty

acid decarboxylase from Jeotgalicoccus species. *Appl Environ Microbiol* **77**, 1718-1727
102. Cirino, P. C., and Arnold, F. H. (2003) A self-sufficient peroxide-driven hydroxylation biocatalyst. *Angew Chem Int Ed Engl* **42**, 3299-3301
103. Lundemo, M. T., and Woodley, J. M. (2015) Guidelines for development and implementation of biocatalytic P450 processes. *Appl Microbiol Biotechnol* **99**, 2465-2483
104. Ma, N., Chen, Z., Chen, J., Chen, J., Wang, C., Zhou, H., Yao, L., Shoji, O., Watanabe, Y., and Cong, Z. (2018) Dual-functional small molecules for generating an efficient cytochrome $P450_{BM3}$ peroxygenase. *Angew Chem Int Ed Engl*
105. Girhard, M., Kunigk, E., Tihovsky, S., Shumyantseva, V. V., and Urlacher, V. B. (2013) Light-driven biocatalysis with cytochrome P450 peroxygenases. *Biotechnol Appl Biochem* **60**, 111-118
106. Wang, Y., Lan, D., Durrani, R., and Hollmann, F. (2017) Peroxygenases en route to becoming dream catalysts. What are the opportunities and challenges? *Curr Opin Chem Biol* **37**, 1-9
107. Joo, H., Lin, Z., and Arnold, F. H. (1999) Laboratory evolution of peroxide-mediated cytochrome P450 hydroxylation. *Nature* **399**, 670-673
108. Wei, Y., Ang, E. L., and Zhao, H. (2017) Recent developments in the application of P450 based biocatalysts. *Curr Opin Chem Biol* **43**, 1-7
109. Guengerich, F. P. (1978) Destruction of heme and hemoproteins mediated by liver microsomal reduced nicotinamide adenine dinucleotide phosphate-cytochrome P-450 reductase. *Biochemistry* **17**, 3633-3639
110. Hrycay, E. G., and O'Brien, P. J. (1971) Cytochrome P-450 as a microsomal peroxidase utilizing a lipid peroxide substrate. *Arch Biochem Biophys* **147**, 14-27
111. Albertolle, M., Phan, T. T. N., Pozzi, A., and Guengerich, F. P. (2018) Sulfenylation of human liver and kidney microsomal cytochromes P450 and other drug metabolizing enzymes as a response to redox alteration. *Mol Cell Proteomics* **17**, 889-900
112. Albertolle, M. E., Kim, D., Nagy, L. D., Yun, C. H., Pozzi, A., Savas, U., Johnson, E. F., and Guengerich, F. P. (2017) Heme-thiolate sulfenylation of human cytochrome P450 4A11 functions as a redox switch for catalytic inhibition. *J Biol Chem* **292**, 11230-11242
113. Sevrioukova, I. F. (2017) High-level production and properties of the cysteine-depleted cytochrome P450 3A4. *Biochemistry* **56**, 3058-3067
114. Schmith, V. D., and Foss, J. F. (2010) Inflammation: planning for a source of pharmacokinetic/pharmacodynamic variability in translational studies. *Clin Pharmacol Ther* **87**, 488-491
115. Lang, C. C., Brown, R. M., Kinirons, M. T., Deathridge, M. A., Guengerich, F. P., Kelleher, D., O'Briain, D. S., Ghishan, F. K., and Wood, A. J. (1996) Decreased intestinal CYP3A in celiac disease: reversal after successful gluten-free diet: a potential source of interindividual variability in first-pass drug metabolism. *Clin Pharmacol Ther* **59**, 41-46
116. Ling, S., Lewanczuk, R. Z., Russell, A. S., Ihejirika, B., and Jamali, F. (2009) Influence of controlled rheumatoid arthritis on the action and disposition of verapamil: focus on infliximab. *J Clin Pharmacol* **49**, 301-311

117. Frye, R. F., Schneider, V. M., Frye, C. S., and Feldman, A. M. (2002) Plasma levels of TNF-α and IL-6 are inversely related to cytochrome P450-dependent drug metabolism in patients with congestive heart failure. *J Card Fail* **8**, 315-319
118. Coutant, D. E., and Hall, S. D. (2018) Disease-drug interactions in inflammatory states via effects on CYP-mediated drug clearance. *J Clin Pharmacol* **58**, 849-863
119. Coutant, D. E., and Hall, S. D. (2018) Disease-drug interactions in inflammatory states via effects on CYP-mediated drug clearance. *J Clin Pharmacol* **58**, 849-863
120. Hoffmann, M. H., and Griffiths, H. R. (2018) The dual role of ROS in autoimmune and inflammatory diseases: Evidence from preclinical models. *Free Radic Biol Med* **125**, 62-71
121. Lee, C. M., Pohl, J., and Morgan, E. T. (2009) Dual mechanisms of CYP3A protein regulation by proinflammatory cytokine stimulation in primary hepatocyte cultures. *Drug Metab Dispos* **37**, 865-872
122. Lee, C. M., Tripathi, S., and Morgan, E. T. (2017) Nitric oxide-regulated proteolysis of human CYP2B6 via the ubiquitin-proteasome system. *Free Radic Biol Med* **108**, 478-486
123. Peralta, D., Bronowska, A. K., Morgan, B., Doka, E., Van Laer, K., Nagy, P., Grater, F., and Dick, T. P. (2015) A proton relay enhances H_2O_2 sensitivity of GAPDH to facilitate metabolic adaptation. *Nat Chem Biol* **11**, 156-163
124. Holmgren, A., Johansson, C., Berndt, C., Lonn, M. E., Hudemann, C., and Lillig, C. H. (2005) Thiol redox control via thioredoxin and glutaredoxin systems. *Biochem Soc Trans* **33**, 1375-1377
125. Johansson, C., Lillig, C. H., and Holmgren, A. (2004) Human mitochondrial glutaredoxin reduces S-glutathionylated proteins with high affinity accepting electrons from either glutathione or thioredoxin reductase. *J Biol Chem* **279**, 7537-7543
126. Mailloux, R. J., and Treberg, J. R. (2016) Protein S-glutathionlyation links energy metabolism to redox signaling in mitochondria. *Redox Biol* **8**, 110-118
127. Gupta, V., Yang, J., Liebler, D. C., and Carroll, K. S. (2017) Diverse redoxome reactivity profiles of carbon nucleophiles. *J Am Chem Soc* **139**, 5588-5595
128. Trujillo, M., Alvarez, B., and Radi, R. (2016) One- and two-electron oxidation of thiols: mechanisms, kinetics and biological fates. *Free Radic Res* **50**, 150-171
129. Fries, K. (1912) Über α-anthrachinon-sulfensäure. *Eur J Inorg Chem* **45**, 2965-2973
130. Bruice, T. C., and Markiw, R. (1957) The synthesis of a disulfenic acid. anthraquinone-1, 4-disulfenic acid. *J Am Chem Soc* **79**, 3150-3153
131. Groitl, B., and Jakob, U. (2014) Thiol-based redox switches. *Biochim Biophys Acta* **1844**, 1335-1343
132. Fernandes, A. P., and Holmgren, A. (2004) Glutaredoxins: glutathione-dependent redox enzymes with functions far beyond a simple thioredoxin backup system. *Antioxid Redox Signal* **6**, 63-74
133. Gupta, V., and Carroll, K. S. (2014) Sulfenic acid chemistry, detection and cellular lifetime. *Biochim Biophys Acta* **1840**, 847-875
134. Pihl, A., and Lange, R. (1962) The interaction of oxidized glutathione, cystamine monosulfoxide, and tetrathionate with the-SH groups of rabbit muscle D-glyceraldehyde 3-phosphate dehydrogenase. *J Biol Chem* **237**, 1356-1362

135. Sanner, T., and Pihl, A. (1963) Studies on the active--SH group of papain and on the mechanism of papain activation by thiols. *J Biol Chem* **238**, 165-171
136. Allison, W. S. (1976) Formation and reactions of sulfenic acids in proteins. *Acc Chem Res* **9**, 293-299
137. Lin, W. S., Armstrong, D. A., and Gaucher, G. M. (1975) Formation and repair of papain sulfenic acid. *Can J Biochem* **53**, 298-307
138. Poole, L. B., and Claiborne, A. (1989) The non-flavin redox center of the streptococcal NADH peroxidase. II. Evidence for a stabilized cysteine-sulfenic acid. *J Biol Chem* **264**, 12330-12338
139. Storz, G., Tartaglia, L. A., and Ames, B. N. (1990) Transcriptional regulator of oxidative stress-inducible genes: direct activation by oxidation. *Science* **248**, 189-194
140. Truong, T. H., Ung, P. M., Palde, P. B., Paulsen, C. E., Schlessinger, A., and Carroll, K. S. (2016) Molecular basis for redox activation of epidermal growth factor receptor kinase. *Cell Chem Biol* **23**, 837-848
141. Zhou, H., Singh, H., Parsons, Z. D., Lewis, S. M., Bhattacharya, S., Seiner, D. R., LaButti, J. N., Reilly, T. J., Tanner, J. J., and Gates, K. S. (2011) The biological buffer bicarbonate/CO_2 potentiates H_2O_2-mediated inactivation of protein tyrosine phosphatases. *J Am Chem Soc* **133**, 15803-15805
142. Fourquet, S., Guerois, R., Biard, D., and Toledano, M. B. (2010) Activation of NRF2 by nitrosative agents and H_2O_2 involves KEAP1 disulfide formation. *J Biol Chem* **285**, 8463-8471
143. Suzuki, T., and Yamamoto, M. (2017) Stress-sensing mechanisms and the physiological roles of the Keap1-Nrf2 system during cellular stress. *J Biol Chem* **292**, 16817-16824
144. Yang, J., Carroll, K. S., and Liebler, D. C. (2016) The expanding landscape of the thiol redox proteome. *Mol Cell Proteomics* **15**, 1-11
145. Alcock, L. J., Perkins, M. V., and Chalker, J. M. (2018) Chemical methods for mapping cysteine oxidation. *Chem Soc Rev* **47**, 231-268
146. Gupta, V., Paritala, H., and Carroll, K. S. (2016) Reactivity, selectivity, and stability in sulfenic acid detection: A comparative study of nucleophilic and electrophilic probes. *Bioconjug Chem* **27**, 1411-1418
147. Zanger, U. M., and Schwab, M. (2013) Cytochrome P450 enzymes in drug metabolism: regulation of gene expression, enzyme activities, and impact of genetic variation. *Pharmacol Ther* **138**, 103-141
148. Tompkins, L. M., and Wallace, A. D. (2007) Mechanisms of cytochrome P450 induction. *J Biochem Mol Toxicol* **21**, 176-181
149. Correia, M. A., Wang, Y., Kim, S. M., and Guan, S. (2014) Hepatic cytochrome P450 ubiquitination: conformational phosphodegrons for E2/E3 recognition? *IUBMB Life* **66**, 78-88
150. Oesch-Bartlomowicz, B., and Oesch, F. (2003) Cytochrome-P450 phosphorylation as a functional switch. *Arch Biochem Biophys* **409**, 228-234
151. Redlich, G., Zanger, U. M., Riedmaier, S., Bache, N., Giessing, A. B., Eisenacher, M., Stephan, C., Meyer, H. E., Jensen, O. N., and Marcus, K. (2008) Distinction between human cytochrome P450 (CYP) isoforms and identification of new phosphorylation sites by mass spectrometry. *J Proteome Res* **7**, 4678-4688

152. Butler, M. A., Lang, N. P., Young, J. F., Caporaso, N. E., Vineis, P., Hayes, R. B., Teitel, C. H., Massengill, J. P., Lawsen, M. F., and Kadlubar, F. F. (1992) Determination of CYP1A2 and NAT2 phenotypes in human populations by analysis of caffeine urinary metabolites. *Pharmacogenetics* **2**, 116-127
153. Rendic, S. (2002) Summary of information on human CYP enzymes: human P450 metabolism data. *Drug Metab Rev* **34**, 83-448
154. Wang, J. S., Neuvonen, M., Wen, X., Backman, J. T., and Neuvonen, P. J. (2002) Gemfibrozil inhibits CYP2C8-mediated cerivastatin metabolism in human liver microsomes. *Drug Metab Dispos* **30**, 1352-1356
155. Yano, J. K., Wester, M. R., Schoch, G. A., Griffin, K. J., Stout, C. D., and Johnson, E. F. (2004) The structure of human microsomal cytochrome P450 3A4 determined by X-ray crystallography to 2.05-Å resolution. *J Biol Chem* **279**, 38091-38094
156. Pirmohamed, M. (2013) Drug-grapefruit juice interactions: two mechanisms are clear but individual responses vary. *BMJ* **346**, f1
157. Fan, F., Ge, Y., Lv, W., Elliott, M. R., Muroya, Y., Hirata, T., Booz, G. W., and Roman, R. J. (2016) Molecular mechanisms and cell signaling of 20-hydroxyeicosatetraenoic acid in vascular pathophysiology. *Front Biosci (Landmark Ed)* **21**, 1427-1463
158. Capdevila, J. H., Wang, W., and Falck, J. R. (2015) Arachidonic acid monooxygenase: Genetic and biochemical approaches to physiological/pathophysiological relevance. *Prostaglandins Other Lipid Mediat* **120**, 40-49
159. Lasker, J. M., Chen, W. B., Wolf, I., Bloswick, B. P., Wilson, P. D., and Powell, P. K. (2000) Formation of 20-hydroxyeicosatetraenoic acid, a vasoactive and natriuretic eicosanoid, in human kidney. Role of Cyp4F2 and Cyp4A11. *J Biol Chem* **275**, 4118-4126
160. Wu, C. C., and Schwartzman, M. L. (2011) The role of 20-HETE in androgen-mediated hypertension. *Prostaglandins Other Lipid Mediat* **96**, 45-53
161. Garcia, V., and Schwartzman, M. L. (2016) Recent developments on the vascular effects of 20-hydroxyeicosatetraenoic acid. *Curr Opin Nephrol Hypertens* **26**, 74-82
162. Gainer, J. V., Bellamine, A., Dawson, E. P., Womble, K. E., Grant, S. W., Wang, Y., Cupples, L. A., Guo, C. Y., Demissie, S., O'Donnell, C. J., Brown, N. J., Waterman, M. R., and Capdevila, J. H. (2005) Functional variant of CYP4A11 20-hydroxyeicosatetraenoic acid synthase is associated with essential hypertension. *Circulation* **111**, 63-69
163. Mayer, B., Lieb, W., Gotz, A., Konig, I. R., Aherrahrou, Z., Thiemig, A., Holmer, S., Hengstenberg, C., Doering, A., Loewel, H., Hense, H. W., Schunkert, H., and Erdmann, J. (2005) Association of the T8590C polymorphism of CYP4A11 with hypertension in the MONICA Augsburg echocardiographic substudy. *Hypertension* **46**, 766-771
164. Gainer, J. V., Lipkowitz, M. S., Yu, C., Waterman, M. R., Dawson, E. P., Capdevila, J. H., and Brown, N. J. (2008) Association of a CYP4A11 variant and blood pressure in black men. *J Am Soc Nephrol* **19**, 1606-1612
165. Laffer, C. L., Gainer, J. V., Waterman, M. R., Capdevila, J. H., Laniado-Schwartzman, M., Nasjletti, A., Brown, N. J., and Elijovich, F. (2008) The T8590C

polymorphism of CYP4A11 and 20-hydroxyeicosatetraenoic acid in essential hypertension. *Hypertension* **51**, 767-772
166. Zhang, R., Lu, J., Hu, C., Wang, C., Yu, W., Ma, X., Bao, Y., Xiang, K., Guan, Y., and Jia, W. (2011) A common polymorphism of CYP4A11 is associated with blood pressure in a Chinese population. *Hypertens Res* **34**, 645-648
167. Williams, J. S., Hopkins, P. N., Jeunemaitre, X., and Brown, N. J. (2011) CYP4A11 T8590C polymorphism, salt-sensitive hypertension, and renal blood flow. *J Hypertens* **29**, 1913-1918
168. Wu, C. C., Gupta, T., Garcia, V., Ding, Y., and Schwartzman, M. L. (2014) 20-HETE and blood pressure regulation: clinical implications. *Cardiol Rev* **22**, 1-12
169. Bodiga, S., Gruenloh, S. K., Gao, Y., Manthati, V. L., Dubasi, N., Falck, J. R., Medhora, M., and Jacobs, E. R. (2010) 20-HETE-induced nitric oxide production in pulmonary artery endothelial cells is mediated by NADPH oxidase, H_2O_2, and PI3-kinase/Akt. *Am J Physiol Lung Cell Mol Physiol* **298**, L564-574
170. Cheng, J., Wu, C. C., Gotlinger, K. H., Zhang, F., Falck, J. R., Narsimhaswamy, D., and Schwartzman, M. L. (2010) 20-hydroxy-5,8,11,14-eicosatetraenoic acid mediates endothelial dysfunction via IkappaB kinase-dependent endothelial nitric-oxide synthase uncoupling. *J Pharmacol Exp Ther* **332**, 57-65
171. Han, Y., Zhao, H., Tang, H., Li, X., Tan, J., Zeng, Q., and Sun, C. (2013) 20-Hydroxyeicosatetraenoic acid mediates isolated heart ischemia/reperfusion injury by increasing NADPH oxidase-derived reactive oxygen species production. *Circ J* **77**, 1807-1816
172. Zeng, Q., Han, Y., Bao, Y., Li, W., Li, X., Shen, X., Wang, X., Yao, F., O'Rourke, S. T., and Sun, C. (2010) 20-HETE increases NADPH oxidase-derived ROS production and stimulates the L-type Ca^{2+} channel via a PKC-dependent mechanism in cardiomyocytes. *Am J Physiol Heart Circ Physiol* **299**, H1109-1117
173. Lakhkar, A., Dhagia, V., Joshi, S. R., Gotlinger, K., Patel, D., Sun, D., Wolin, M. S., Schwartzman, M. L., and Gupte, S. A. (2016) 20-HETE-induced mitochondrial superoxide production and inflammatory phenotype in vascular smooth muscle is prevented by glucose-6-phosphate dehydrogenase inhibition. *Am J Physiol Heart Circ Physiol* **310**, H1107-1117
174. Savas, U., Machemer, D. E., Hsu, M. H., Gaynor, P., Lasker, J. M., Tukey, R. H., and Johnson, E. F. (2009) Opposing roles of peroxisome proliferator-activated receptor alpha and growth hormone in the regulation of CYP4A11 expression in a transgenic mouse model. *J Biol Chem* **284**, 16541-16552
175. Savas, U., Wei, S., Hsu, M. H., Falck, J. R., Guengerich, F. P., Capdevila, J. H., and Johnson, E. F. (2016) 20-Hydroxyeicosatetraenoic acid (HETE) dependent hypertension in human cytochrome P450 (CYP) 4A11 transgenic mice: normalization of blood pressure by sodium restriction, hydrochlorothiazide, or blockade of the type 1 angiotensin II receptor *J Biol Chem* **291**, 16904-16919
176. Niwayama, S., Kurono, S., and Matsumoto, H. (2003) Synthesis of ^{13}C-labeled iodoacetanilide and application to quantitative peptide analysis by isotope differential mass spectrometry. *Bioorg Med Chem Lett* **13**, 2913-2916
177. Seo, Y. H., and Carroll, K. S. (2011) Quantification of protein sulfenic acid modifications using isotope-coded dimedone and iododimedone. *Angew Chem Int Ed Engl* **50**, 1342-1345

178. Sreedhar, B., Reddy, P. S., and Madhavi, M. (2007) Rapid and catalyst-free α-halogenation of ketones using *N*-halosuccinamides in DMSO. *Synthetic Commun* **37**, 4149-4156
179. Goswami, P., Ali, S., Khan, M. M., and Khan, A. T. (2007) Selective and effective oxone-catalysed α-iodination of ketones and 1, 3-dicarbonyl compounds in the solid state. *Arkivoc* **15**, 82-89
180. Shriner, R. L., and Todd, H. R. (1943) 5,5-Dimethyl-1,3-cyclohexanedione. *Organic Syntheses* **Collective Vol 2**, 200-202
181. Kawashima, H., Naganuma, T., Kusunose, E., Kono, T., Yasumoto, R., Sugimura, K., and Kishimoto, T. (2000) Human fatty acid *ω*-hydroxylase, *CYP4A11*: determination of complete genomic sequence and characterization of purified recombinant protein. *Arch Biochem Biophys* **378**, 333-339
182. Hanna, I. H., Teiber, J. F., Kokones, K. L., and Hollenberg, P. F. (1998) Role of the alanine at position 363 of cytochrome P450 2B2 in influencing the NADPH- and hydroperoxide-supported activities. *Arch Biochem Biophys* **350**, 324-332
183. Guengerich, F. P. (2005) Reduction of cytochrome b5 by NADPH-cytochrome P450 reductase. *Arch Biochem Biophys* **440**, 204-211
184. Sandhu, P., Guo, Z., Baba, T., Martin, M. V., Tukey, R. H., and Guengerich, F. P. (1994) Expression of modified human cytochrome P450 1A2 in *Escherichia coli*: stabilization, purification, spectral characterization, and catalytic activities of the enzyme. *Arch Biochem Biophys* **309**, 168-177
185. Bajpai, P., Srinivasan, S., Ghosh, J., Nagy, L. D., Wei, S., Guengerich, F. P., and Avadhani, N. G. (2014) Targeting of splice variants of human cytochrome P450 2C8 (CYP2C8) to mitochondria and their role in arachidonic acid metabolism and respiratory dysfunction. *J Biol Chem* **289**, 29614-29630
186. Hanna, I. H., Kim, M. S., and Guengerich, F. P. (2001) Heterologous expression of cytochrome P450 2D6 mutants, electron transfer, and catalysis of bufuralol hydroxylation: the role of aspartate 301 in structural integrity. *Arch Biochem Biophys* **393**, 255-261
187. Hosea, N. A., Miller, G. P., and Guengerich, F. P. (2000) Elucidation of distinct ligand binding sites for cytochrome P450 3A4. *Biochemistry* **39**, 5929-5939
188. Guengerich, F. P. (2014) Analysis and characterization of enzymes and nucleic acids relevant to toxicology. in *Hayes' Principles and Methods of Toxicology* (Hayes, A. W., and Kruger, C. L. eds.), 6th Ed., CRC Press-Taylor & Francis Boca Raton, FL. pp 1905-1964
189. Vaclavikova, R., Soucek, P., Svobodova, L., Anzenbacher, P., Simek, P., Guengerich, F. P., and Gut, I. (2004) Different in vitro metabolism of paclitaxel and docetaxel in humans, rats, pigs, and minipigs. *Drug Metab Dispos* **32**, 666-674
190. Yamazaki, H., Gillam, E. M., Dong, M. S., Johnson, W. W., Guengerich, F. P., and Shimada, T. (1997) Reconstitution of recombinant cytochrome P450 2C10(2C9) and comparison with cytochrome P450 3A4 and other forms: effects of cytochrome P450-P450 and cytochrome P450-b5 interactions. *Arch Biochem Biophys* **342**, 329-337
191. Yamazaki, H., Nakano, M., Imai, Y., Ueng, Y. F., Guengerich, F. P., and Shimada, T. (1996) Roles of cytochrome b5 in the oxidation of testosterone and nifedipine

by recombinant cytochrome P450 3A4 and by human liver microsomes. *Arch Biochem Biophys* **325**, 174-182
192. Pallan, P. S., Wang, C., Lei, L., Yoshimoto, F. K., Auchus, R. J., Waterman, M. R., Guengerich, F. P., and Egli, M. (2015) Human cytochrome P450 21A2, the major steroid 21-hydroxylase: Structure of the enzyme progesterone substrate comples and the rate-limiting C-H bond cleavage. *J Biol Chem* **290**, 13128-13143
193. Shimada, T., and Guengerich, F. P. (2006) Inhibition of human cytochrome P450 1A1-, 1A2-, and 1B1-mediated activation of procarcinogens to genotoxic metabolites by polycyclic aromatic hydrocarbons. *Chem Res Toxicol* **19**, 288-294
194. Yu, A. M., Dong, H. J., Lang, D., and Haining, R. L. (2001) Characterization of dextromethorphan *O*- and *N*-demethylation catalyzed by highly purified recombinant human CYP2D6. *Drug Metab. Dispos.* **29**, 1362-1365
195. Gupta, V., and Carroll, K. S. (2016) Profiling the reactivity of cyclic C-nucleophiles towards electrophilic sulfur in cysteine sulfenic acid. *Chem Sci* **7**, 400-415
196. Hansen, R. E., and Winther, J. R. (2009) An introduction to methods for analyzing thiols and disulfides: Reactions, reagents, and practical considerations. *Anal Biochem* **394**, 147-158
197. Tabb, D. L., Fernando, C. G., and Chambers, M. C. (2007) MyriMatch: highly accurate tandem mass spectral peptide identification by multivariate hypergeometric analysis. *Journal of proteome research* **6**, 654-661
198. Kim, S. M., Wang, Y., Nabavi, N., Liu, Y., and Correia, M. A. (2016) Hepatic cytochromes P450: structural degrons and barcodes, posttranslational modifications and cellular adapters in the ERAD-endgame. *Drug Metab Rev* **48**, 405-433
199. Holman, J. D., Ma, Z. Q., and Tabb, D. L. (2012) Identifying proteomic LC-MS/MS data sets with Bumbershoot and IDPicker. *Curr Protoc Bioinformatics* **Chapter 13**, Unit 13.17
200. Schilling, B., Rardin, M. J., MacLean, B. X., Zawadzka, A. M., Frewen, B. E., Cusack, M. P., Sorensen, D. J., Bereman, M. S., Jing, E., Wu, C. C., Verdin, E., Kahn, C. R., Maccoss, M. J., and Gibson, B. W. (2012) Platform-independent and label-free quantitation of proteomic data using MS1 extracted ion chromatograms in skyline: application to protein acetylation and phosphorylation. *Mol Cell Proteomics* **11**, 202-214
201. Sun, R., Fu, L., Liu, K. K., Tian, C. P., Yang, Y., Tallman, K. A., Porter, N. A., Liebler, D. C., and Yang, J. (2017) Chemoproteomics reveals chemical diversity and dynamics of 4-oxo-2-nonenal modifications in cells. *Mol Cell Proteomics* **16**, 1789-1800
202. Patil, P. V., and Ballou, D. P. (2000) The use of protocatechuate dioxygenase for maintaining anaerobic conditions in biochemical experiments. *Anal. Biochem.* **286**, 187-192
203. Burleigh, B. D., Jr., Foust, G. P., and Williams, C. H., Jr. (1969) A method for titrating oxygen-sensitive organic redox systems with reducing agents in solution. *Anal. Biochem.* **27**, 536-544
204. Guengerich, F. P., Krauser, J. A., and Johnson, W. W. (2004) Rate-limiting steps in oxidations catalyzed by rabbit cytochrome P450 1A2. *Biochemistry* **43**, 10775-10788

205. Searle, B. C. (2010) Scaffold: a bioinformatic tool for validating MS/MS-based proteomic studies. *Proteomics* **10**, 1265-1269
206. Kurono, S., Kurono, T., Komori, N., Niwayama, S., and Matsumoto, H. (2006) Quantitative proteome analysis using D-labeled *N*-ethylmaleimide and ^{13}C-labeled iodoacetanilide by matrix-assisted laser desorption/ionization time-of-flight mass spectrometry. *Bioorg Med Chem* **14**, 8197-8209
207. Zabet-Moghaddam, M., Kawamura, T., Yatagai, E., and Niwayama, S. (2008) Electrospray ionization mass spectroscopic analysis of peptides modified with *N*-ethylmaleimide or iodoacetanilide. *Bioorg Med Chem Lett* **18**, 4891-4895
208. Lin, T. Y., and Kim, P. S. (1989) Urea dependence of thiol-disulfide equilibria in thioredoxin: confirmation of the linkage relationship and a sensitive assay for structure. *Biochemistry* **28**, 5282-5287
209. Gupta, V., and Carroll, K. S. (2014) Sulfenic acid chemistry, detection and cellular lifetime. *Biochim Biophys Acta* **1840**, 847-875
210. Parsonage, D., and Claiborne, A. (1995) Analysis of the kinetic and redox properties of NADH peroxidase C42S and C42A mutants lacking the cysteine-sulfenic acid redox center. *Biochemistry* **34**, 435-441
211. Muller, D. N., Schmidt, C., Barbosa-Sicard, E., Wellner, M., Gross, V., Hercule, H., Markovic, M., Honeck, H., Luft, F. C., and Schunck, W. H. (2007) Mouse Cyp4a isoforms: enzymatic properties, gender- and strain-specific expression, and role in renal 20-hydroxyeicosatetraenoic acid formation. *Biochem J* **403**, 109-118
212. Chalkley, R. J., Baker, P. R., Huang, L., Hansen, K. C., Allen, N. P., Rexach, M., and Burlingame, A. L. (2005) Comprehensive analysis of a multidimensional liquid chromatography mass spectrometry dataset acquired on a quadrupole selecting, quadrupole collision cell, time-of-flight mass spectrometer: II. New developments in Protein Prospector allow for reliable and comprehensive automatic analysis of large datasets. *Mol Cell Proteomics* **4**, 1194-1204
213. Omura, T., and Sato, R. (1964) The carbon monoxide-binding pigment of liver microsomes. II. Solubilization, purification, and properties. *J Biol Chem* **239**, 2379-2385
214. Imai, Y., Horie, S., Yamano, T., and Iizuka, T. (1978) Molecular properties. in *Cytochrome P-450* (Sato, R., and Omura, T. eds.), Academic Press, New York. pp 37-135
215. Murakami, K., and Mason, H. S. (1967) An electron spin resonance study of microsomal fex. *J Biol Chem* **242**, 1102-1110
216. Franklin, M. R. (1972) The incomplete conversion of hepatic cytochrome P-450 to P-420 by mercurials. *Mol Pharmacol* **8**, 711-721
217. Malinouski, M., Zhou, Y., Belousov, V. V., Hatfield, D. L., and Gladyshev, V. N. (2011) Hydrogen peroxide probes directed to different cellular compartments. *PLoS One* **6**, e14564
218. Kuthan, H., and Ullrich, V. (1982) Oxidase and oxygenase function of the microsomal cytochrome P450 monooxygenase system. *Eur J Biochem* **126**, 583-588
219. Anfinsen, C. B., and Haber, E. (1961) Studies on the reduction and re-formation of protein disulfide bonds. *J Biol Chem* **236**, 1361-1363

220. Guengerich, F. P., Martin, M. V., Beaune, P. H., Kremers, P., Wolff, T., and Waxman, D. J. (1986) Characterization of rat and human liver microsomal cytochrome P-450 forms involved in nifedipine oxidation, a prototype for genetic polymorphism in oxidative drug metabolism. *J Biol Chem* **261**, 5051-5060
221. Guengerich, F. P., Hosea, N. A., and Martin, M. V. (1998) Purification of cytochromes P450: products of bacterial recombinant expression systems. *Methods Mol Biol* **107**, 77-83
222. Devarie-Baez, N. O., Silva Lopez, E. I., and Furdui, C. M. (2016) Biological chemistry and functionality of protein sulfenic acids and related thiol modifications. *Free Radic Res* **50**, 172-194
223. Choudhury, K., Sundaramoorthy, M., Hickman, A., Yonetani, T., Woehl, E., Dunn, M. F., and Poulos, T. L. (1994) Role of the proximal ligand in peroxidase catalysis: crystallographic, kinetic, and spectral studies of cytochrome *c* peroxidase proximal ligand mutants. *J Biol Chem* **269**, 20239-20249
224. Marnett, L. J., Weller, P., and Battista, J. R. (1986) Comparison of the peroxidase activity of hemeproteins and cytochrome P-450. in *Cytochrome P-450* (Ortiz de Montellano, P. R. ed.), Plenum Press, New York. pp 29-76
225. Everse, J., Everse, K. E., and Grisham, M. B. (1991) *Peroxidases in Chemistry and Biology, Volumes I and II*, CRC Press, Boca Raton, FL
226. Martinez, S., Wu, R., Sanishvili, R., Liu, D., and Holz, R. (2014) The active site sulfenic acid ligand in nitrile hydratases can function as a nucleophile. *J Am Chem Soc* **136**, 1186-1189
227. Forman, H. J., Davies, M. J., Kramer, A. C., Miotto, G., Zaccarin, M., Zhang, H., and Ursini, F. (2017) Protein cysteine oxidation in redox signaling: Caveats on sulfenic acid detection and quantification. *Arch Biochem Biophys* **617**, 26-37
228. Hsu, M. H., Baer, B. R., Rettie, A. E., and Johnson, E. F. (2017) The crystal structure of cytochrome P450 4B1 (CYP4B1) monooxygenase complexed with octane discloses several structural adaptations for *ω*-hydroxylation. *J Biol Chem* **292**, 5610-5621
229. Imig, J. D., Zou, A. P., Stec, D. E., Harder, D. R., Falck, J. R., and Roman, R. J. (1996) Formation and actions of 20-hydroxyeicosatetraenoic acid in rat renal arterioles. *Am J Physiol* **270**, R217-227
230. Sun, C. W., Falck, J. R., Harder, D. R., and Roman, R. J. (1999) Role of tyrosine kinase and PKC in the vasoconstrictor response to 20-HETE in renal arterioles. *Hypertension* **33**, 414-418
231. Hazelton, G. A., and Lang, C. A. (1980) Glutathione contents of tissues in the aging mouse. *Biochem J* **188**, 25-30
232. Hoch, U., and Ortiz de Montellano, P. R. (2001) Covalently linked heme in cytochrome P4504A fatty acid hydroxylases. *J Biol Chem* **276**, 11339-11346
233. LeBrun, L. A., Hoch, U., and Ortiz de Montellano, P. R. (2002) Autocatalytic mechanism and consequences of covalent heme attachment in the cytochrome P4504A family. *J Biol Chem* **277**, 12755-12761
234. Jiang, X. L., Gonzalez, F. J., and Yu, A. M. (2011) Drug-metabolizing enzyme, transporter, and nuclear receptor genetically modified mouse models. *Drug Metab Rev* **43**, 27-40

235. Aguiar, M., Masse, R., and Gibbs, B. F. (2005) Regulation of cytochrome P450 by posttranslational modification. *Drug Metab Rev* **37**, 379-404
236. Munoz-Clares, R. A., Gonzalez-Segura, L., Murillo-Melo, D. S., and Riveros-Rosas, H. (2017) Mechanisms of protection against irreversible oxidation of the catalytic cysteine of ALDH enzymes: Possible role of vicinal cysteines. *Chem Biol Interact* **276**, 52-64
237. Pundir, C. S., Deswal, R., and Narwal, V. (2017) Quantitative analysis of hydrogen peroxide with special emphasis on biosensors. *Bioprocess Biosyst Eng* **41**, 313-329
238. Nordblom, G. D., White, R. E., and Coon, M. J. (1976) Studies on hydroperoxide-dependent substrate hydroxylation by purified liver microsomal cytochrome P-450. *Arch Biochem Biophys* **175**, 524-533
239. Joo, H., Lin, Z. L., and Arnold, F. H. (1999) Laboratory evolution of peroxide-mediated cytochrome P450 hydroxylation. *Nature* **399**, 670-673
240. Shoji, O., and Watanabe, Y. (2014) Peroxygenase reactions catalyzed by cytochromes P450. *J Biol Inorg Chem* **19**, 529-539
241. Matthews, S., Belcher, J. D., Tee, K. L., Girvan, H. M., McLean, K. J., Rigby, S. E., Levy, C. W., Leys, D., Parker, D. A., Blankley, R. T., and Munro, A. W. (2017) Catalytic determinants of alkene production by the cytochrome P450 peroxygenase $OleT_{JE}$. *J Biol Chem* **292**, 5128-5143
242. Matsumura, H., Wakatabi, M., Omi, S., Ohtaki, A., Nakamura, N., Yohda, M., and Ohno, H. (2008) Modulation of redox potential and alteration in reactivity via the peroxide shunt pathway by mutation of cytochrome P450 around the proximal heme ligand. *Biochemistry* **47**, 4834-4842
243. Miseta, A., and Csutora, P. (2000) Relationship between the occurrence of cysteine in proteins and the complexity of organisms. *Mol Biol Evol* **17**, 1232-1239
244. Crooks, G. E., Hon, G., Chandonia, J. M., and Brenner, S. E. (2004) WebLogo: a sequence logo generator. *Genome Res* **14**, 1188-1190
245. Sirim, D., Widmann, M., Wagner, F., and Pleiss, J. (2010) Prediction and analysis of the modular structure of cytochrome P450 monooxygenases. *BMC Struct Biol* **10**, 34

Figure A1. Representative MS/MS Spectra of P450 recombinant 1A2. Some annotated spectra produced by protein prospector MS-Product (http://prospector.ucsf.edu/prospector/cgi-bin/msform.cgi?form=msproduct)

Cys158-containing peptide alkylated with d_0-dimedone

LAQNALNTFSIASDPASSSSC*YLEEHVSK (Light)

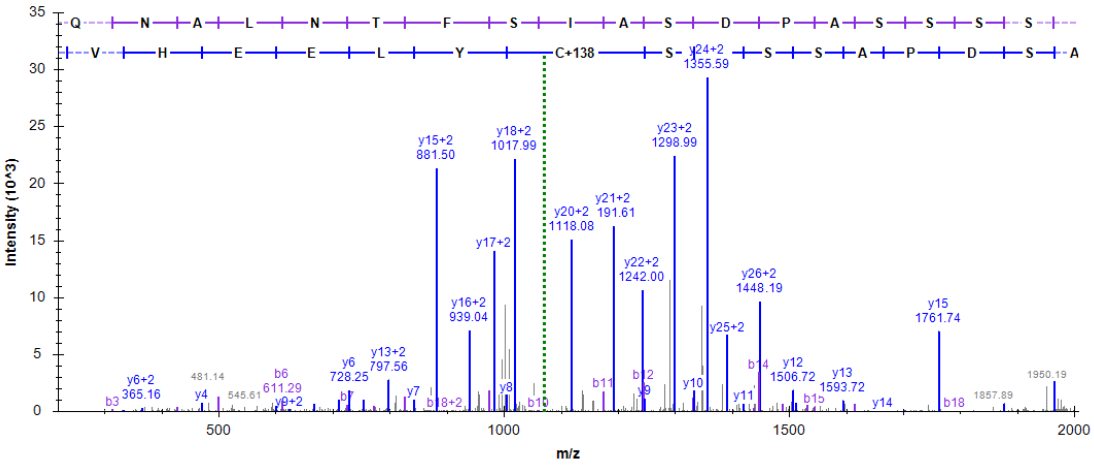

Cys158-containing peptide alkylated with d_6-dimedone

LAQNALNTFSIASDPASSSSC*YLEEHVSK (Heavy)

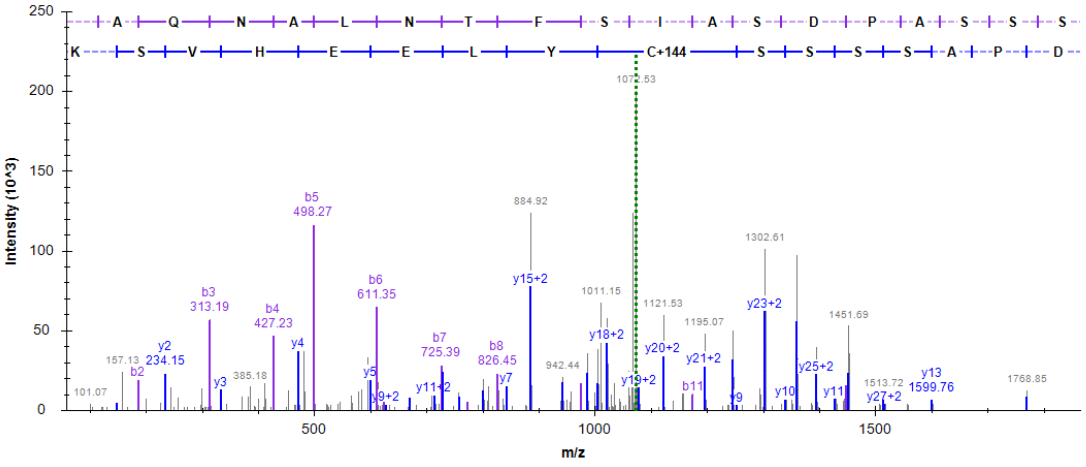

Representative XIC peaks integrated for Cys158-containing peptide:

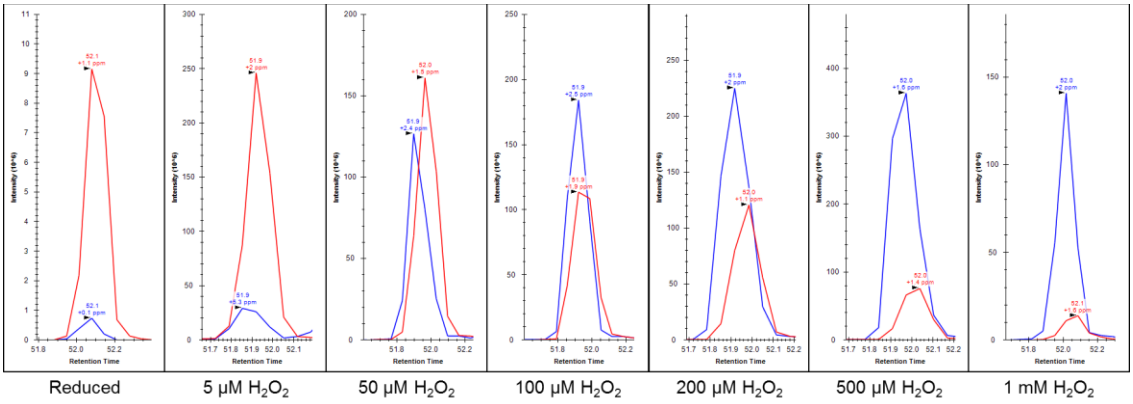

Cys457-containing peptide alkylated with d_0-dimedone

C*IGEVLAK (Light)

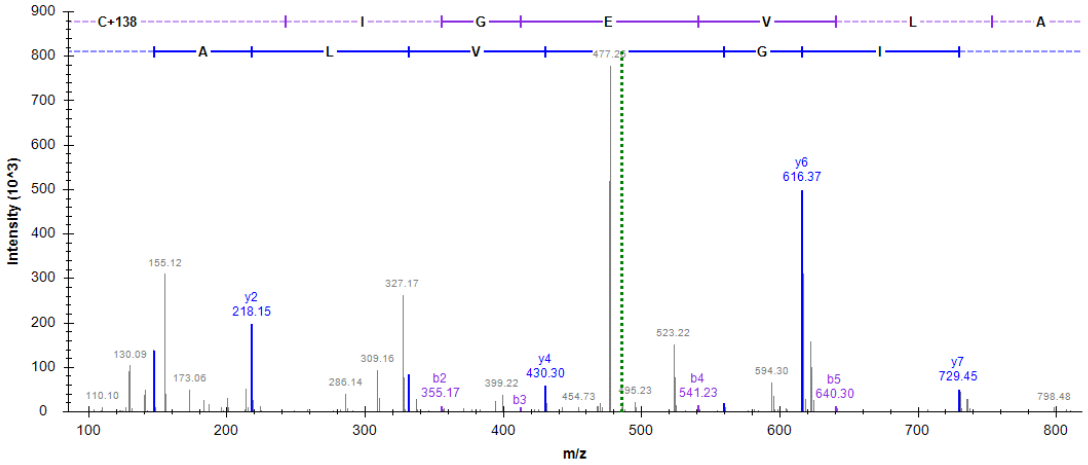

Cys457-containing peptide alkylated with d_6-dimedone

C*IGEVLAK (Heavy)

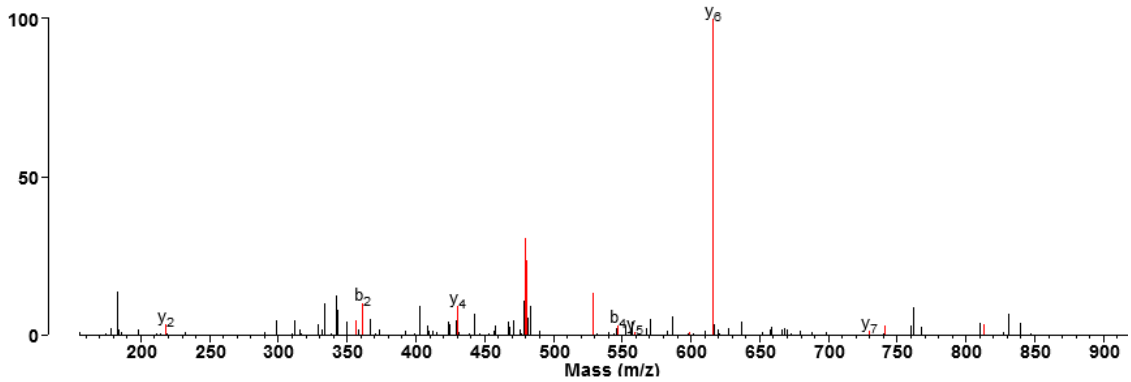

Representative XIC peaks integrated for Cys457-containing peptide:

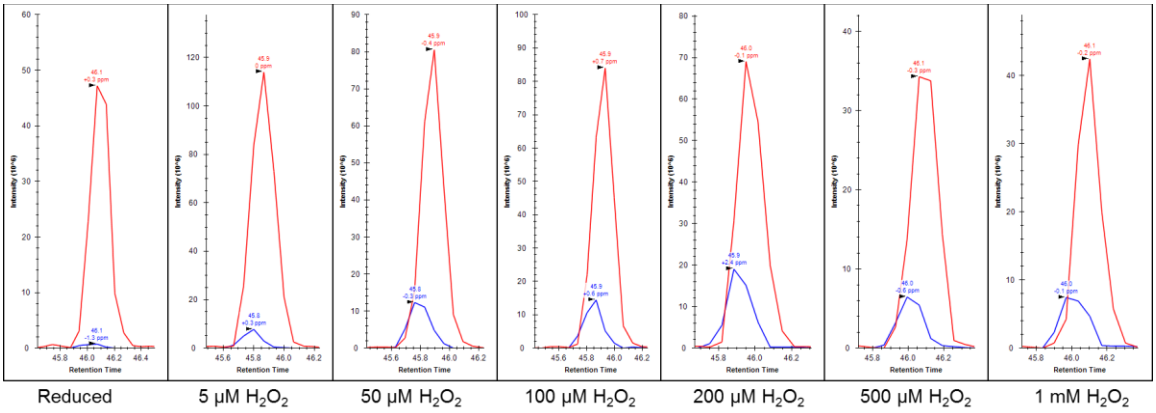

Cys503-containing peptide alkylated with d_0-dimedone

C*EHVQAR (Light)

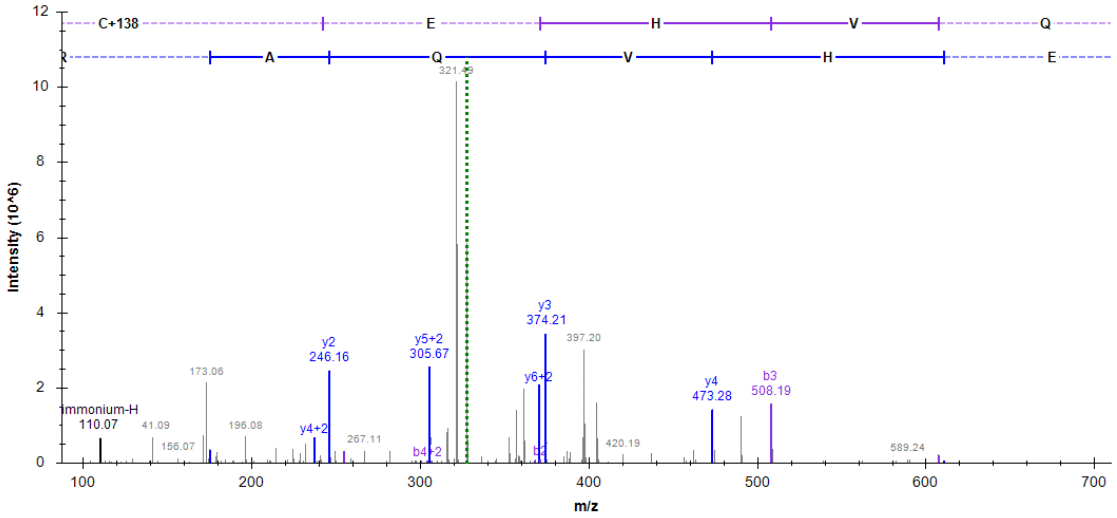

Cys503-containing peptide alkylated with d_6-dimedone

C*EHVQAR (Heavy)

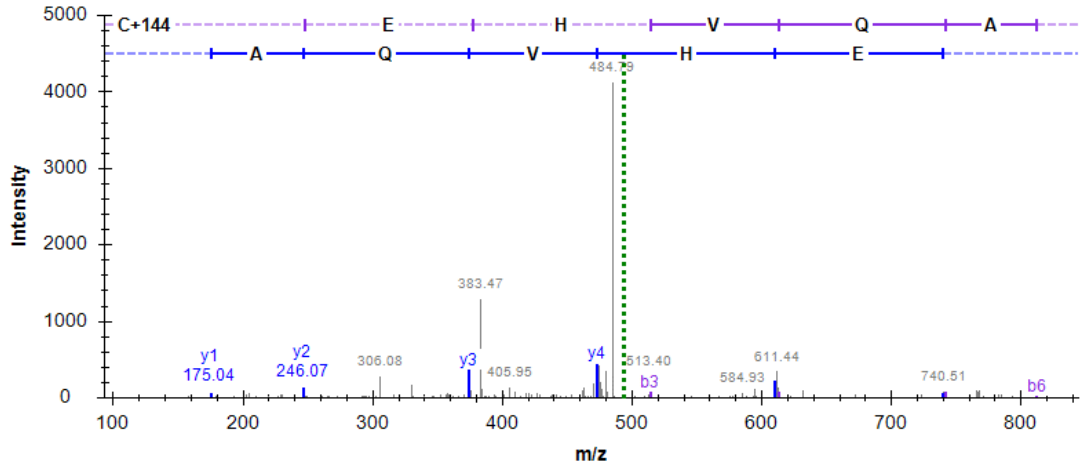

Representative XIC peaks integrated for Cys503-containing peptide:

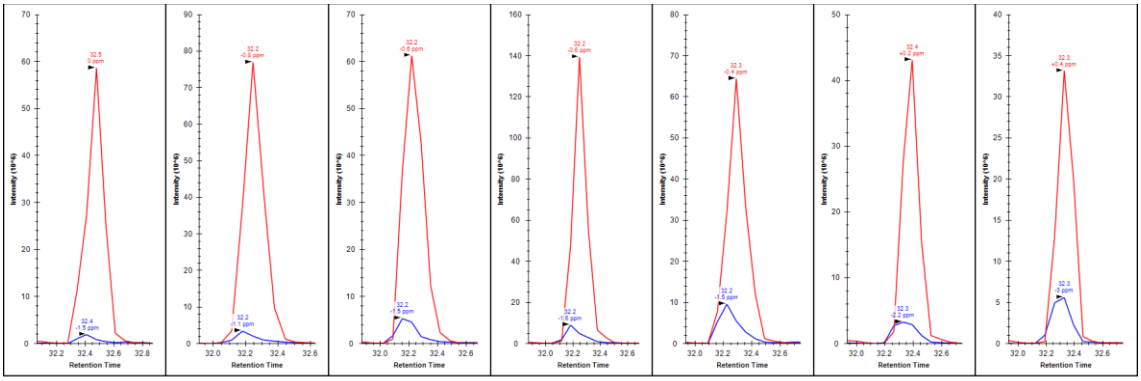

Reduced | 5 μM H_2O_2 | 50 μM H_2O_2 | 100 μM H_2O_2 | 200 μM H_2O_2 | 500 μM H_2O_2 | 1 mM H_2O_2

Figure A2. Representative MS/MS Spectra of P450 recombinant 2C8. Some annotated spectra produced by protein prospector MS-Product (http://prospector.ucsf.edu/prospector/cgi-bin/msform.cgi?form=msproduct)

Cys50-containing peptide alkylated with d_0-dimedone

DIC*K (Light)

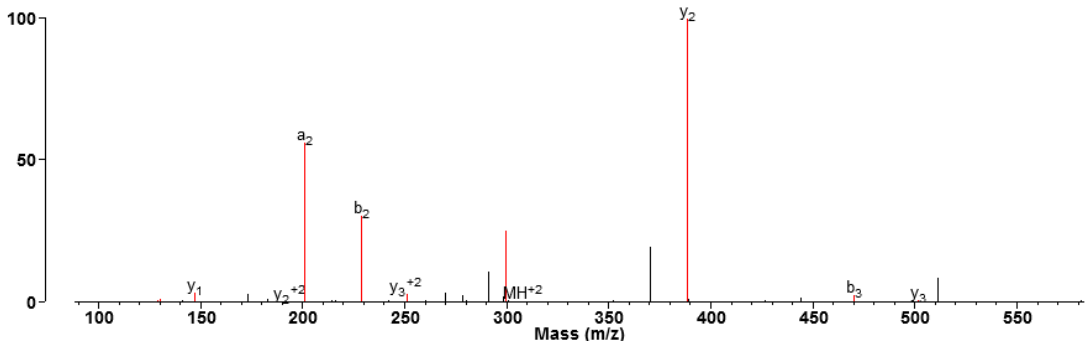

Cys50-containing peptide alkylated with d_6-dimedone

DIC*K (Heavy)

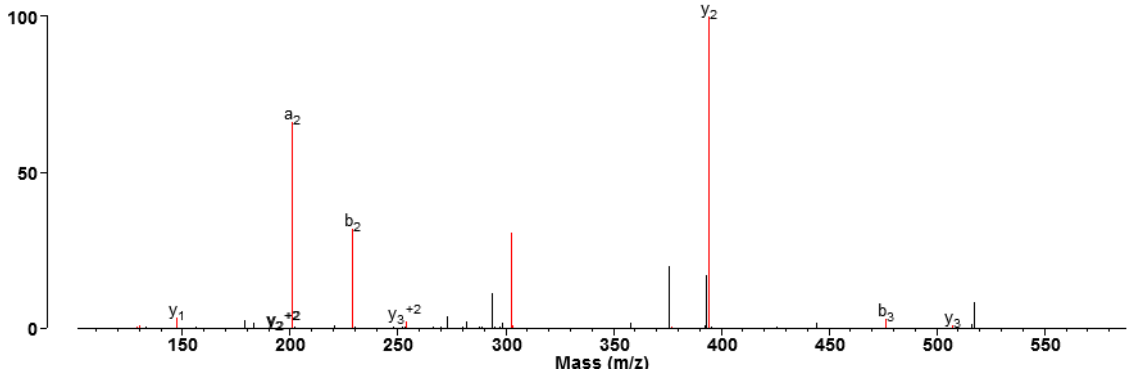

Representative XIC peaks integrated for Cys50-containing peptide:

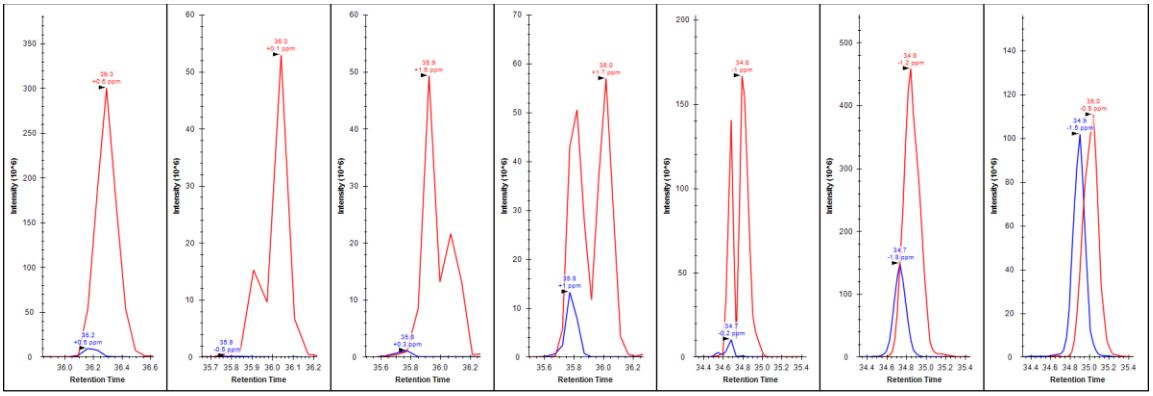

Reduced | 5 μM H_2O_2 | 50 μM H_2O_2 | 100 μM H_2O_2 | 200 μM H_2O_2 | 500 μM H_2O_2 | 1 mM H_2O_2

Cys149-containing peptide alkylated with d_0-dimedone

VQEEAHC*LVEELR (Light)

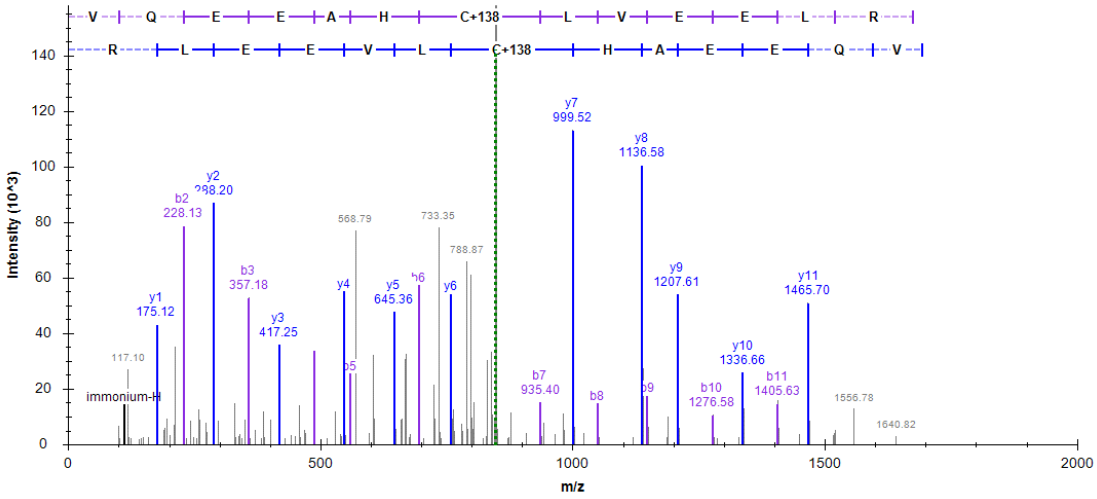

Cys149-containing peptide alkylated with d_6-dimedone

VQEEAHC*LVEELR (Heavy)

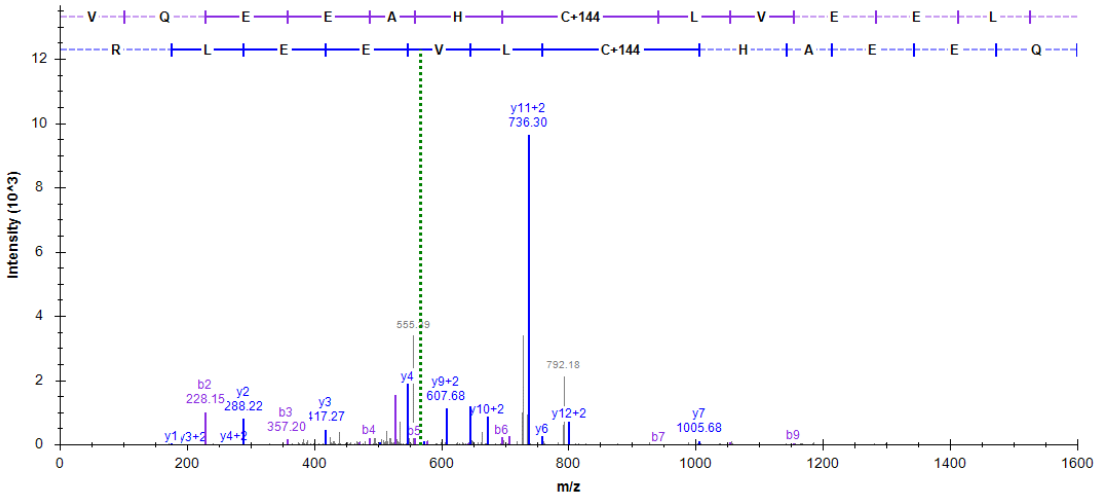

Representative XIC peaks integrated for Cys151-containing peptide:

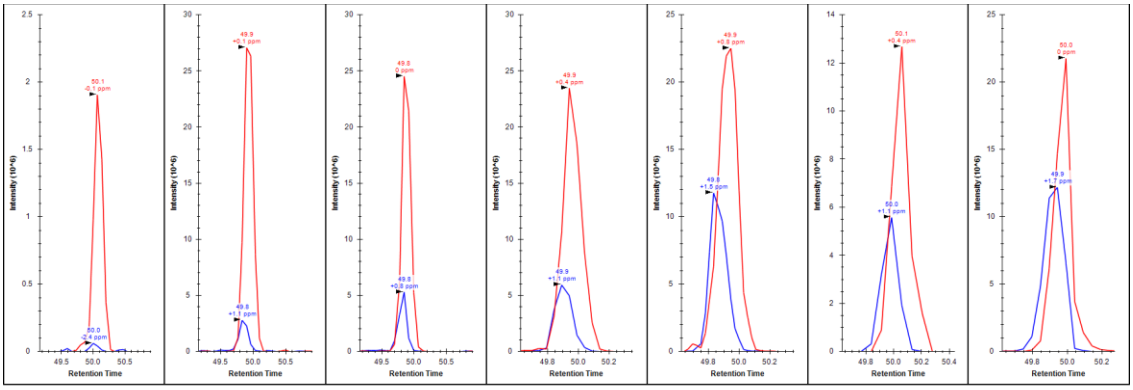

Cys264-containing peptide alkylated with d_0-dimedone

DFIDC*FLIK (Light)

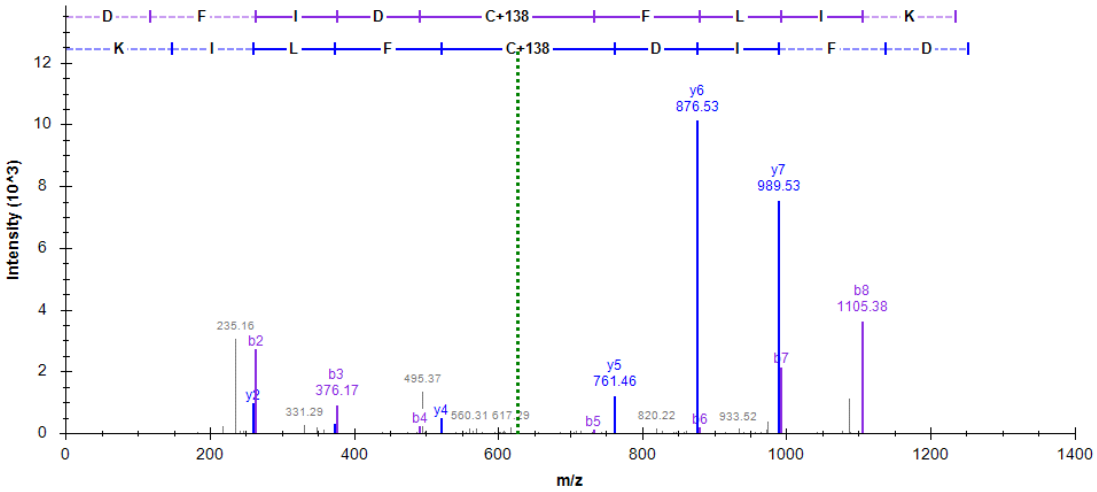

Cys264-containing peptide alkylated with d_6-dimedone

DFIDC*FLIK (Heavy)

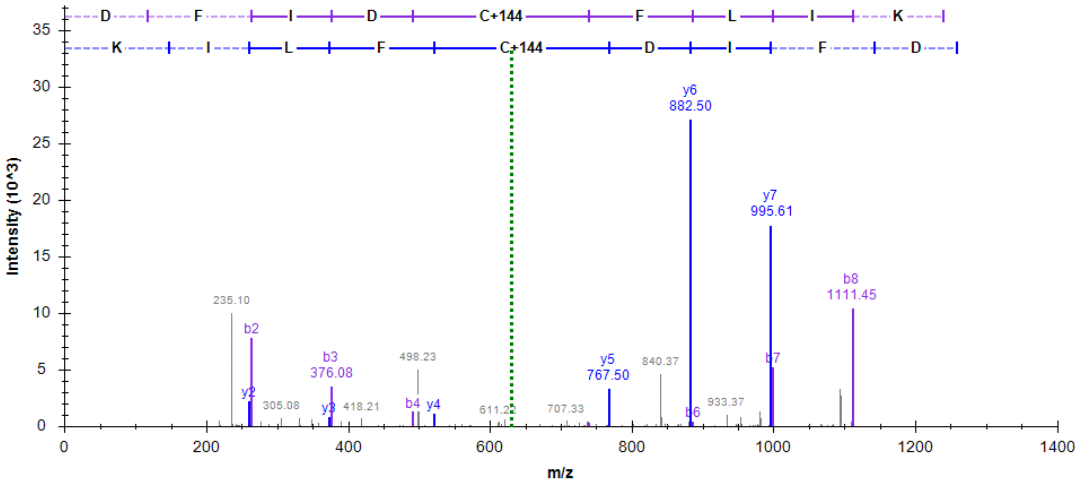

Representative XIC peaks integrated for Cys264-containing peptide:

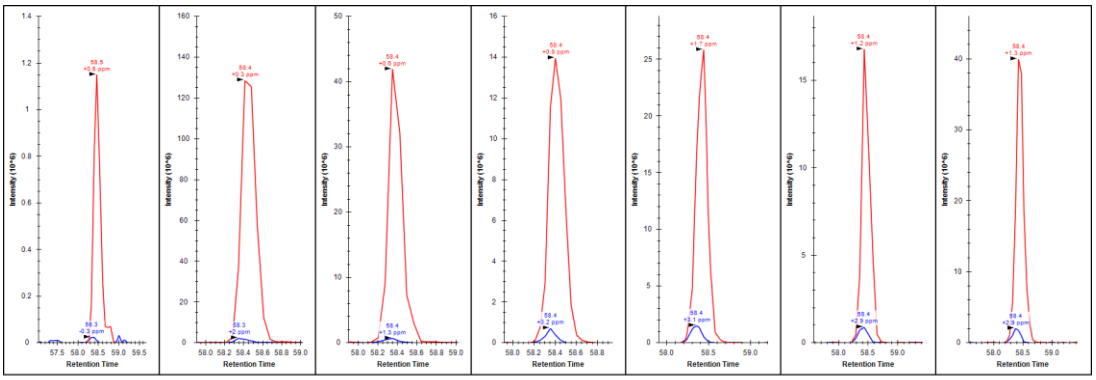

Cys337-containing peptide alkylated with d_0-dimedone

SPC*MQDR (Light)

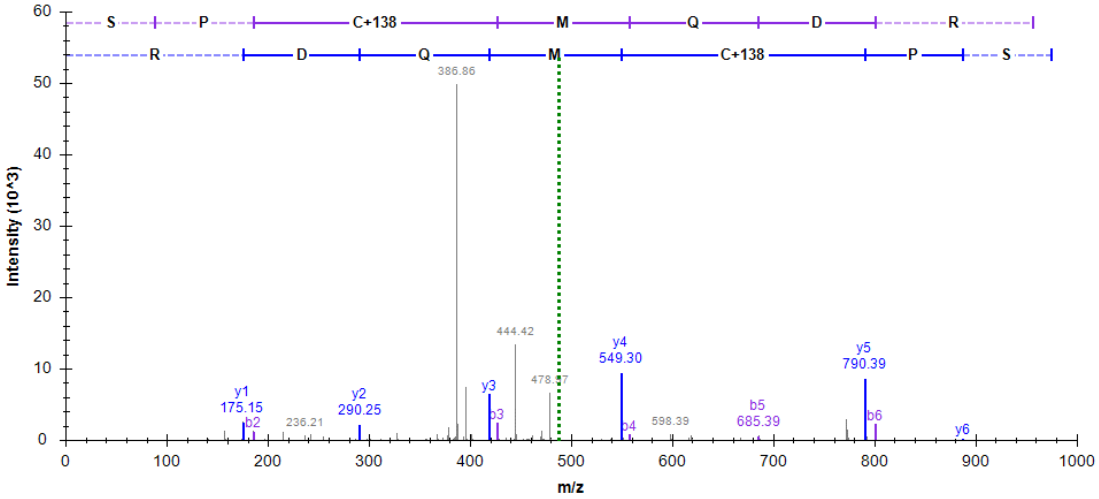

Cys337-containing peptide alkylated with d_6-dimedone

SPC*MQDR (Heavy)

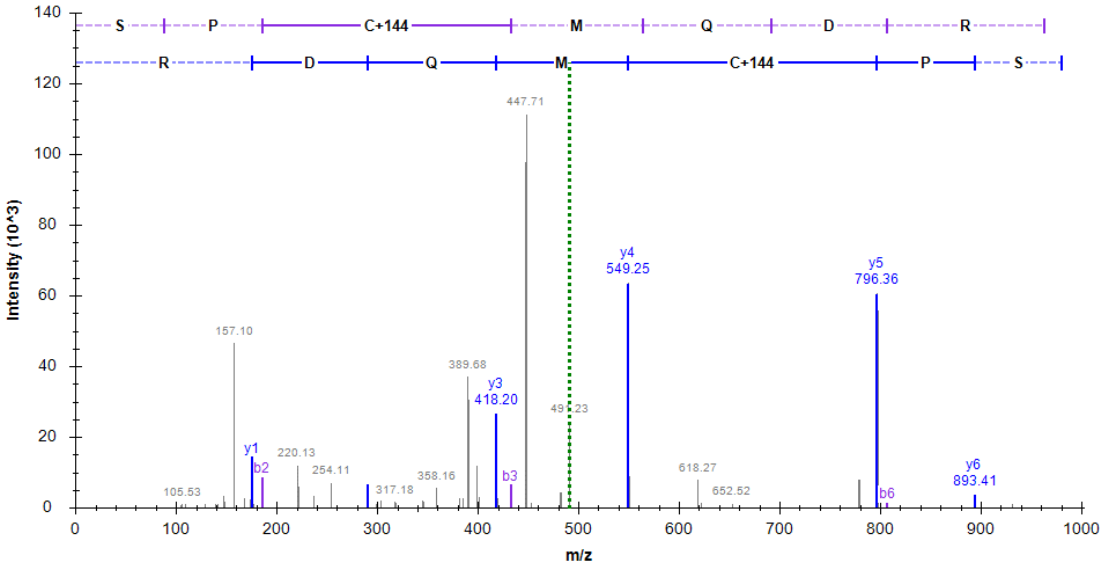

Representative XIC peaks integrated for Cys338-containing peptide:

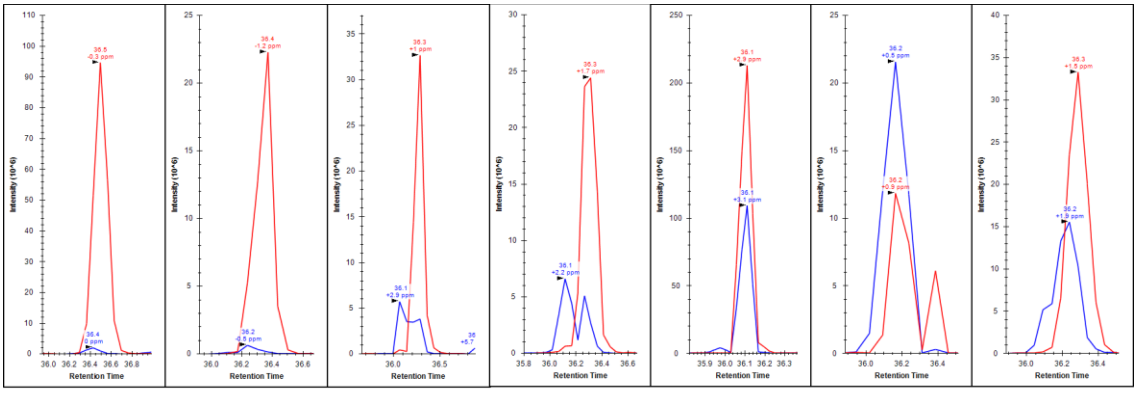

Cys434-containing peptide alkylated with d_0-dimedone

IC*AGEGLAR (Light)

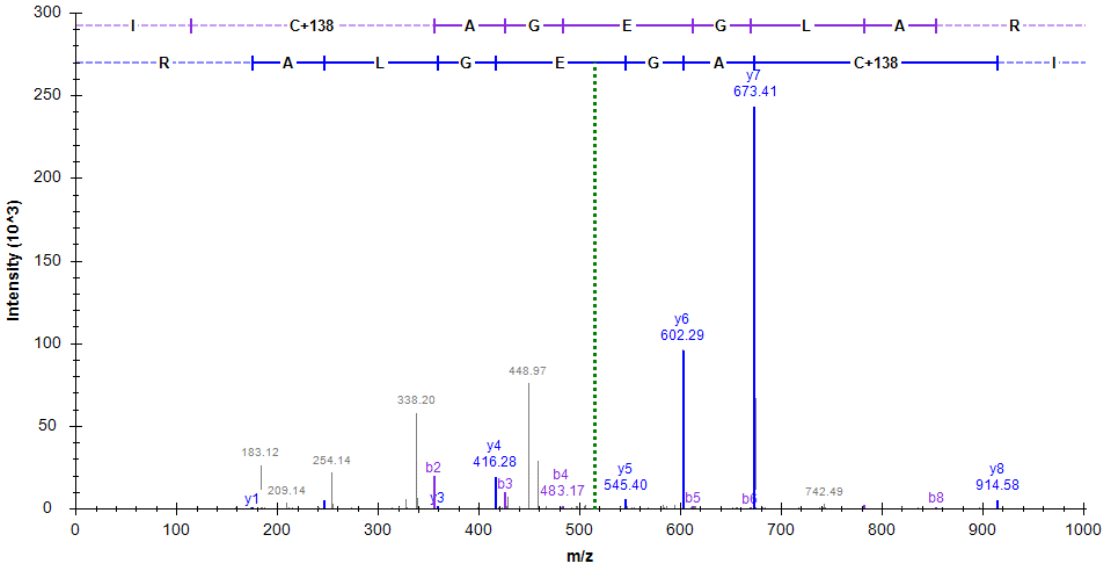

Cys434-containing peptide alkylated with d_6-dimedone

IC*AGEGLAR (Heavy)

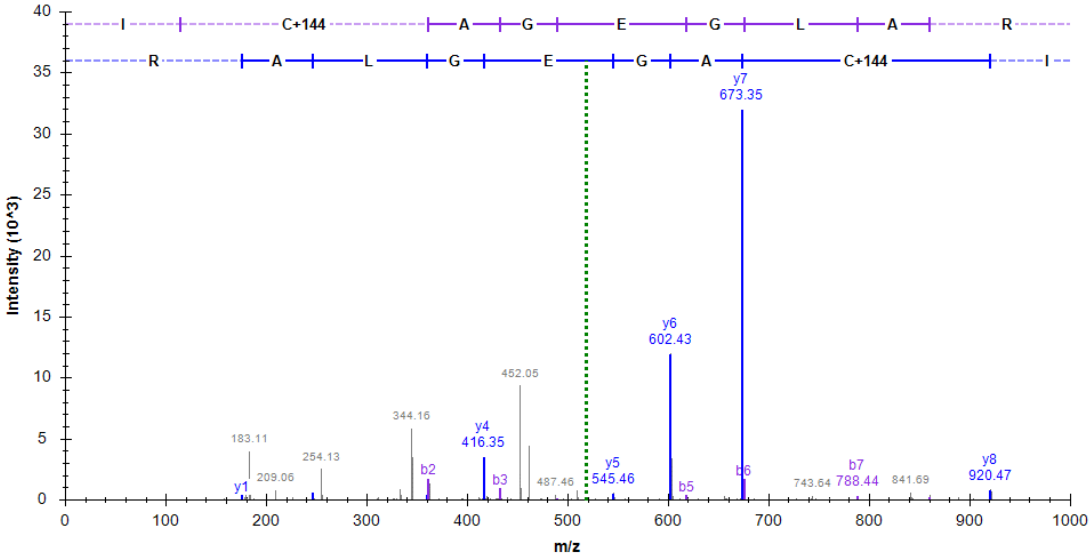

Representative XIC peaks integrated for Cys434-containing peptide:

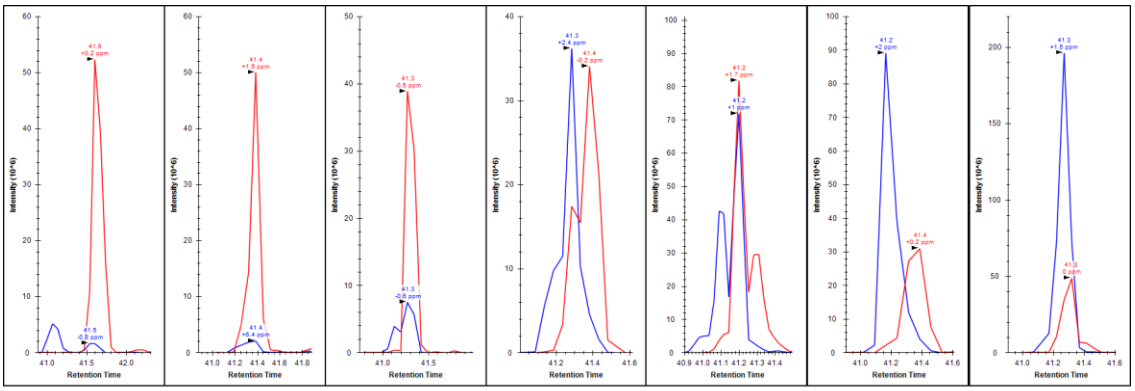

Figure A3. Representative MS/MS Spectra of P450 recombinant 2D6. Some annotated spectra produced by protein prospector MS-Product (http://prospector.ucsf.edu/prospector/cgi-bin/msform.cgi?form=msproduct)

Cys190-containing peptide alkylated with d_0-dimedone

AVSNVIASLTC*GR (Light)

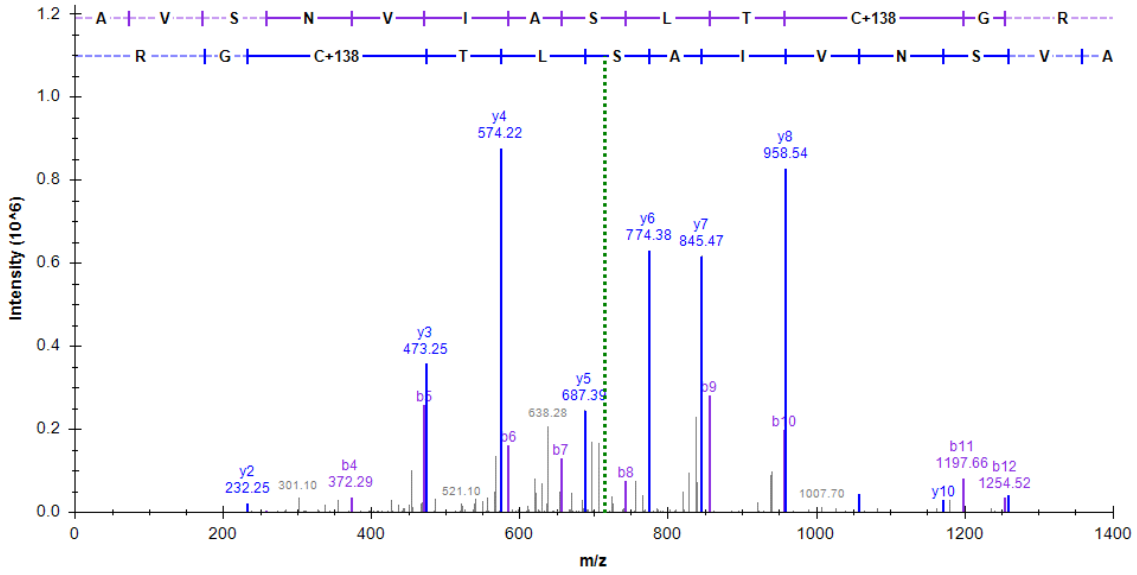

Cys190-containing peptide alkylated with d_6-dimedone

AVSNVIASLTC*GR (Heavy)

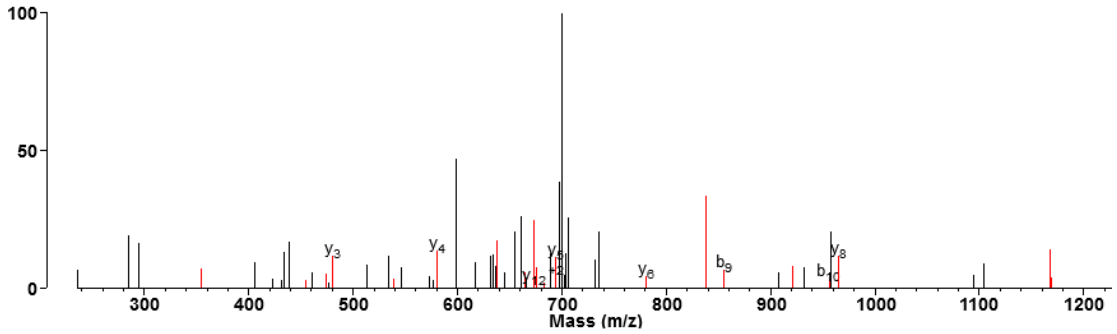

Representative XIC peaks integrated for Cys190-containing peptide:

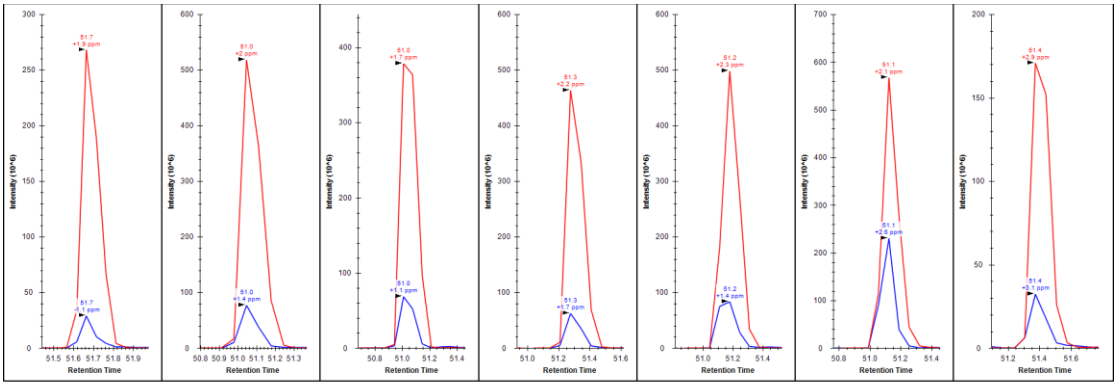

Cys442-containing peptide alkylated with d_0-dimedone

AC*LGEPLAR (Light)

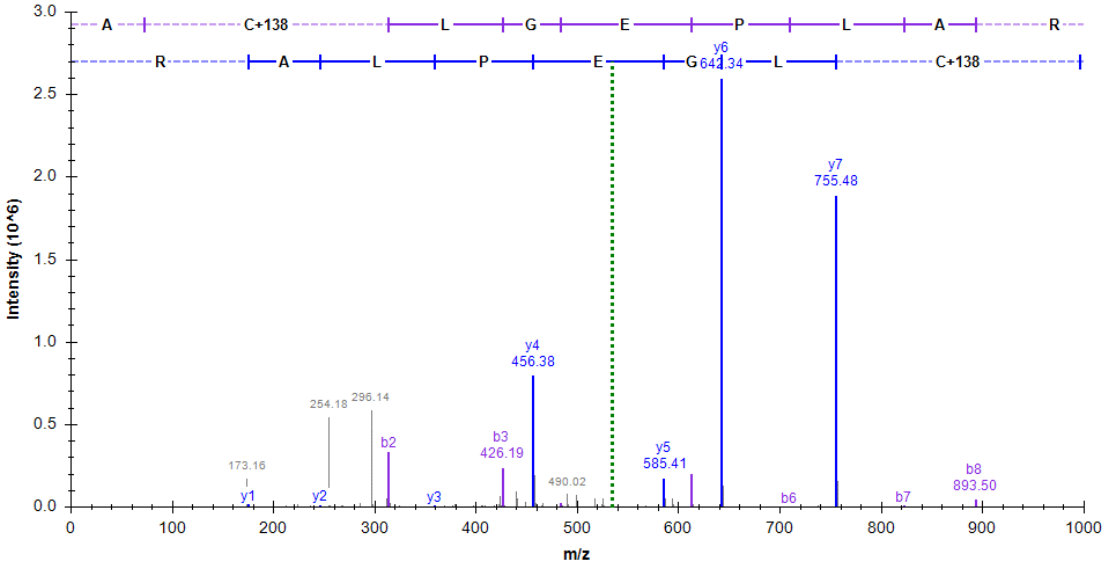

Cys442-containing peptide alkylated with d_6-dimedone

AC*LGEPLAR (Heavy)

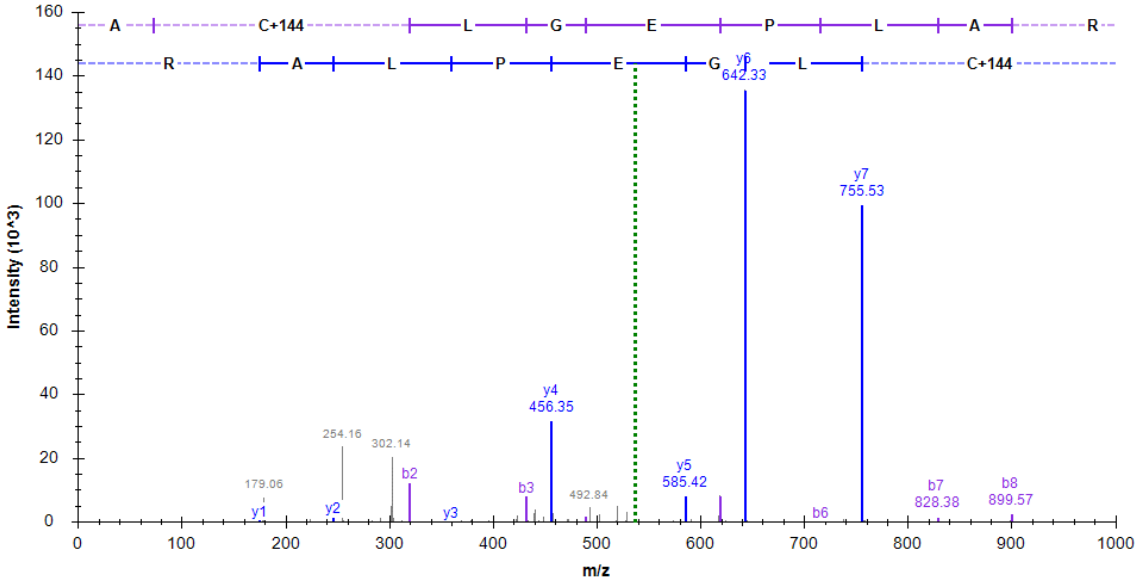

Representative XIC peaks integrated for Cys443-containing peptide:

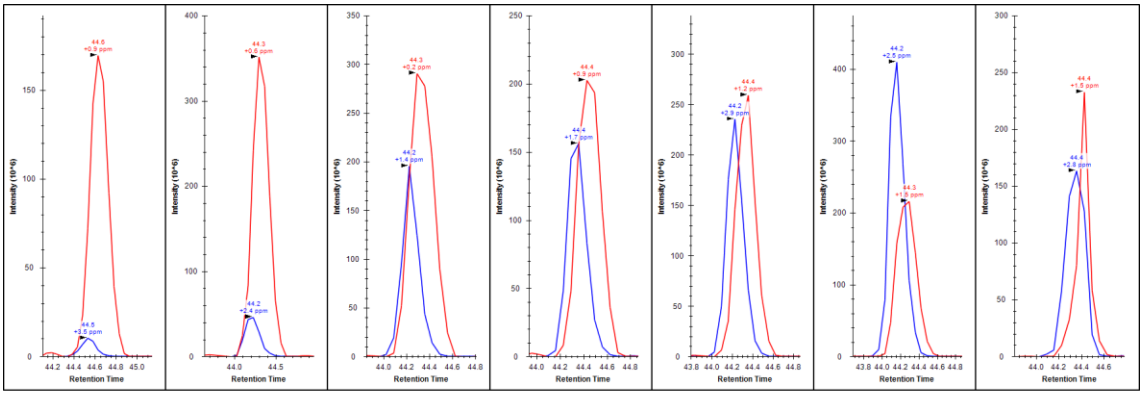

Figure A4. Representative MS/MS Spectra of P450 recombinant 3A4. Some annotated spectra produced by protein prospector MS-Product (http://prospector.ucsf.edu/prospector/cgi-bin/msform.cgi?form=msproduct)

Cys96-containing peptide alkylated with d_0-dimedone

EC*YSVFTNR (Light)

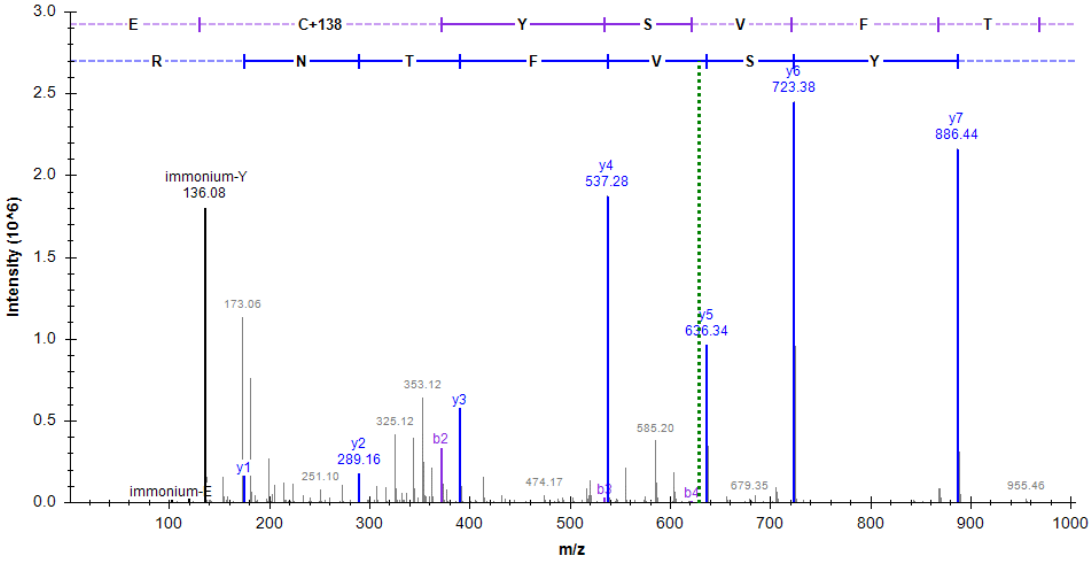

Cys96-containing peptide alkylated with d_6-dimedone

EC*YSVFTNR (Heavy)

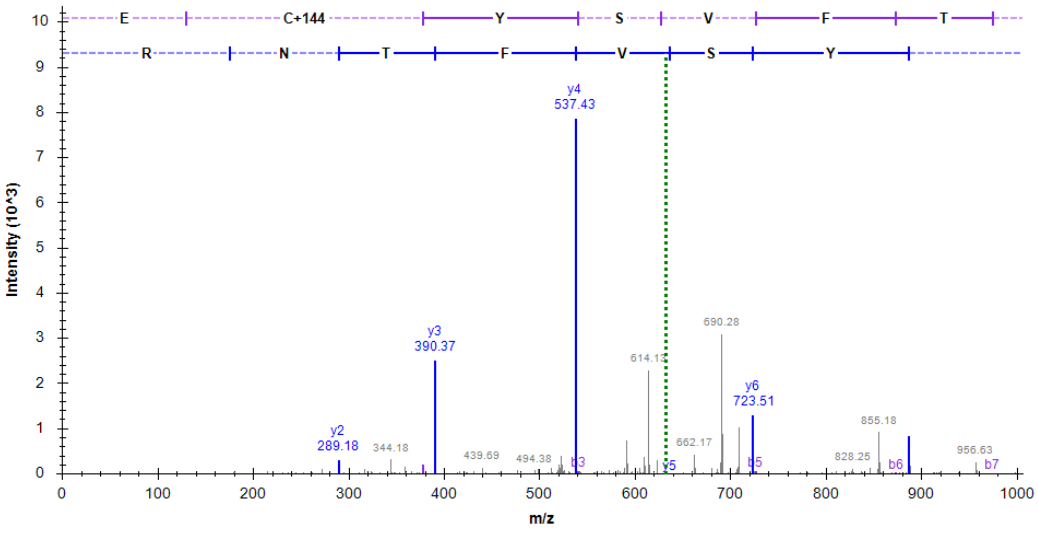

Representative XIC peaks integrated for Cys98-containing peptide:

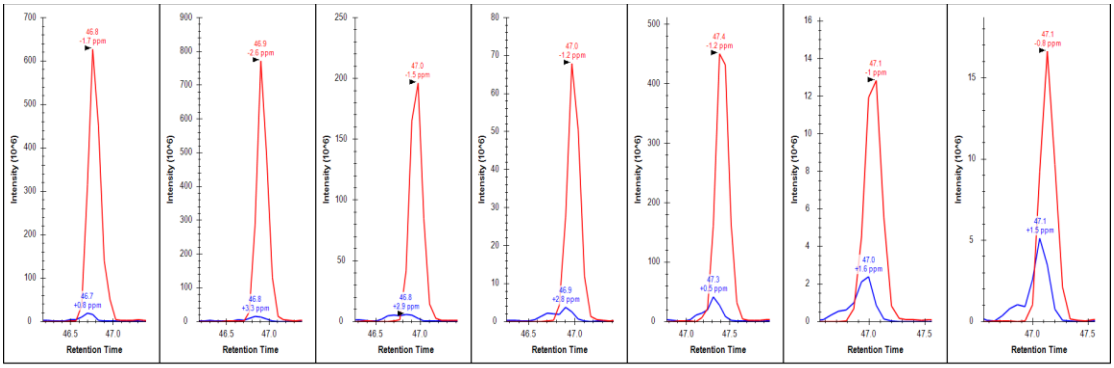

Cys376-containing peptide alkylated with d_0-dimedone

LERVC*K (Light)

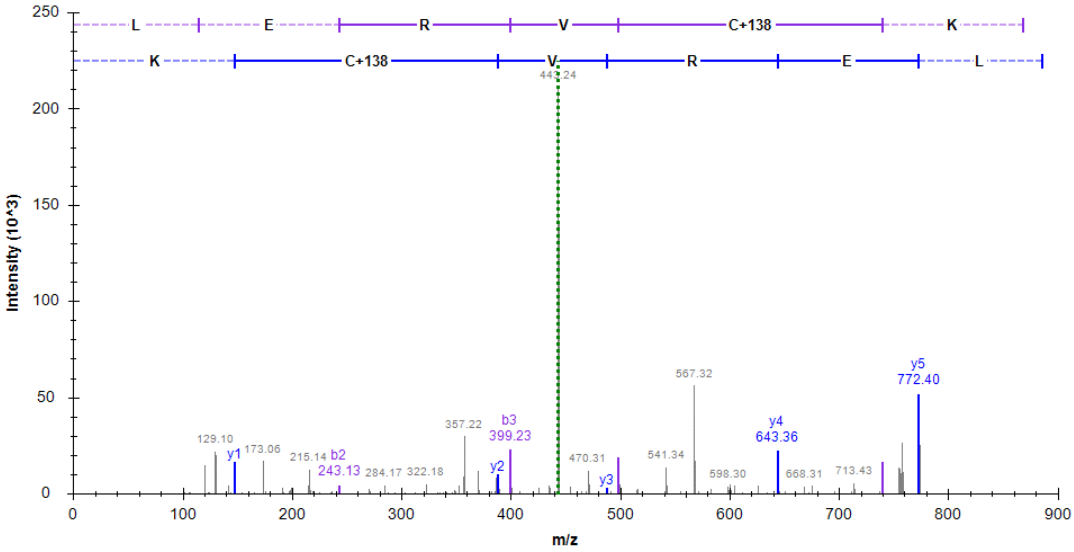

Cys376-containing peptide alkylated with d_6-dimedone

LERVC*K (Heavy)

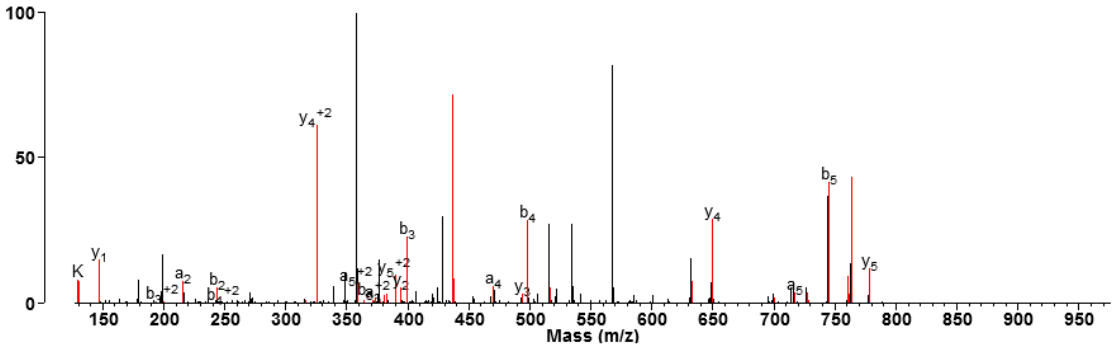

Representative XIC peaks integrated for Cys376-containing peptide:

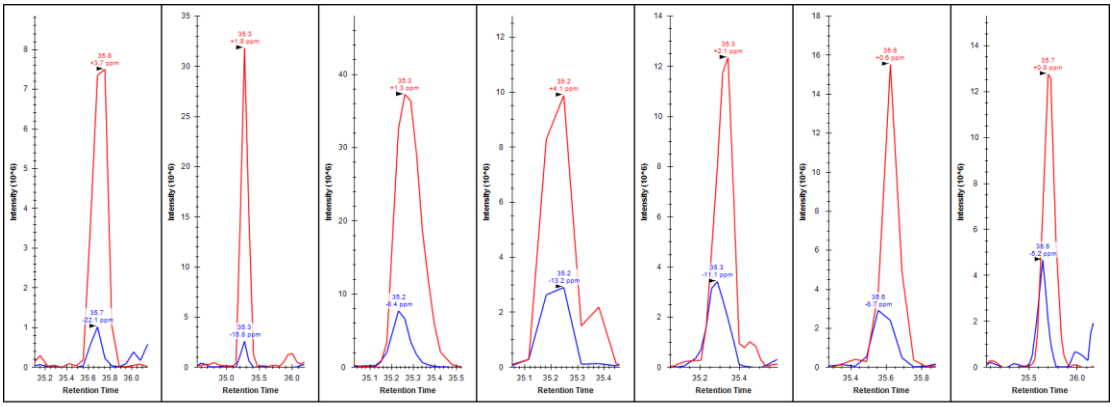

Reduced | 5 μM H_2O_2 | 50 μM H_2O_2 | 100 μM H_2O_2 | 200 μM H_2O_2 | 500 μM H_2O_2 | 1 mM H_2O_2

Cys440-containing peptide alkylated with d_0-dimedone

NC*IGMR (Light)

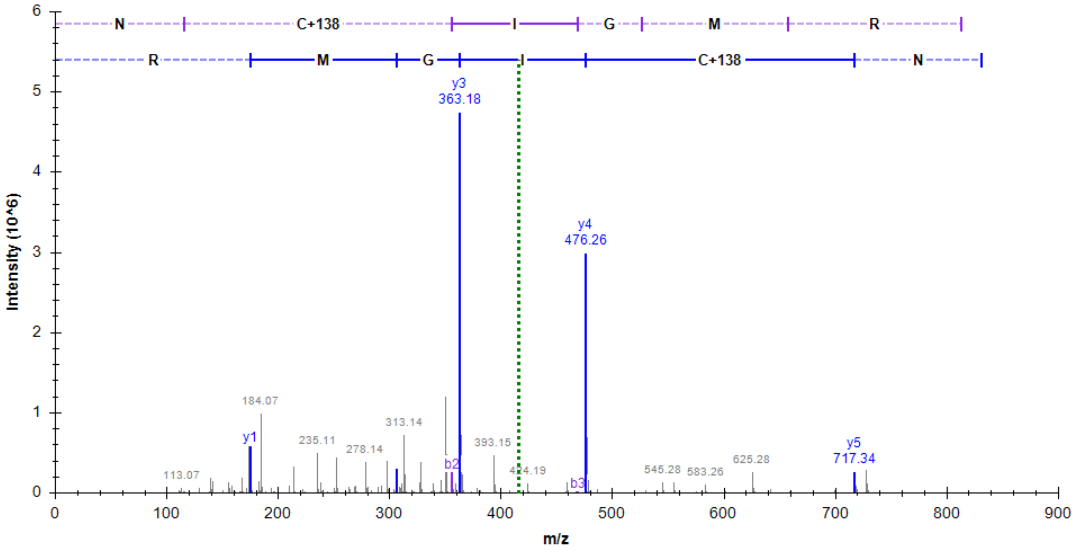

Cys440-containing peptide alkylated with d_6-dimedone

NC*IGMR (Heavy)

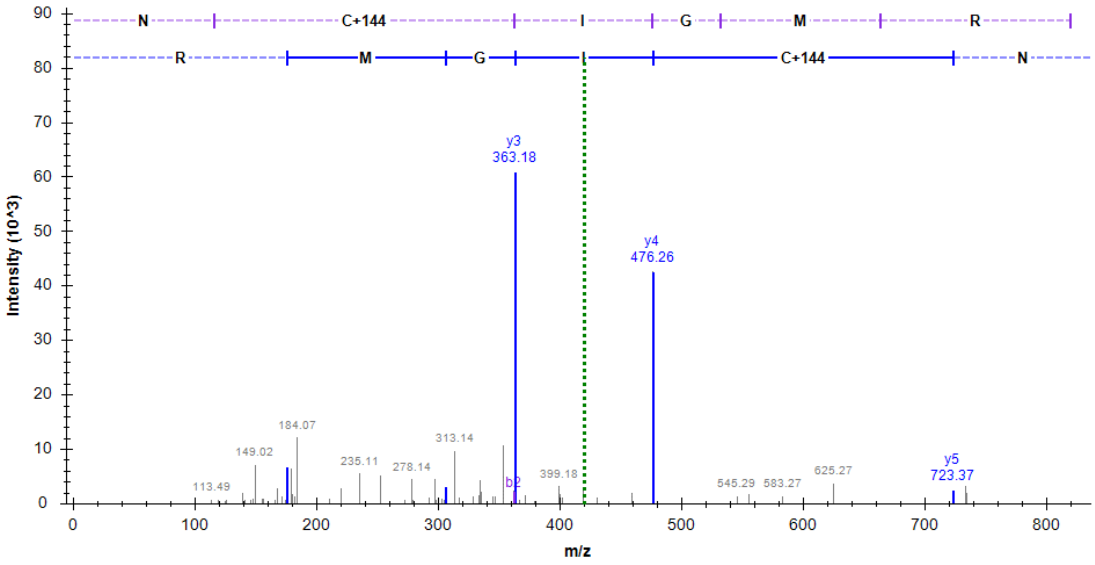

Representative XIC peaks integrated for Cys440-containing peptide:

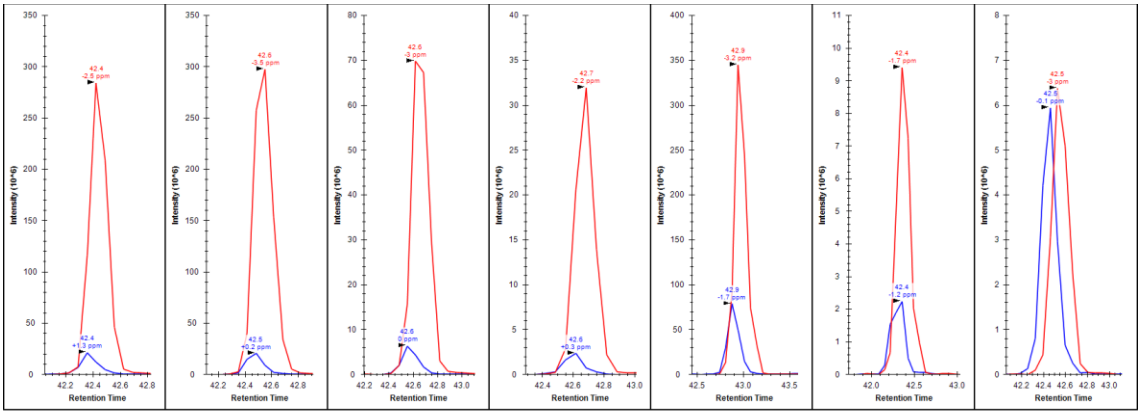

Cys467-containing peptide alkylated with d_0-dimedone

VLQNFSFKPC*K (Light)

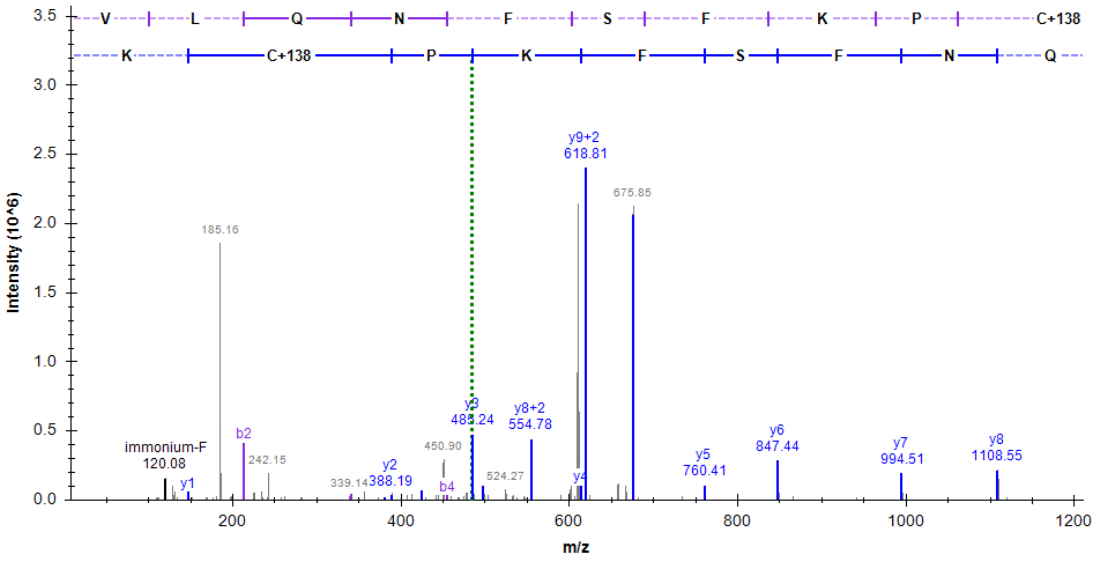

Cys467-containing peptide alkylated with d_6-dimedone

VLQNFSFKPC*K (Heavy)

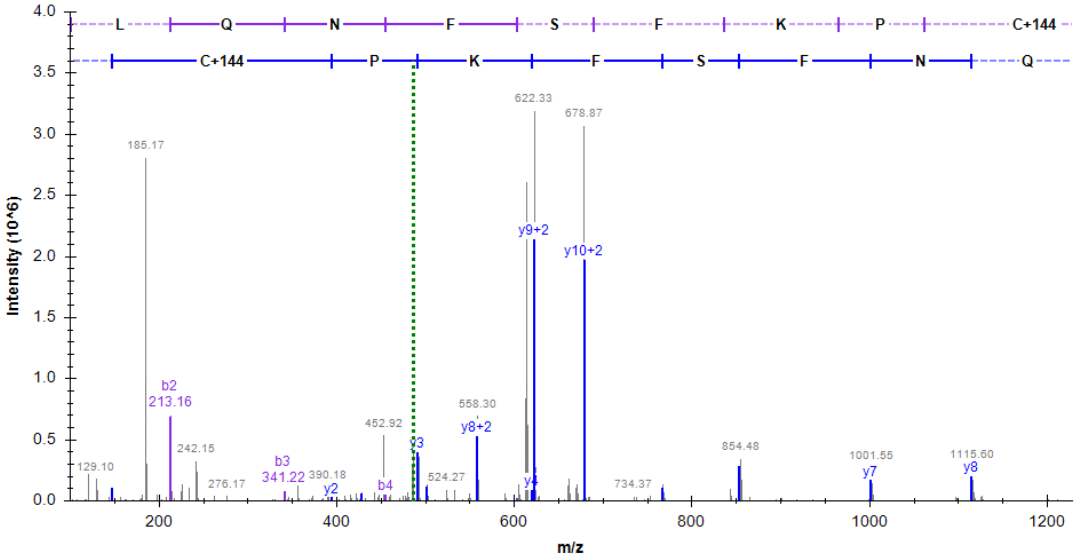

Representative XIC peaks integrated for Cys467-containing peptide:

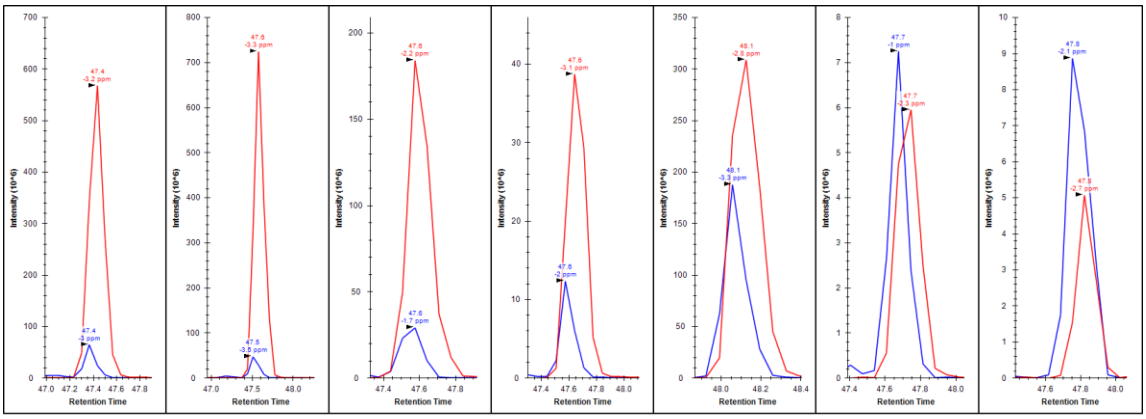

Figure A5. Hyperoxidation of P450 3A4 Cys467. MS/MS Spectra of hyperoxidized Cys-467

VLQNFSFKP**C**(SO_2)K

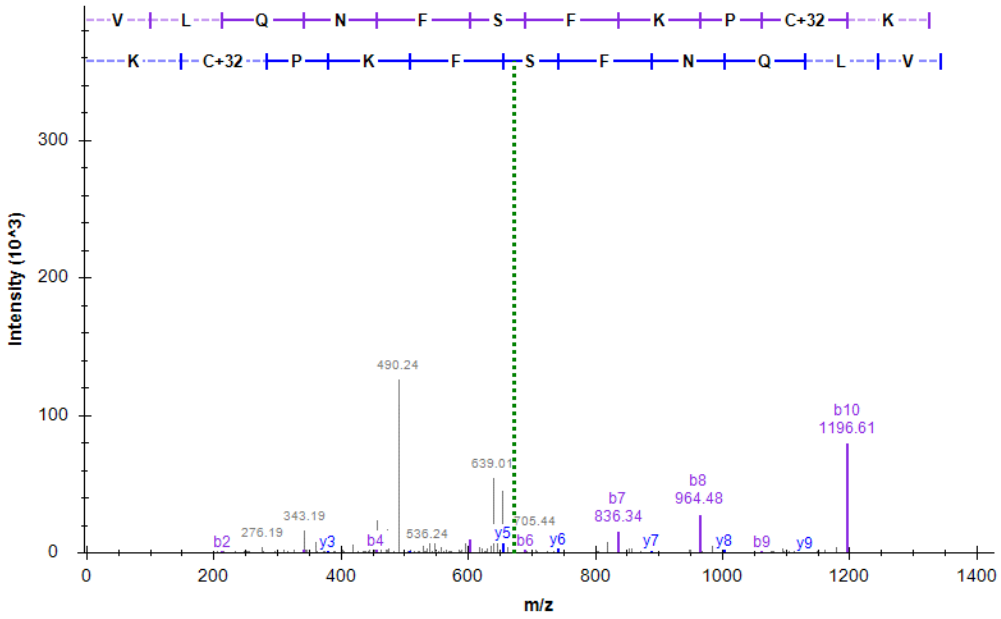

VLQNFSFKP**C**(SO_3)K